

# FLUIDIC EMERGENCY ROLL CONTROL SYSTEM

Contract NAS2-5467 Task IV

Prepared for  
National Aeronautics and Space Administration  
Ames Research Center  
Moffett Field, California

By  
K. B. Haefner and T. S. Honda  
General Electric Company  
Specialty Fluidics Operation  
Schenectady, New York

March 1973

(NASA-CR-114588) FLUIDIC EMERGENCY ROLL  
CONTROL SYSTEM Final Report (General  
Electric Co.) 98 p HC \$7.00 CSCL 01C

N74-10048

Unclas  
G3/02 21506



## Foreword

This final report was prepared by the General Electric Company for the System Engineering Facility of the Ames Research Center, National Aeronautics and Space Administration, Moffett Field, California, under Task IV, Contract NAS2-5467. The Ames Project Engineer was Mr. D. M. Chisel.

## TABLE OF CONTENTS

	<u>Page</u>
List of Figures	i
List of Tables	iii
SECTION 1      Introduction and Summary	1-1
2      Conclusions and Recommendations	2-1
Conclusions	2-1
Recommendations	2-2
3      ERC System Design Specifications	3-1
FET	3-1
Hot Gas Generator	3-2
4      FET Design Modifications	4-1
5      Hot Gas Generator Design	5-1
6      Solid Propellant Gas Generator Test	6-1
7      Test Plan Definition and Test Hardware	7-1
Static Cold Gas Tests	7-1
Dynamic Cold Gas Tests	7-3
Dynamic Hot Gas Tests	7-11
8      Cold and Hot Gas Test Results-Unit No. 1	8-1
Static Cold Gas Tests	8-1
Dynamic Cold Gas Tests	8-6
Hot Gas Tests	8-8
9      FET Modifications	9-1
10      Cold and Hot Gas Tests-Unit No. 2	10-1
Cold Gas Tests	10-1
Hot Gas Tests	10-8
APPENDIX A      Engineering Specification ES-PT-1	
APPENDIX B(a)   Test Plan 1290-141 for Fluidic Emergency Thruster System (Thiokol Chemical Corporation)	
(b) Engineering Specification ES-PT-2	
Hot Gas Test Procedure	

# LIST OF FIGURES

<u>Figure</u>		<u>Page</u>
1-1	Emergency Roll Control Installation	1-2
4-1	Torque Motor Enclosure Redesign	4-3
5-1	Motor Assembly	5-2
5-2	Ballistic Characterization of TP-Q-3074A, Rate and $K_n$ Versus Pressure	5-3
5-3	Propellant Grain-Inhibited	5-4
5-4	Gas Generator Pressure Schedule	5-5
6-1	Hot Gas Generator Test #1 (Pressure Versus Time)	6-2
6-2	Test #1 Pressure vs Time (Temperature Ambient)	6-3
6-3	Test #2 Pressure vs Time (Temperature +60F)	6-4
6-4	Test #2 Pressure vs Time (Temperature +60F)	6-5
7-1	Schematic of Cold Tests	7-2
7-2	Functional Diagram, Fluidic Emergency Thruster and Aircraft System Simulator	7-4
7-3	Aircraft Analog Simulation	7-5
7-4	Attitude Control Simulator Breadboard	7-7
7-5	Electronic Logic Board No. 1	7-8
7-6	Electronic Logic	7-9
7-7	FET-Aircraft System Simulation Gain Distribution	7-10
7-8	Schematic of Hot Gas Test	7-12
8-1	FET Null Offset Versus Supply Pressure	8-3
8-2	FET Saturation Characteristic	8-4
8-3	FET Hysteresis Characteristic	8-5
8-4	Cold Gas Test Data - FET-Simulated Aircraft Stabilization Characteristic	8-7
8-5	Cold Gas Test Data - FET-Simulated Stabilization Characteristic	8-9
8-6	Cold Gas Test Data - FET-Simulated Aircraft Stabilization Characteristic	8-10
8-7	Test Setup Employed During Dynamic Cold and Hot Gas Runs	8-11
8-8	Test Setup Prior to Firing	8-12
8-9	Phase Plane Plot of FET Closed Loop Performance on Hot Gas #1	8-14
8-10	FET After Firing	8-15

# LIST OF FIGURES (CONT.)

<u>Figure</u>		<u>Page</u>
8-11	Torque Motor Housing After Firing	8-16
8-12	Time Trace of FET Performance First 1.4 Seconds	8-17
9-1	Sketch of Modified Torque Motor Housing	9-2
9-2	Spring Force Versus Deflection	9-4
9-3	Flapper Deflection Versus Volts Input With Magnetic Field Strength Reduced by 1000 Gauss	9-5
10-1	Cold Gas Test-FET No. 2	10-2
10-2	Cold Gas Test-FET No. 2	10-3
10-3	Cold Gas Test-FET No. 2	10-4
10-4	Cold Gas Test-FET No. 2	10-5
10-5	Cold Gas Test-FET No. 2	10-6
10-6	Hot Gas Test-FET No. 2	10-9
10-7	Photograph of Post-Firing Unit No. 2	10-10
10-8	Pressure Versus Time Hot Gas Test No. 2	10-11
10-9	Torque Motor Voltage and $\Delta P_c$ vs. Time Hot Gas Test No. 2	10-12
10-10	Temperature vs. Time, Hot Gas Test No. 2	10-13
10-11	Partial Disassembly of FET After Hot Gas Test No. 2	10-16
10-12	Complete Disassembly of FET After Hot Gas Test No. 2	10-17

## LIST OF TABLES

<u>Table</u>		<u>Page</u>
3-1	Summary of FET Requirements	3-1
3-2	Specifications for ERC Hot Gas Generator	3-2
4-1	Fluidic Emergency Thruster Torque Motor Specifications	4-2
8-1	Summary of Design Goals and Measured Values Obtained with FET No. 1	8-6
10-1	Summary of the Performance of FET No. 2 and Goals Specified in ES-PT-1	10-7

## Section 1

### INTRODUCTION AND SUMMARY

This report summarizes the work accomplished under Task IV, which is a continuation of the contract NAS-2-5467.

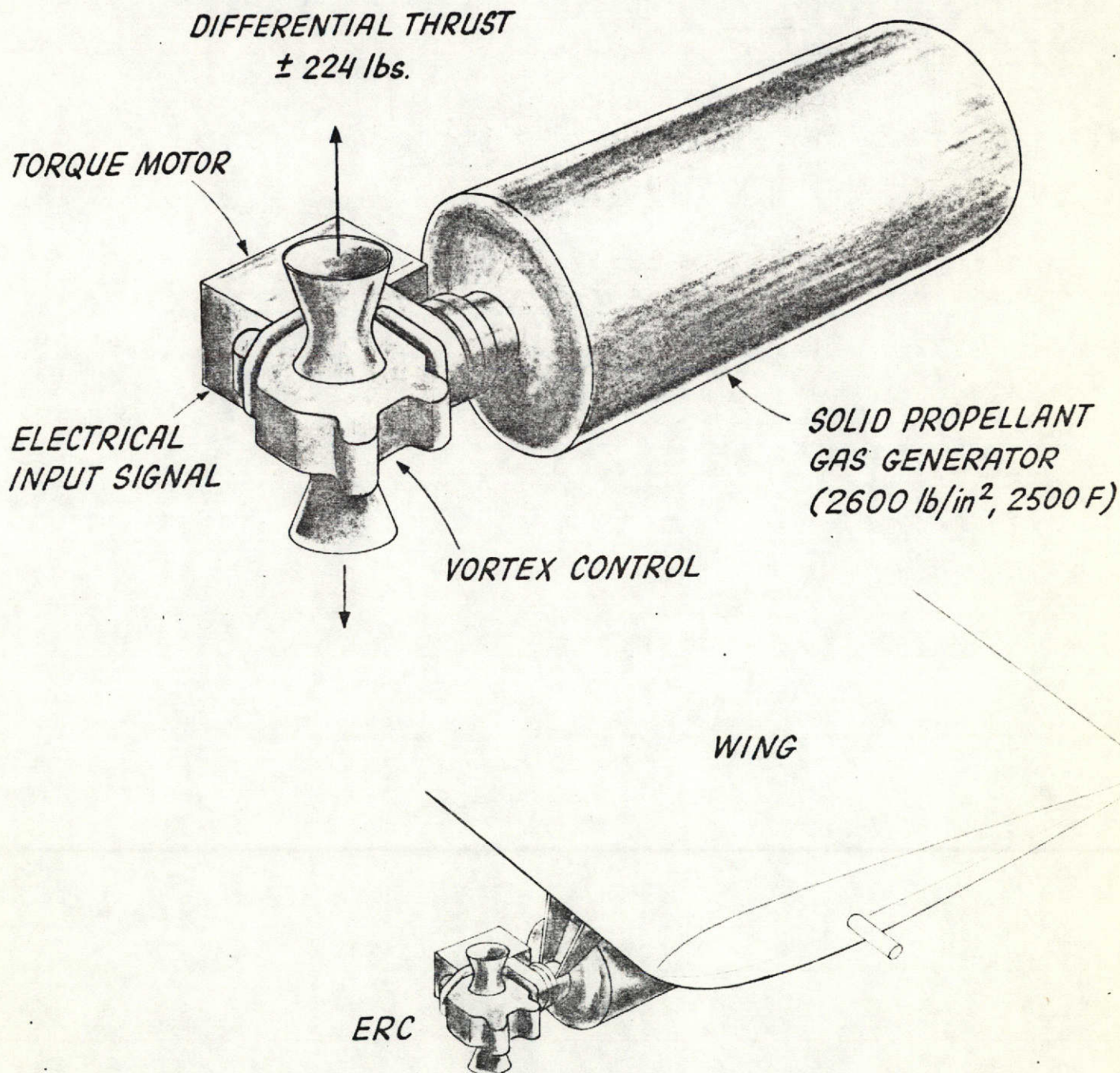
As a result of the design, development, and fabrication study accomplished on Task III of contract NAS-2-5467, the Fluidic Emergency Roll Control (ERC) System concept was proven feasible as a method of aircraft stabilization in the event of a primary flight control failure. The fluidic control units were designed to provide a roll torque proportional to an electrical command as operated by two diametrically opposed thrust nozzles located at the wing tips.

The fluidic emergency roll control system evaluated in this task is shown in a typical conceptual package installation in Figure 1-1. The control package consists of a solid propellant gas generator, two diametrically opposed vortex valve modulated thrust nozzles, and an electromagnetic torque motor. The gas generator is ignited on an emergency command signal from the flight control logic and the differential thrust output is modulated proportionately via an electrical signal to the torque motor from the flight control computer.

The specific objective of this portion of the program was to fabricate, assemble, and test three ERC systems and evaluate the systems while operating on hot gas. The program was accomplished in accordance with the following program plan:

- The Fluidic Emergency Thruster (FET) hardware designed and fabricated on Task III was modified with the objective of attaining the goals outlined in the design specification ES-PT-1.
- A design, fabrication, and test evaluation program was accomplished with Thiokol to build and test a solid propellant hot gas generator. The hot gas generator was designed to provide a preprogrammed pressure schedule vs. time for a total burn of 5 seconds duration.
- The modified FET was evaluated using high pressure cold gas as the operating medium to obtain static and dynamic performance characteristics.
- After satisfactory completion of the cold gas tests, the FET and the solid propellant gas generator were tested as a complete ERC system. The tests were performed at the Thiokol rocket test facility in Elkton, Maryland. The objective of

# EMERGENCY ROLL CONTROL FOR VTOL



## EMERGENCY ROLL CONTROL INSTALLATION X14 VTOL

Figure 1-1



the tests were to evaluate the dynamic performance of the ERC system while controlling a simulated aircraft. The dynamic performance was observed employing a closed loop simulation of the ERC, consisting of a breadboard of the electronic control, an analog simulation of the aircraft, and the actual hardware. Three hot gas tests were planned on the program, but due to technical difficulties and funding, only two tests were accomplished.

## Section 2

### CONCLUSIONS AND RECOMMENDATIONS

#### CONCLUSIONS

The basic objectives of the ERC Task IV development program were to:

1. Develop Hot Gas Generator for ERC.
2. Modify FET hardware to meet design goals.
3. Integrate Hot Gas Generator with FET and accomplish dynamic hot gas firing.

With the exception of objective no. 2, the major goals of the fabrication and test evaluation were accomplished.

The hot gas generator was successfully developed and tested by Thiokol. When mated to an equivalent orifice of 0.350 inches diameter the gas generator met all the performance specifications with respect to pressure profile, initial transient and burn time.

The method of machining the solid propellant grain as a means of pre-programming the three supply pressures vs. a time schedule has definitely been proven feasible. The shaped grain provides adequate timing accuracy for generating the different pressure levels required in the mechanization of the ERC.

Several modifications were performed on the FET in order to meet the design goals outlined in Task III of this contract. The major goals to be accomplished by the modifications were:

1. Eliminate the torque motor instability at high pressures.
2. Increase maximum thrust.

In order to achieve these design goals, the modifications were limited to reworking existing hardware within the confines of the program scope. Three basic modifications were performed which included:

1. Increasing the area of the thrust nozzle.
2. Increasing the supply pressure to the vortex valve.
3. Increasing the size of the first stage torque motor.

As a result of the testing accomplished on two FET units, it became evident that the maximum thrust could not be obtained with the present design. The major reason for not achieving the thrust design

goals is attributed to the limited size of the first stage. As a result of limited control from the existing first stage design, the increased vortex valve supply pressure was negated by a reduced vortex valve turndown.

The increased force output of the new torque motor did increase the proportional range of supply pressure from 600 psi to 1700 psi but was not adequate to encompass the full range of 2500 psi.

Although the FET did not meet the design specifications, the major goal of fabricating vortex valves for modulating the flow of hot gases was achieved. As will be cited in the recommendations, the maximum thrust and unstable output deficiencies can be corrected by a redesign of the FET first stage control.

The FET was successfully integrated with the hot gas generator for two hot gas firings. The first test revealed a deficiency in the structural design of the torque motor housing which was corrected for the second hot gas firing test. The final hot gas firing of the complete ERC demonstrated a successful dynamic control of the simulated vehicle and satisfactory functional performance of the hardware. The gas generator pressures were in excess of the desired values by 30%, which was due to the reduced effective orifice size of the FET. For an FET of the desired thrust output, the hot gas generator will provide the specified pressure output. Post firing examination of the ERC system revealed no seal failures, and subsequent testing of the FET torque motor after the hot gas tests validated that the first stage control was still functional with a reduced gain.

On the basis of the hot gas test firing results it can be concluded that the ERC control concept, employing non-moving part vortex valves for modulating thrust and a preprogrammed hot gas generator pressure output, is a feasible approach for controlling an STOL aircraft in an emergency situation.

#### RECOMMENDATIONS

As a result of the testing performed on Task IV, it has been determined that the major design problems of the ERC system exist in the FET. If the FET design goals are to be achieved, three definite areas of improvement can be identified which relate to a complete redesign of the FET first stage:

1. Increase the control flow of first stage.
2. Redesign the first stage to accommodate a dry torque motor.
3. Increase the size of the torque motor to eliminate the instability.

The increased control flow from the first stage will provide the capability of increasing the turndown of the vortex valves at the higher supply pressures, which will enable the existing vortex valve design to produce the desired maximum thrust. The test results indicate that with the present configuration, a maximum of 600 psi is now available for producing thrust at the nozzle. If a turndown of 4.5 can be obtained at 1000 psi, the existing vortex valves will be adequate for generating 200 lb. thrust.

It is considered essential that a dry torque motor be employed in any future design in order to stay within the weight limitation of the ERC system. The wet torque motor presently employed requires an additional 3.6 lb. of weight for the high pressure housing which increases the total weight of the FET from 4.5 to 9.1 lb. By employing a dry torque motor the housing required for the torque motor is eliminated, thus the target weight of 4.7 lb. can be met.

The instability of the vortex valve output and the excessive null offset is due to insufficient spring rate in the torque motor. In order to correct this problem it is necessary to increase the stiffness of the torque motor to a value which provides a positive spring rate and exceeds the pressure forces on the flapper. Test data indicates that the pressure forces are higher than the values based on the calculated data. The 20 lb. torque motor force output is adequate for the FET application, but the redesigned torque motor will require an increased spring rate of 2000 lb./in., which is two times the spring rate of the present torque motor. The increased spring rate will not allow the maximum travel of 0.020 inches at 0 pressure, but the torque motor will be capable of full travel at the minimum operating pressure of 800 psi due to the reduction in effective spring by the pressure forces.

### Section 3

#### ERC SYSTEM DESIGN SPECIFICATIONS

The Emergency Roll Control is composed of two basic components:

1. The Fluidic Emergency Thruster, (FET),
2. The Hot Gas Generator.

The FET was designed and fabricated by General Electric and the Hot Gas Generator by Thiokol.

The system design specification for the units fabricated were established on a previous study analysis and test under Task III conducted for NASA which is summarized in the Final Report for NAS-2-5467.

The system design specifications defined the requirements for the overall ERC system to be tested, including the FET and gas propellant provided by Thiokol.

The specifications were based on a thorough design study analysis and preliminary hot gas tests conducted with hydrazine by NASA with the hardware fabricated by General Electric on Task III.

#### FET

A summary of the FET requirements is presented in Table 3-1.

Table 3-1

Maximum Differential Thrust	224 lb.
Gas Temperature	2000F
Operating Time	5 sec.
Weight	4.6 lb.
Electrical Input	+10 volts @ 0.25 amps
Maximum Operating Pressure	2500 psi
Proof Pressure	4000 psi
Null Offset	+15% max.
Proportional Output	800 - 2500 psi
Gain @ 800 psia	10 lb./volt

In order to effectively evaluate the characteristics of the FET, an Engineering Performance Test Procedure was written which outlines the test procedure to follow in generating test data for substantiating the FET specifications. The Performance Test Procedure methods are detailed in the specification ES-PT-1, Appendix A.

The verification tests were conducted using compressed air as the operating gas. At the completion of the cold gas tests the FET was mated with the Hot Gas Generator and was operated using the gases provided from burning a solid propellant.

#### HOT GAS GENERATOR

The Hot Gas Generator was designed by Thiokol in accordance with the requirements established from Task III.

The primary objectives of the Hot Gas Generator design for this program were to meet the pressure schedule and total impulse requirements. The motor case was not optimized with respect to weight and volume but was designed to provide the required pressure profile at the minimum cost.

The Hot Gas Generator consisted of a solid propellant grain, an igniter, and a high pressure case. The specifications shown in Table 3-2 were provided to Thiokol for the design of the ERC Hot Gas Generator.

Table 3-2

1. Pressure Schedule:	2500 psi -	4 sec.
	1300 psi -	1.2 sec.
	800 psi -	3.4 sec.
2. Load Orifice:	0.35 inches dia.	
3. Initial Pressure Rise:	0.1 sec.	
4. Maximum Gas Temperature	2000F	
5. Total Burn Time:	5 sec.	

The tests verifying the ERC specifications were initially conducted by testing each component, the FET and Hot Gas Generator individually; the final tests were performed at Thiokol with the Hot Gas Generator and the FET as one unit.

## Section 4

### FET DESIGN MODIFICATIONS

Based on the results of Task III tests conducted at NASA/Ames, design modifications to upgrade the FET performance were made. In order to achieve the design thrust objective of 224 lbs. thrust at 2500 psig supply pressure, the calculated vortex valve supply orifice diameter was increased from 0.25 inch to 0.3125 inch. Correspondingly, the first stage flapper nozzle flow area and the vortex valve outlet were increased to maintain a vortex valve turndown ratio of 5.0. The flapper nozzle equivalent diameter of 0.180 inch and a null clearance of .018 inch was specified. The vortex valve outlet diameter was increased from 0.4 to 0.45 inch, i.e., the maximum possible by rework of the existing hardware.

Subsequent testing of the FET operating on cold gas, with various size throttling orifices for the vortex valve supply led to the selection of an orifice diameter of 0.280. This selection was made on the basis of obtaining the maximum thrust from the FET at 2500 psi.

The torque motor instability evidenced in the Task III tests and the increased flapper displacement required to increase thrust output, necessitated changes in the torque motor specifications. Instability of the torque motor flapper resulted from cancellation of the mechanical spring rate by the flapper nozzle force gradient at high operating pressures. Increasing the net spring constant to at least 1000 lb./in. from 400 lb./in. was calculated to provide stable proportional control up to 2400 psig supply pressure. The stroke requirement was increased from +0.015 inch to +0.020 inch. These changes in the torque motor were not readily achieved in the D. G. O'Brien model 124 torque motor used in Task III. An alternate torque motor was therefore procured from Servotronics, Inc. The torque motor specifications are shown in Table 4-1.

Since procurement of a dry coil torque motor meeting the FET requirements necessitated additional development effort, a wet coil design was selected to adhere to the scope of development effort planned. This approach, however, resulted in the redesign of the torque motor enclosure as shown in Drawing No. 55-519405, Figure 4-1, to withstand the maximum anticipated system supply pressure. The use of the wet coil torque motor was undertaken as an expediency for the accomplishment of the primary objective of demonstrating the FET operation with a hot gas generator in the planned time schedule. A flightworthy FET design requires a dry coil torque motor redesign effort.

Table 4-1

FLUIDIC EMERGENCY THRUSTER  
TORQUE MOTOR SPECIFICATIONS

Torque Motor - Servotronics, Model 20-4A-16

Stroke:	Torque motor will be capable of stroking plus or minus 0.02 inch while a six (6) pound or greater aiding load is applied.
Stiffness:	Flapper position will be less than 0.02 inch from mid-position when coil current is zero and aiding load is 18 pounds.
Force Output:	With rated coil current applied and six (6) pound aiding load, flapper will stroke 0.02 inch minimum.
Output Radius:	Torque motor output will be measured at 0.005 plus or minus 0.5 inches below mounting base.
Rated Coil Current:	250 milliamperes
Coil Resistance:	80 plus or minus 5 ohms/coil at 77 degrees Fahrenheit all performance testing to be done with parallel coil hook-up (40 ohms).
Dimensions:	2.2 x 2.39 x 2.10 high

Mechanical Features:

Flame baffle on flapper

High temperature (5 sec. at 2000 degrees Fahrenheit flame) resistant flapper

Withstand high pressure submergence

Wet coil construction

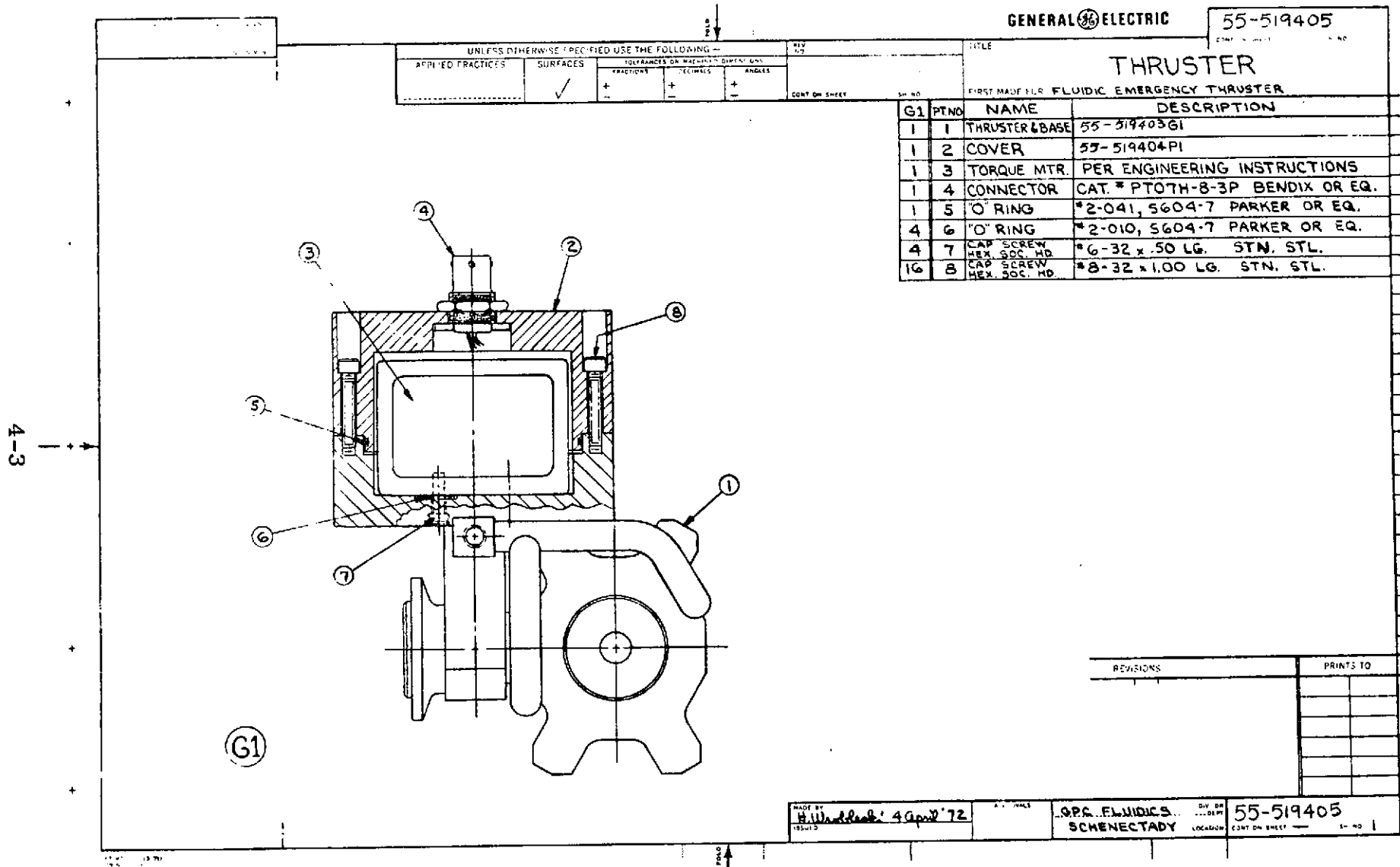
Size to fit within cover having ID 3.19 inch or larger

Teflon lead wire insulation

Mechanical stops to limit flapper overtravel

Weight, less than 1.75 lbs.





## Section 5

### HOT GAS GENERATOR DESIGN

The Hot Gas Generator design consisted of minor modifications of the existing Thiokol TE-T-509 heavy wall, high pressure control test motor. Its design is shown on Thiokol Drawing DE 24847 (Figure 5-1). The headcap of the standard TE-T-509 was modified to accept a special igniter, and the aft closure was reworked to accommodate the FET. For the preliminary orifice tests, the aft closure was designed with a graphite insert.

The propellant grain was machined from a cured cylinder of Thiokol propellant TP-Q-3074A. The grain ballistic characterization is shown in Figure 5-2. The grain was machined as shown in Thiokol Drawing DE 24791 (Figure 5-3) to provide the pressure vs. time schedule shown in Figure 5-4.

The motor chamber was designed to contain an inert spacer to reduce the free volume and serve as a positioner for the propellant grain. The spacer was made of TAD-320B, an epoxy polyamide adhesive material used in Poseidon gas generator inhibitors.

The igniter was designed to use a number of loosely packed TP-Q-3074A propellant cubes, which are ignited by two grams of BKNO<sub>3</sub> pellets. The propellant and pellets are separated by a perforated metal screen. The pellets are initiated by a Halex 1196A squib with the following electrical characteristics:

No fire current:	max. 0.5 amps
Min. fire current:	3.0 amps
Resistance:	0.25 $\pm$ .05 ohms
Voltage:	28 VDC

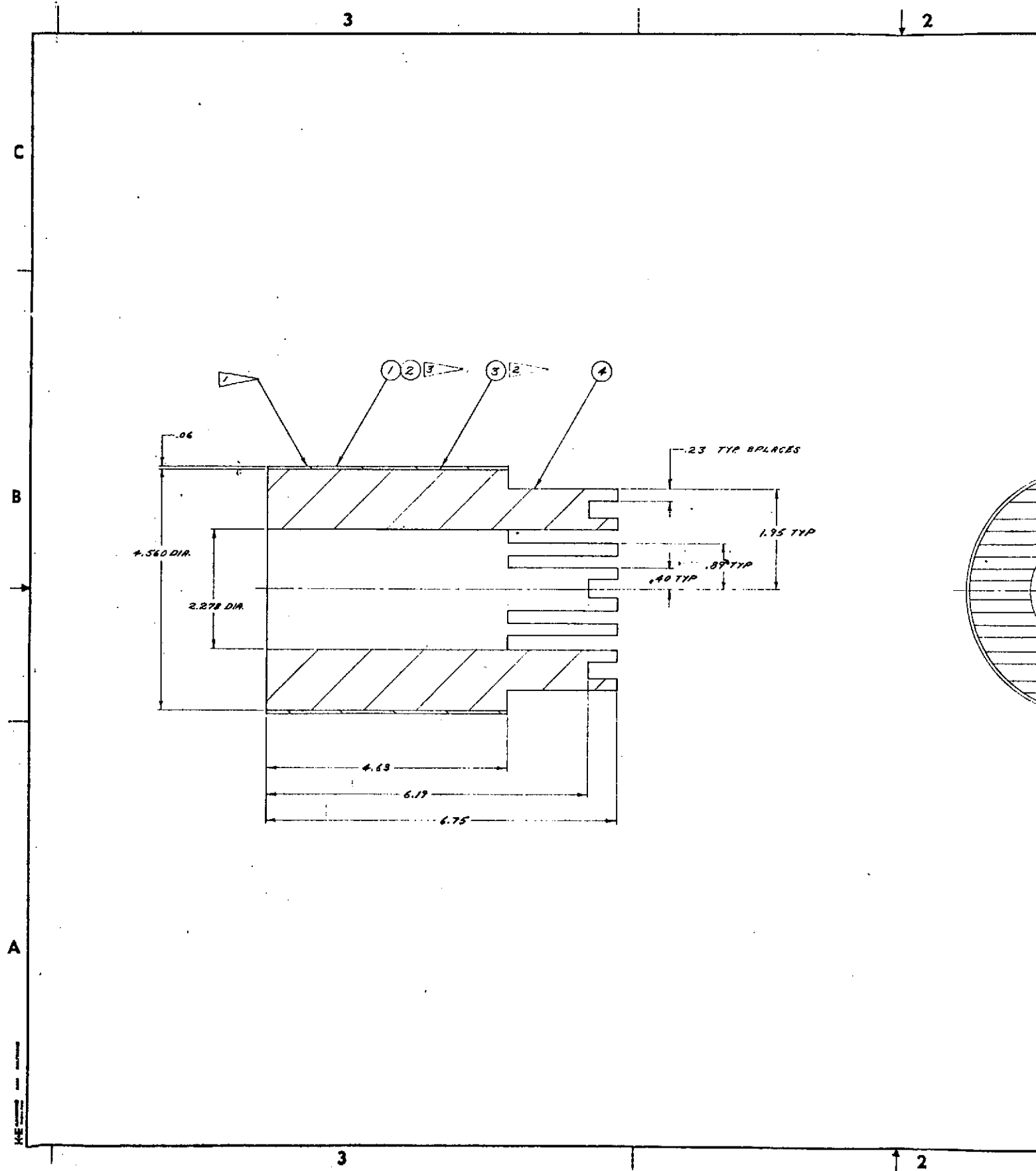
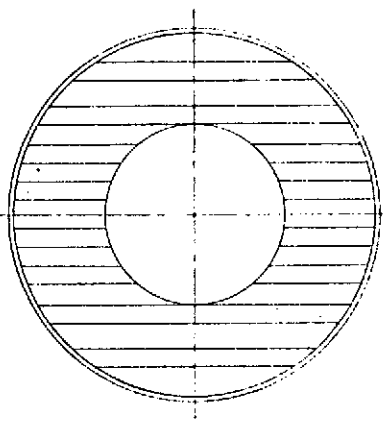


Figure 5-1

REVISIONS			
SYM	DESCRIPTION	DATE	APPROVED

- NOTES:
- 1. PART M. (PIN.....) TO BE MARKED PER T.C.C. SPEC. P10001-6.
  - 2. PRIME PROPELLANT (ITEM 4) SURFACE WITH ADHESIVE (ITEM 3).
  - 3. COAT WITH ADHESIVE (ITEM 2) BEFORE APPLYING NYLON STOCKINET (ITEM 1).



E24791

UNLESS OTHERWISE SPECIFIED: DIMENSIONS ARE IN INCHES TOLERANCES .XX = ±.030. .XXX = ±.010 ANGULAR ± 30° FRACTIONS ± 1/16 BREAK SHARP EDGES .003-.015 ALL SMALL FILLETS .020-.040 R THREADS PER FED. HANDBOOK AND SUPPLEMENTS DIMENSIONING PER MIL-STD-8 WELD SYMBOLS PER JAN-STD-19 SURFACE ROUGHNESS SYMBOLS PER MIL-STD-10 ALL FINISHED SURFACES			AR 4 AR 3 AR 2 AR 1 -01	ITEM NO. 4 3 2 1 1	CODE IDENT 	PART OR IDENTIFYING NO. TCC TA-D-3074 TCC TA-G-301 TCC TA-D-3208 NYLON STOCKINET 	NOMENCLATURE OR DESCRIPTION PROPELLANT ADHESIVE ADHESIVE 	MATERIAL 	SPECIFICATION T.C.C. NE1031 
LIST OF MATERIAL OR PARTS LIST									
DRAWN CHECKED ENGR ENGR USER STRESS SAFETY APPROV			BY DATE J.D. BISHOP 12/26/71 D.L. BISHOP 1/1/72 J.M. BISHOP 1/1/72 			Thiokol CHEMICAL CORPORATION ELKTON DIVISION ELKTON, MARYLAND			
DESIGN ACTIVITY APPROVAL 			CODE IDENT NO. 07299			SIZE D E24791			
SCALE 1/2			WEIGHT			CALC ACTUAL SHEET			

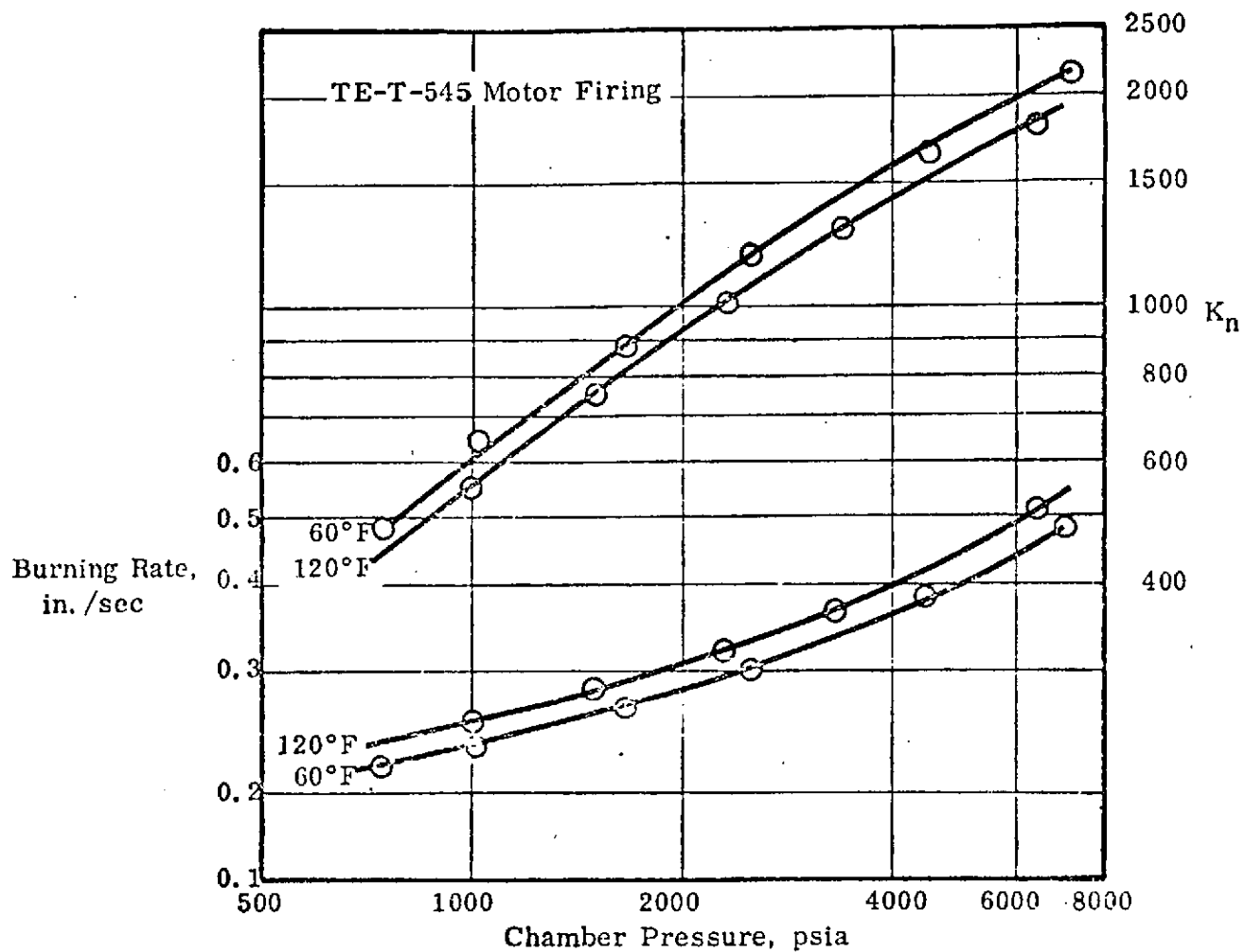


FIGURE 5-2 BALLISTIC CHARACTERIZATION OF TP-Q-3074A, RATE AND  $K_n$  VERSUS PRESSURE



EFFECTIVITY	REVISIONS			
	SYM	DESCRIPTION	DATE	APPROVED

## NOTES:

1. ASSEMBLY NO. (ASSY) TO BE MARKED PER T.C.C. SPEC. P10001-1.
2. APPLY LUBRICANT (ITEM 3) TO ENTIRE SURFACE OF O-RINGS PRIOR TO ASSEMBLY.

G.SODIA TYP REF

E24847

DASH NO.	MODEL NO.	REVISION	ITEM NO.	CODE IDENT	PART OR IDENTIFYING NO.	NOMENCLATURE OR DESCRIPTION	MATERIAL	SPECIFICATION	
			1	9	E24844-01	AFT CLOSURE ASSY			
			1	0	E24792-01	CASE, FILLED			
			1	7	E24791-01	PROPELLANT GR. INHIBITED			
			AR	6	T.C.C. TA-D-3208	ADHESIVE		T.C.C. ESP-37	
			2	5	83259	2-252	O-RING	BUNN N-506-7	
			1	4	E19647-01	CRA HEAD			
			AR	5		LUBRICANT		MIL-G-4343	
			1	2	83259	2-122	O-RING	BUNN N-506-7	
			1	1	E24795-01	IGNITER ASSEMBLY			
			-01	ITEM NO.	CODE IDENT	PART OR IDENTIFYING NO.	NOMENCLATURE OR DESCRIPTION	MATERIAL	SPECIFICATION

USED ON			UNLESS OTHERWISE SPECIFIED: DIMENSIONS ARE IN INCHES		DRAWN		CHECKED		ENGR		ENGR		ENGR		USER		STRESS		SAFETY		APPROV	
DASH NO.	MODEL NO.	REVISION	XX ± .030	XX ± .010	XX ± .030	XX ± .010	XX ± .030	XX ± .010	XX ± .030	XX ± .010	XX ± .030	XX ± .010	XX ± .030	XX ± .010	XX ± .030	XX ± .010	XX ± .030	XX ± .010	XX ± .030	XX ± .010	XX ± .030	XX ± .010
-01	T.E.T. 618-1	FINAL																				

LIST OF MATERIAL OR PARTS LIST		THICKOL. CHEMICAL CORPORATION ELKTON DIVISION ELKTON, MARYLAND	
MOTOR ASSEMBLY			

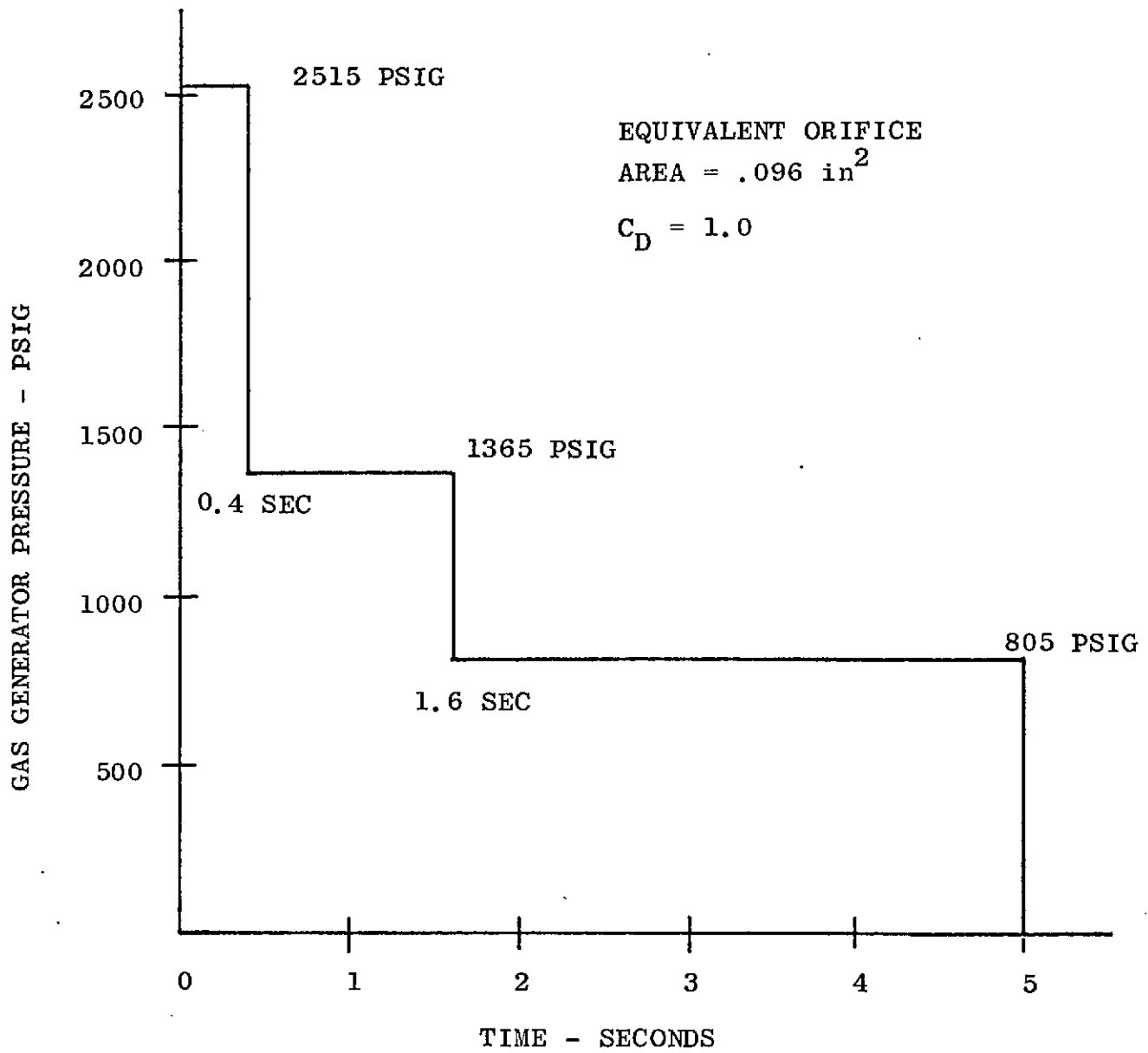
DESIGN ACTIVITY APPROVAL	CODE IDENT NO.	SIZE
J. L. G. 7/13/71	07299	D E24847

SCALE	WEIGHT	CALC	ACTUAL	SHEET

# GAS GENERATOR PRESSURE SCHEDULE

Figure 5-4





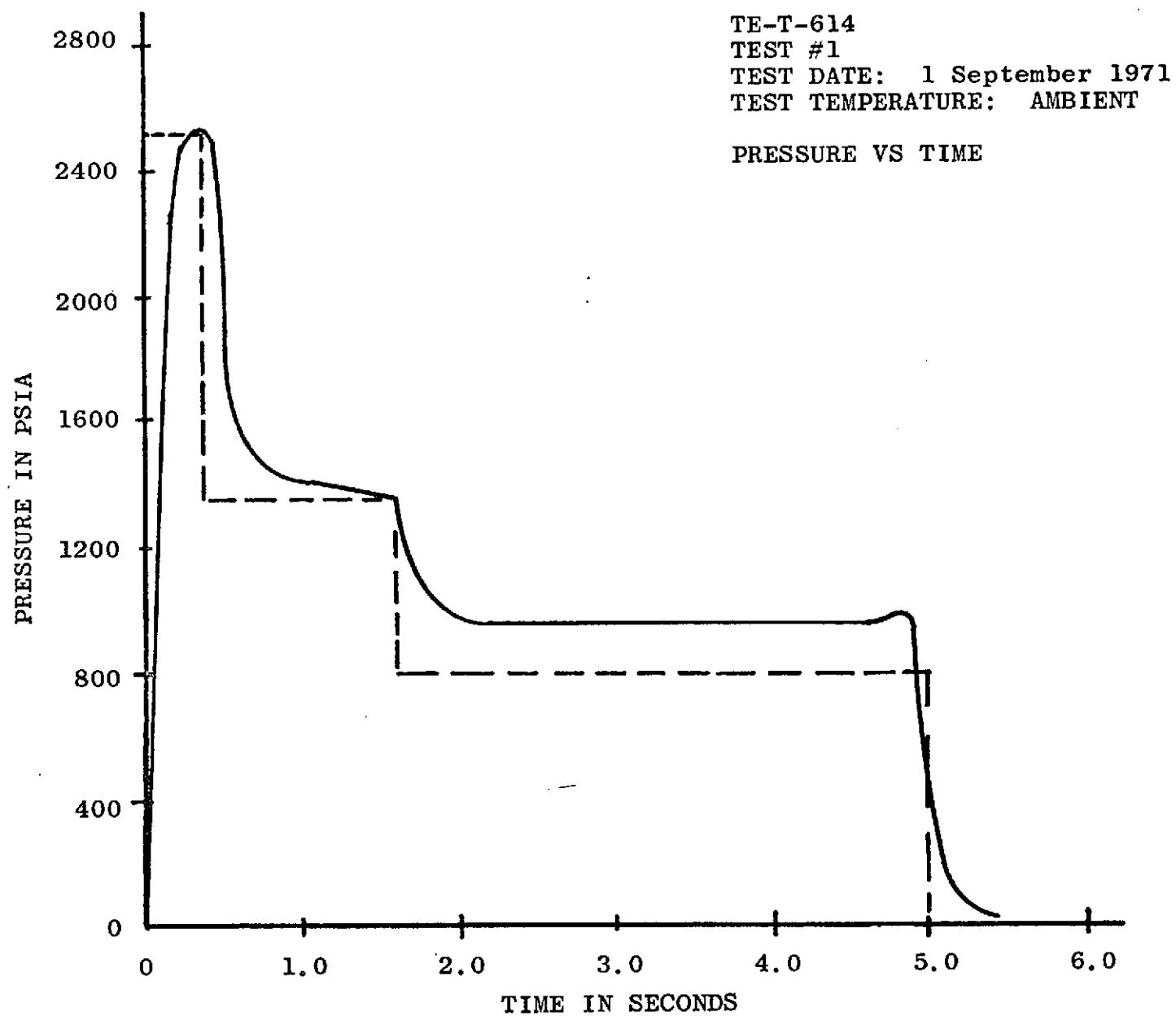
## Section 6

### SOLID PROPELLANT GAS GENERATOR TEST

Two ballistic test firings of the Hot Gas Generator with an equivalent orifice of 0.350 inch diameter were conducted to establish conformance to the pressure vs. time schedule specified in the design. The results of initial firing are shown in Figures 6-1 and 6-2. Figure 6-1 shows that the actual pressure schedule developed deviates slightly from the design goal. The grain shape was modified for the second test to achieve closer approximation of the design schedule. The results of the second firing is shown in Figure 6-3.

Figure 6-2 shows that the pressure rise delay after ignition was approximately 0.2 seconds during the first test firing. Since a 0.2 second rise time was considered to be detrimental to system performance, the igniter pyrogen charge was increased to provide a faster pressure buildup of less than 0.1 second. The second controlled ballistic firing of the hot gas propellant was conducted with the modification in the igniter design. The second test result shown in Figure 6-4 shows that the pressure rise time was reduced to approximately 0.050 second. The desired rise time and pressure schedule were thus achieved on the second firing. Subsequent hot gas test firings were conducted with the FET in place of the equivalent orifice and with the grain shape and pyrogen charge established in the second ballistic firing. The results of these tests are discussed in a later section under ERC system hot gas tests.

Figure 6-1 HOT GAS GENERATOR TEST #1



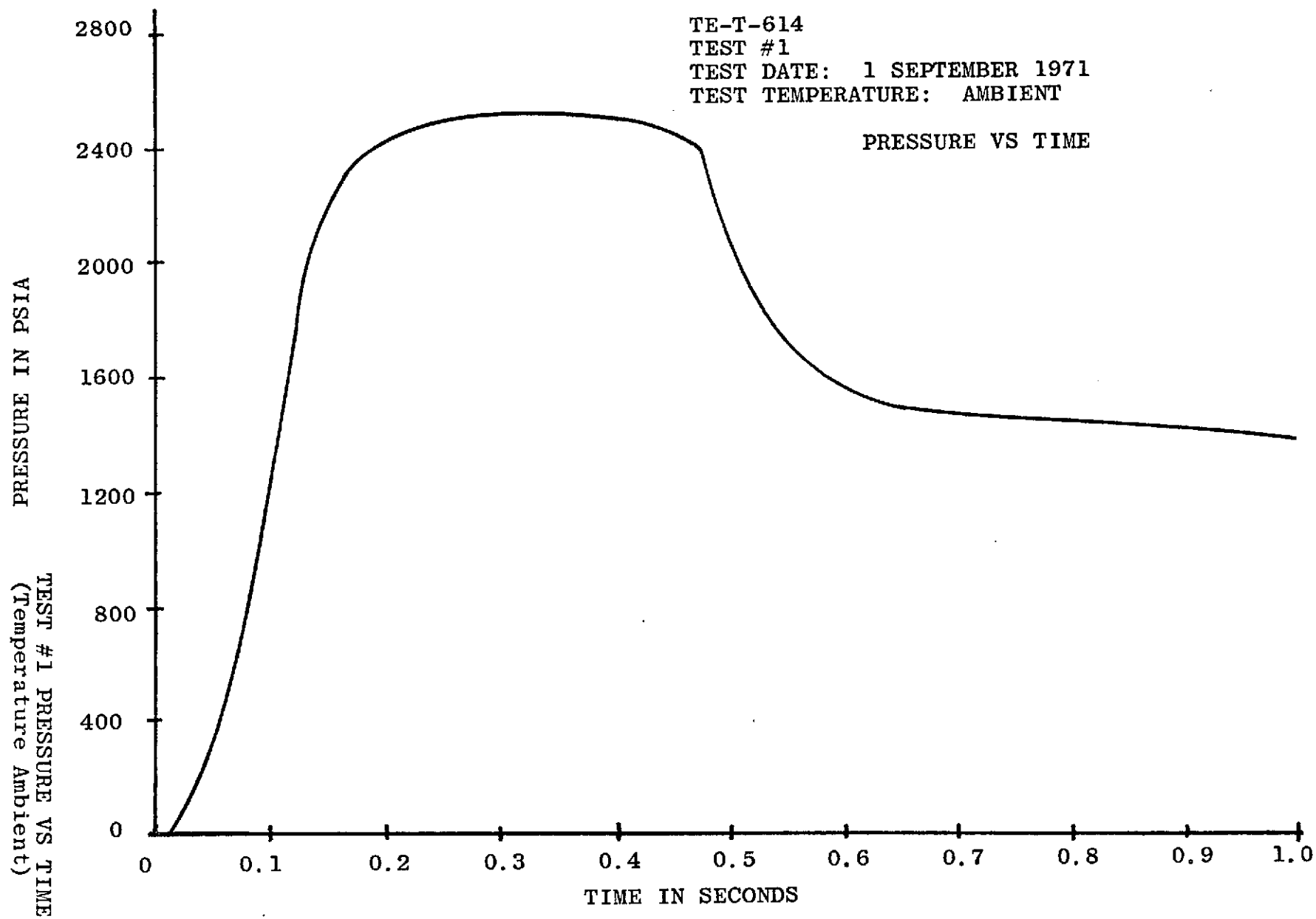


Figure 6-2

TE-T-614  
TEST #2  
TEST DATE: 1 OCTOBER 1971  
TEST TEMPERATURE: +60°F

PRESSURE VS TIME

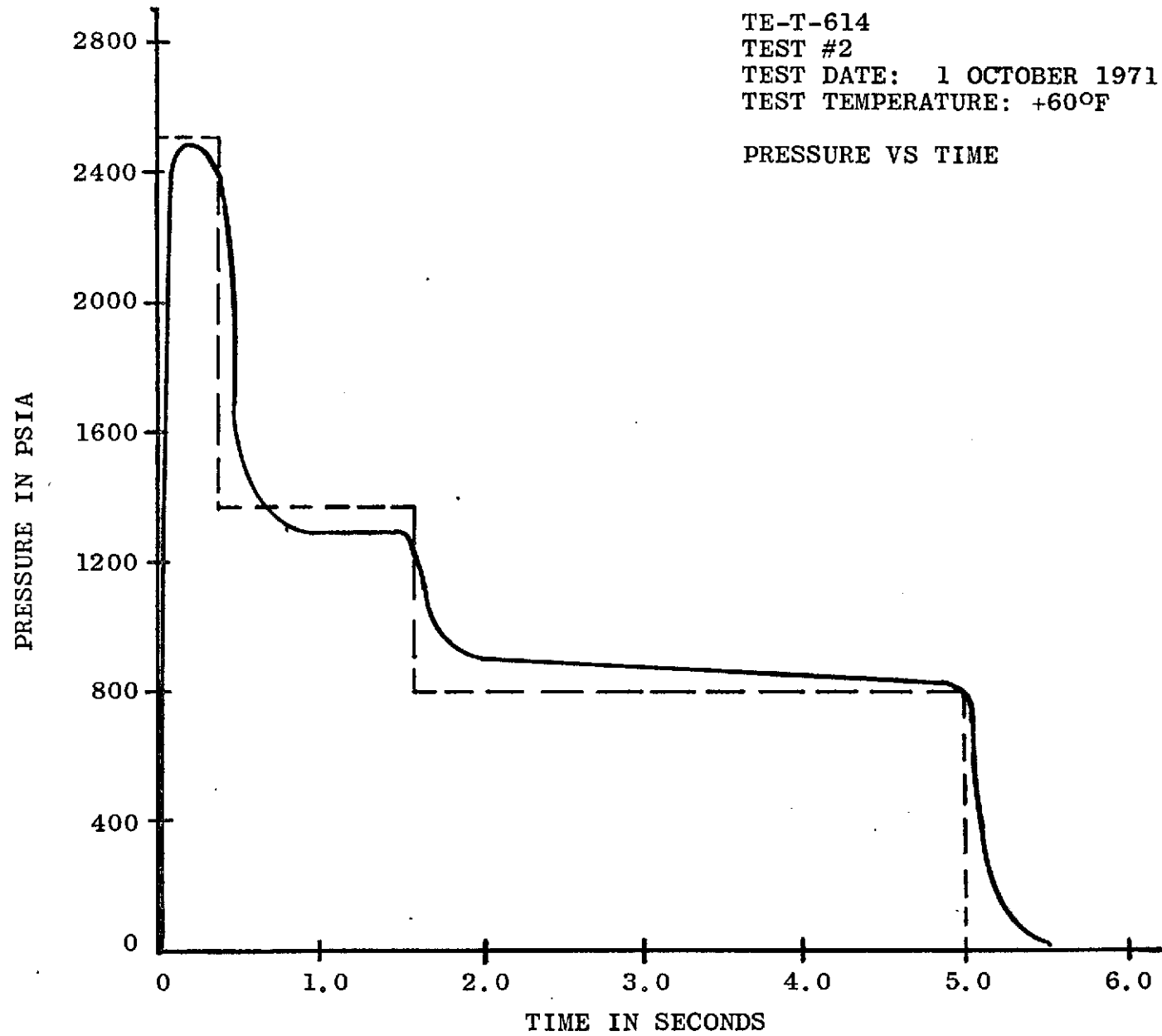


Figure 6-3  
TEST #2 PRESSURE VS TIME  
(Temperature +60°F)

9-9

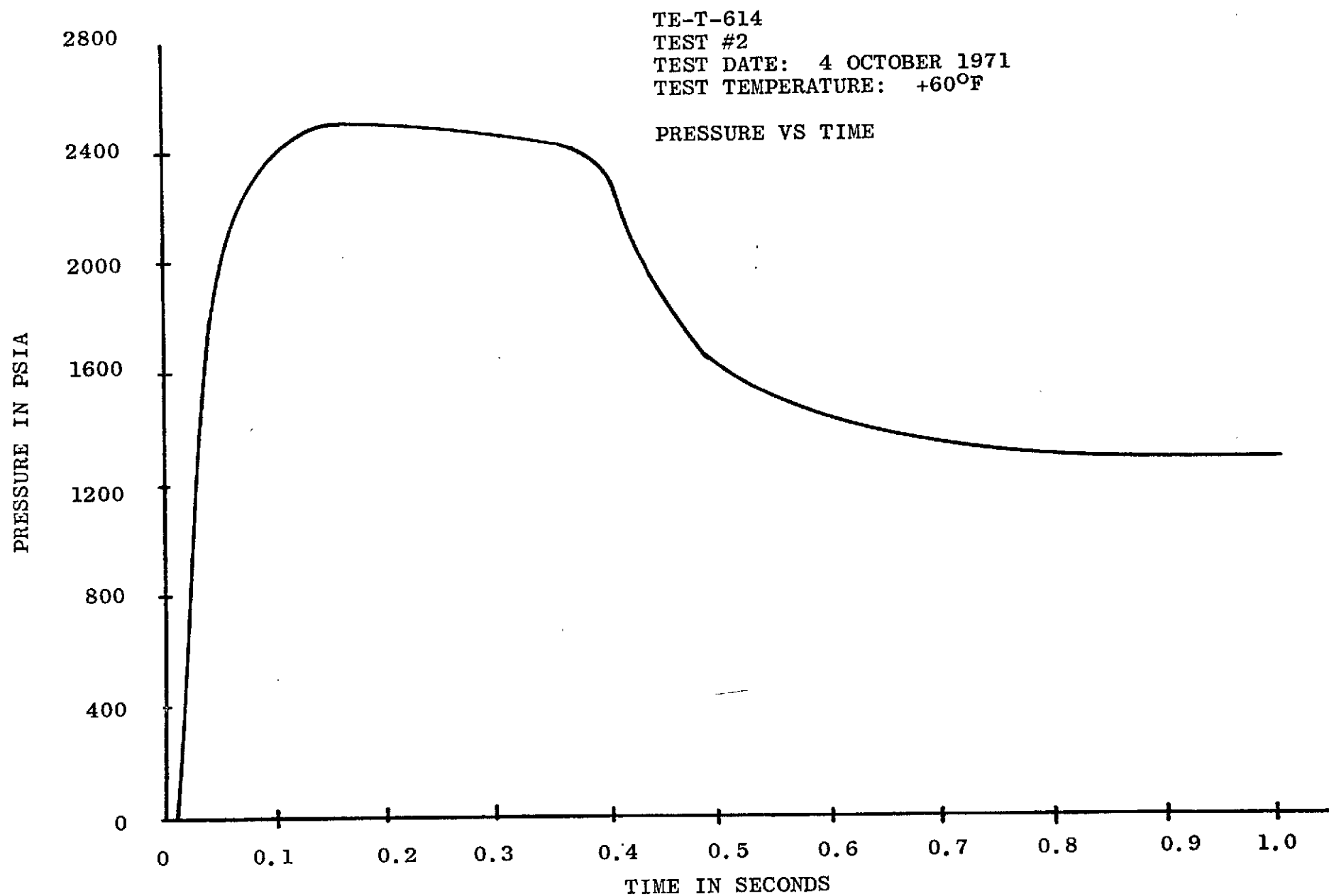


Figure 6-4

TEST #2 PRESSURE VS TIME  
(Temperature +60F)

## Section 7

### TEST PLAN DEFINITION AND TEST HARDWARE

In order to provide an effective demonstration of the ERC performance, a test plan was defined to furnish data on the static as well as the dynamic ERC characteristics. The tests were divided into three categories:

1. Static Cold Gas Tests
2. Dynamic Cold Gas Tests
3. Dynamic Hot Gas Tests

The static cold gas tests were conducted to provide data with respect to static gain, hysteresis, and change in performance parameters under different operating conditions. The dynamic cold gas tests were performed using an analog simulation of the aircraft and an attitude control simulator in conjunction with the FET hardware. These tests were conducted operating the FET as a closed loop system at various operating pressures in order to ascertain the response characteristics of the ERC control.

The dynamic hot gas tests were carried out at Thiokol with the hot gas generator furnishing power to the FET. The hot gas tests were performed in a manner similar to the cold gas dynamic tests in that the ERC was evaluated closed loop, using an electronic breadboard of the control logic and an aircraft simulation.

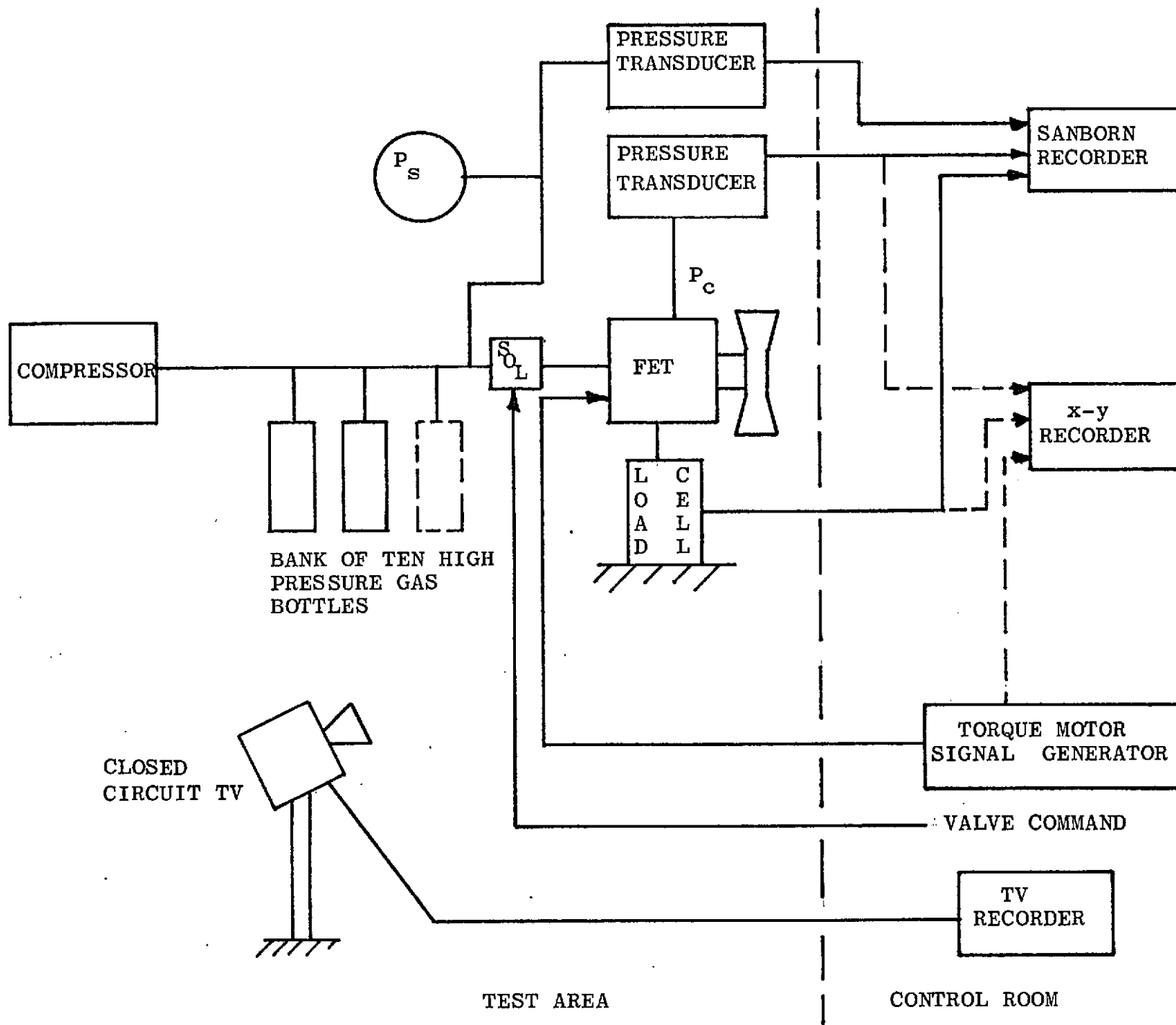
#### STATIC COLD GAS TESTS

The cold gas tests were set up to provide the data outlined in the Engineering Performance Test Procedure, Appendix A.

The FET was mounted to a 250 pound load cell which furnished an electrical indication of the thrust output. A schematic of the cold test hardware is presented in Figure 7-1.

The cold gas high pressure supply was provided by a compressor which charged 10, 1.5 cu.ft. bottles to a pressure of 2500 psig. A high pressure solenoid was employed to activate the air supply to the FET when a test was to be performed. The FET, compressor, gas storage, and a closed circuit TV monitor were all located in remote hazardous test bay areas.

The FET was instrumented, in addition to the load cell, with two pressure transducers to measure supply pressure and the differential control pressure to the vortex valves. Each of the electrical instrumentation outputs was recorded on a Sanborn Recorder or, as necessary, on an X-Y recorder.



SCHEMATIC OF COLD TESTS

Figure 7-1

The TV monitor was utilized to record all tests and provide a permanent record of the performance as well as any failure which might occur.

The storage capacity of the gas bottles provided a blowdown test time of 40 seconds for a pressure range of 2500 to 800 psi. A time of 1.5 hrs./1000 psi was required to charge the system. The mechanization of the test setup did not permit any constant pressure test runs to be conducted.

The static cold gas tests performed included:

1. Low pressure static gain curves.
2. Hysteresis.
3. Null shift with pressure.
4. Saturation.
5. Maximum thrust.
6. Stability performance.

Each of these tests is defined in detail in ES-PT-1, Appendix A.

#### DYNAMIC COLD GAS TESTS

The dynamic cold gas tests were performed by employing a dynamic simulation of the aircraft and a breadboard of the electronic logic (attitude control simulator) furnished by NASA. (Figure 7-2 is a schematic of the ERC closed loop simulation). The FET was instrumented to provide an electrical signal proportional to the control pressure applied to the FET vortex valve. This signal was used as the electrical output proportional to FET thrust and with suitable gain was employed as the input to the analog computer. The analog computer was mechanized to furnish a simple second order inertial model of aircraft with no damping, Figure 7-3. The aircraft was simulated as two integrators in series with suitable switches for initial conditions and computer hold functions. Three inputs to the analog computer were required, one from the FET ( $\Delta P$ ) or simulated FET, an electrical input from the electrical joy stick which was used to control the aircraft during the manual control mode, and an automatic torque disturbance. Transistor switching circuits in the attitude control simulator provided the logic necessary for switching the manual joy stick signal and the disturbance torque out of the loop when the automatic mode assumed control. Two outputs from the analog computer; aircraft rate ( $\dot{\theta}$ ) and attitude ( $\theta$ ) were used as inputs to the attitude control simulator.

The attitude control simulator was originally used by NASA to simulate the FET and control logic in a control analysis study performed on Task III. Several modifications to the attitude



control simulator had to be implemented in order to make it compatible with the dynamic cold gas and hot gas tests. When received from NASA the electronics were on two separate breadboards on a loose mounting structure. These breadboards were modified and mounted in a Plexiglas case, Figure 7-4, to permit a more efficient handling of the electronics and provide a convenient interface between the analog computer and the FET. A schematic of the electronics appears in Figures 7-5 and 7-6. Board #2 sums the two inputs  $\theta$  and  $\dot{\theta}$  from the analog computer and compares the sum with a set reference. When the sum of the two signals exceeds the set reference, the FET is automatically fired if the fire switch is in the automatic mode. Board #1 provides a simulation of the FET which generates a maximum thrust vs. time profile and voltage output proportional to the sum of the  $\theta$  and  $\dot{\theta}$  signal. The modifications to the electronics included adding a switch which would eliminate the saturation of the attitude control output signal and a relay which was actuated by the fire command. The switch for adding or deleting the saturation characteristic enabled the electronics to be used either as a simulated FET or as the control signal to the actual FET when performing the dynamic closed loop tests. The relay was employed to fire the squibb on the Hot Gas Generator for the hot gas tests.

In order to close the loop with the actual FET hardware it was necessary to adjust the gain of the torque motor amplifier and FET ( $\Delta P$ ) transducer such that the desired gain was achieved when coupled to the analog computer. A block diagram of the gains selected is presented in Figure 7-7. The gains selected were determined based on the FET static gain measurements. As per Figure 7-7, two gains were selected to provide the desired gain distribution. The gain of the FET changes with supply pressure and the gain selected corresponds to the supply pressure (1300 psi) where the closed loop system will be controlling the vehicle proportionally.

The torque motor amplifier, the FET, and the pressure transducer plus amplifier were installed in the overall control loop as shown in Figure 7-2.

The cold gas tests were run at various pressures during the blowdown of the gas storage system. For each test, during the blowdown, the system was displaced  $25^\circ$  in angle with a small positive rate. The angle was permitted to exceed the fire limits at a slow rate which automatically activated the ERC and enabled the response of the system to be observed. The gain of the system was not varied to compensate for pressure variation. The performance of the system was evaluated over the entire pressure range of 2500 psi to 800 psi.



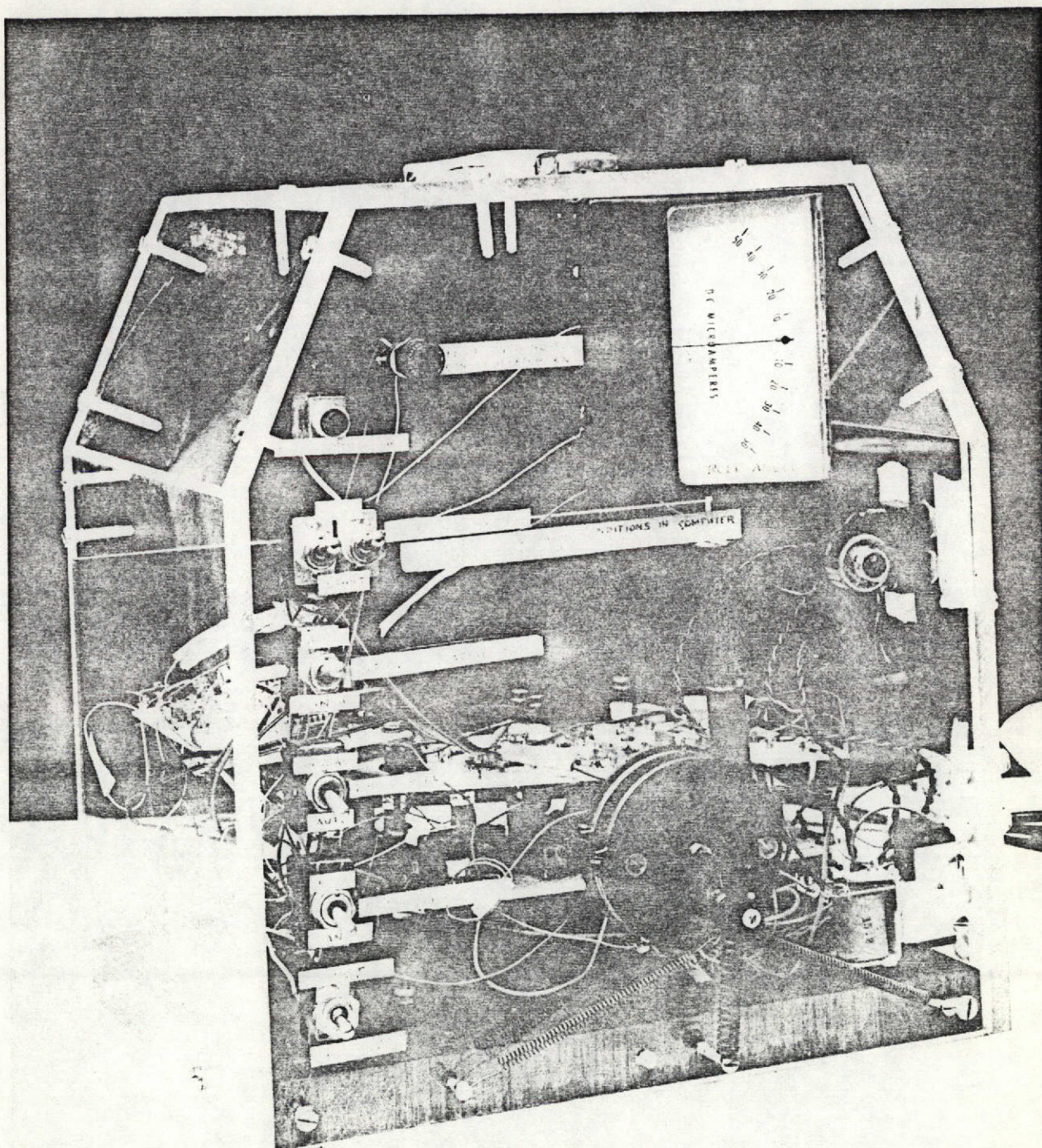
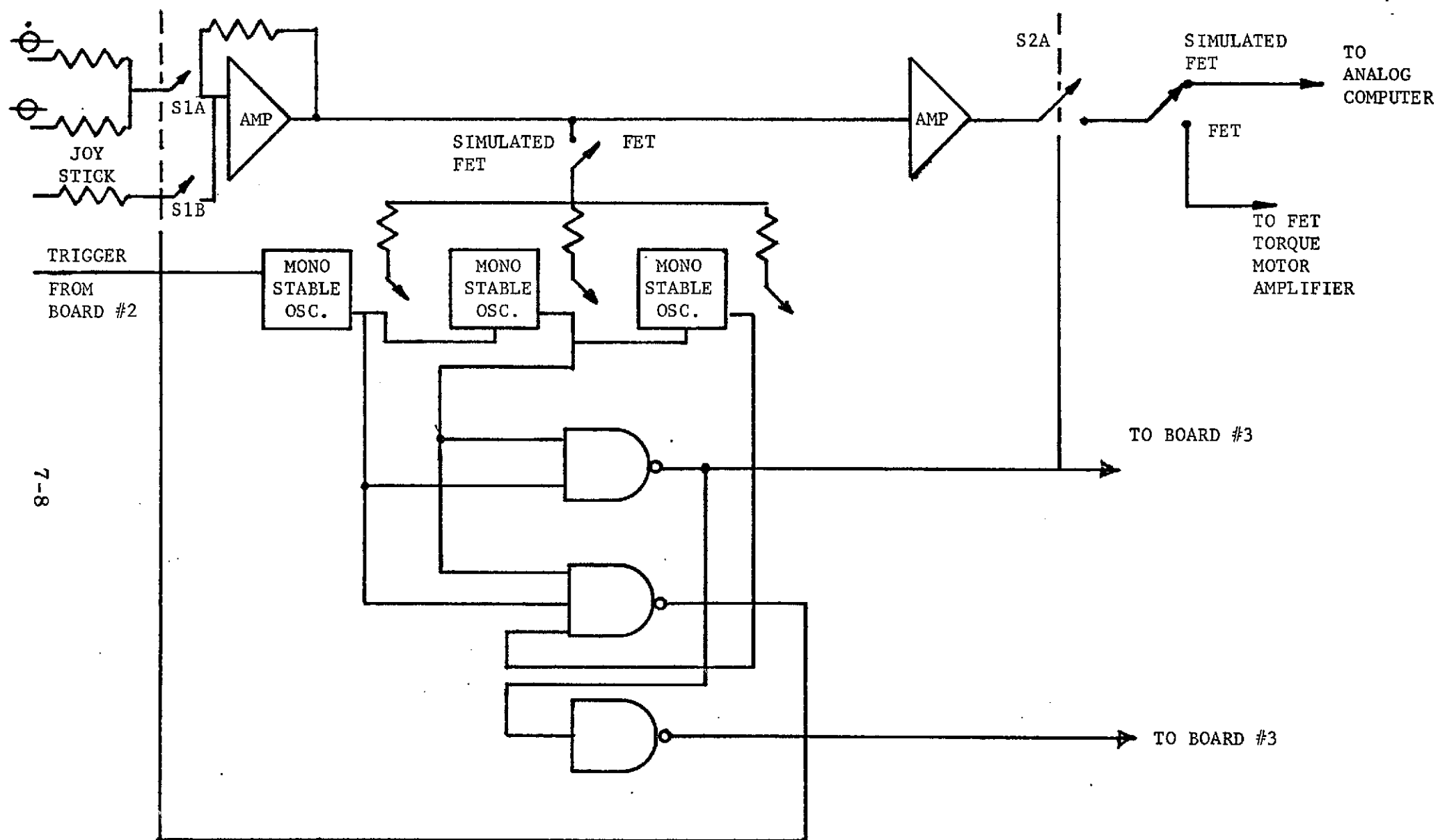
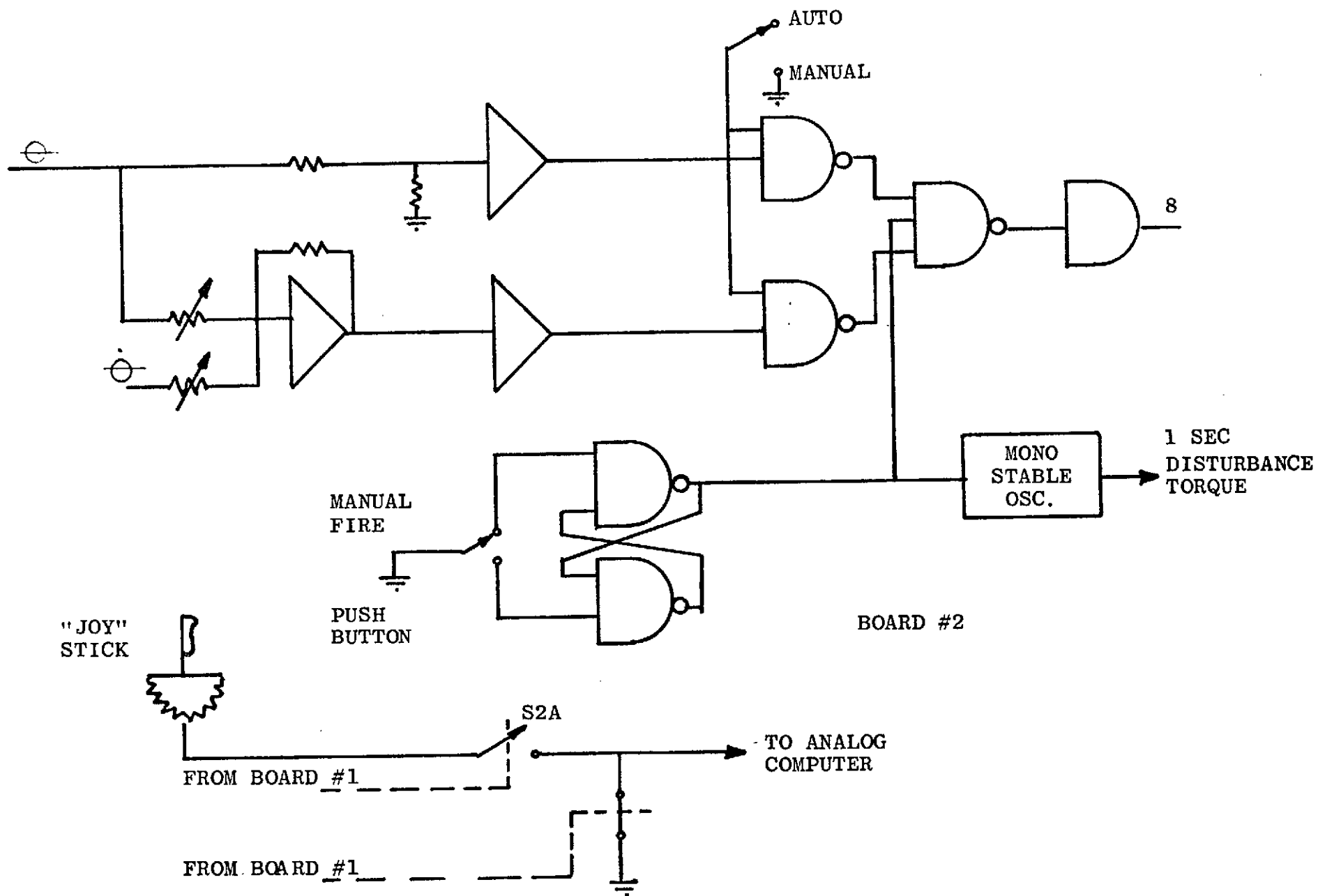


Figure 7-4 Attitude Control Simulator Breadboard



ELECTRONIC LOGIC BOARD #1

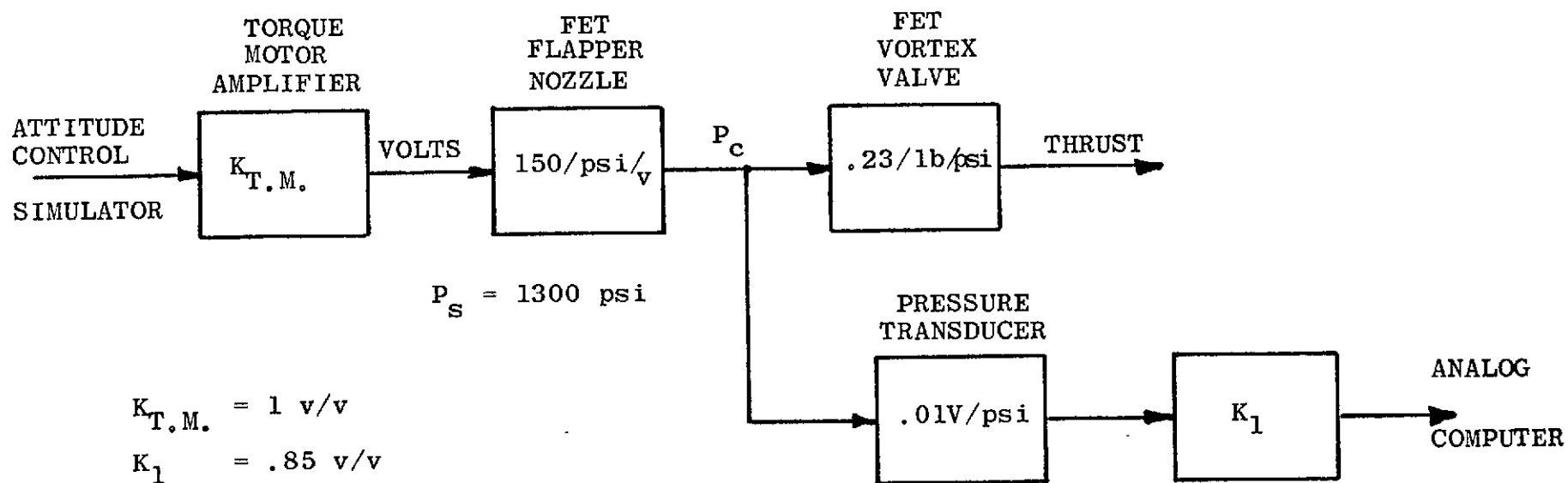
Figure 7-5



ELECTRONIC LOGIC

Figure 7-6





## FET AIRCRAFT SYSTEM SIMULATION

## GAIN DISTRIBUTION

Figure 7-7

## DYNAMIC HOT GAS TESTS

The hot gas tests were conducted using a standard model of a Thiokol hot gas generator, the FET, and the attitude control simulator plus the aircraft simulation to operate the ERC system in a closed loop manner. The purpose of the tests was to ascertain the overall dynamic performance of the ERC system and the compatibility of the hot gas generator with the FET.

The main objectives of the test were to demonstrate the

1. Functional closed loop performance of the thruster.
2. Temperature rise in critical areas.
3. Generator ballistic performance when coupled to the FET.

A test plan was completed by Thiokol and General Electric outlining the tests to be performed and the instrumentation required. The test plan is included in Appendix B of this report. The initial test plan called for Thiokol to perform high flow cold gas tests which is outlined in the hot gas test procedure. These tests were later revised to be run with a single bottle of N<sub>2</sub> operating with a 1/8 inch orifice. The purpose of the low flow cold gas tests was to confirm signal polarity and instrumentation outputs. The hot gas tests were performed to furnish the data outlined in ES-PT-2, Appendix B.

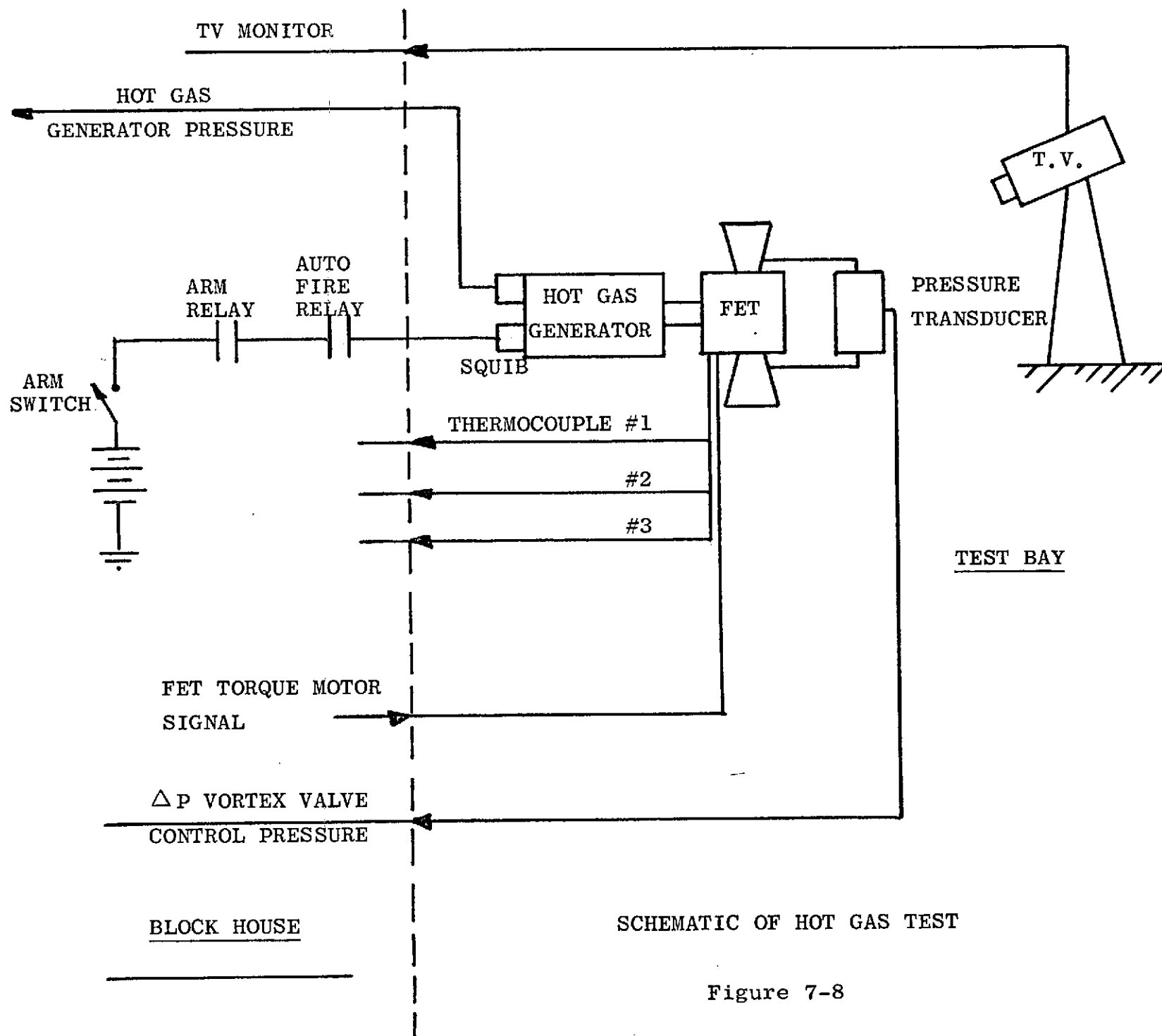
A schematic of the test setup is shown in Figure 7-8. The FET was electronically controlled in the same manner as described in the cold gas tests, only in this case, the pressure time profile would be in accordance with the automatic firing mode as provided by the hot gas generator. In the test bay area the FET was instrumented with three thermocouples which monitored critical temperature areas on the unit. These included:

1. The vortex valve case
2. The torque motor enclosure
3. The gas inlet

The hot gas generator was also instrumented with a pressure transducer to monitor the supply pressure to the FET. The remaining interfaces between the Block House and the test bay area included:

1. The torque motor command signal
2. The firing circuit
3. The TV monitor

Each of the electrical interface signals was recorded on an oscillograph during the simulated cold gas run and the hot gas firing. A recording was also made of the TV monitor output. In



SCHEMATIC OF HOT GAS TEST

Figure 7-8

addition to the electrical signals just cited, the  $\theta$  and  $\dot{\theta}$  signals from the analog simulation were recorded on the oscillograph and the X-Y recorder.

In both hot gas tests a dry run was conducted using the nitrogen bottle as the supply. With the satisfactory completion of the dry run, the hot gas generator was activated and the ERC system was automatically fired by the attitude control simulator. An immediate post firing inspection of the unit was conducted to ascertain whether any structural failures had occurred.



## Section 8

### COLD AND HOT GAS TEST RESULTS-UNIT #1

#### STATIC COLD GAS TESTS

The first unit with the design modifications cited in Section 4 was evaluated in accordance with ES-PT-1, paragraph 3.3. Since the tests were conducted with a varying supply pressure the data obtained on each run exhibits the effects of changing supply pressure and has to be accounted for in interpreting the results. Earlier tests with unit #1 indicated that a torque motor stability problem existed at pressures in excess of 1300 psi. In order to minimize the latching problem, magnetic shorting bars were added to the torque motor in an effort to increase the overall spring rate and thus increase the pressure at which instability occurs. The reduction in magnetic field has the disadvantage of degrading the gain of the torque motor; therefore, the amount of demagnetization is limited. The addition of the magnetic shorting bars increased the FET latching pressure to 1750 psi. Further reduction of the magnetic field strength was not deemed advisable due to the loss of gain which would result at the lower pressures.

The test results indicate that the original assumptions used in establishing the torque motor force requirements are invalid. In the force calculation, it was assumed that the approximate force on the flapper was the product of the differential control pressure ( $\Delta P_c$ ) to the vortex valve and the nozzle projected area ( $A_n$ ). For  $\Delta P_c = 750$  psi (at  $P_s = 2500$  psig) and  $A_n = 0.023$  in<sup>2</sup>, the force required is 17.3 pounds and the net spring rate of the torque motor must be at least 865 lbs/in. The torque motor was designed accordingly to provide 18 to 20 pounds mid-position force and a net spring rate of 1000 lbs/in. Further analysis of the flapper force leads to the conclusion that the pressure acting on the open side of the flapper as it approaches full stroke is greater than the actual control pressure measured. This is explained by the fact that the flapper nozzle curtain and the nozzle projected areas become equal at full flapper stroke. Consequently, a series orifice pressure drop is established. Thus, the actual pressure acting on the flapper area is intermediate of the supply and control pressures. The differential pressure across the flapper at  $P_s = 2500$  psig calculated on the basis of the revised assumption is approximately 1250 psi. The torque motor should, therefore, have a mid-position force capability of 20 pounds and a net spring rate of at least 1500 lbs/in. Electromagnetic torque motors of the desired performance are feasible but not available as a standard commercially available component. It is apparent that thrusters of the current size and larger will require a new torque motor development or the incorporation of an additional stage of fluidic amplification.

Since proportional control is desired from the ERC at pressures less than 1350 psi, the performance of the FET #1 was deemed acceptable for the hot gas tests. Even though the FET exhibited a latching characteristic at pressures in excess of 1350 psi, a torque motor input of less than 10 volts was of sufficient magnitude to command the thrust in the desired direction during the initial acquisition of the vehicle in the simulated closed loop runs.

A null shift characteristic for unit #1 is presented in Figure 8-1. Although the FET does not meet the requirements of ES-PT-1, paragraph 3.3.1-Null Offset, and 3.3.2-Stability, over the entire pressure range, it does maintain the required null during the proportional range of automatic control from 1350 down to 800 psi. The maximum thrust is 150 lb. which allows a total deviation of  $\pm 23$  lb. for the null variation. As indicated on the null vs. supply pressure curve, the null is within the limits for supply pressures below 1400 psi and exhibits proportional output characteristics for supply pressure less than 1300 psia.

The maximum thrust generated by the FET is less than the goal of 220 lb. The data presented in Figure 8-1 shows a maximum value of 150 lb. It was found during subsequent recalibrations of the load cell that the 150 lb. was in error and that the true thrust was 110 lbs. The main reason for the reduced thrust is due to the reduced turndown of the FET vortex valve. The program scope did not permit any further improvement in vortex turndown but several methods of achieving increased thrust are cited in the report under Recommendations.

Figure 8-2 is a static gain curve of the FET run at 1000 psi to 850 psi. The X-Y recording of thrust vs. input voltage verifies that output saturation is achieved at a voltage less than 10 volts. As was mentioned previously, the thrust calibration on these curves is in error and should be reduced by 25%. The true static gain in the linear range of operation is approximately 10 lb/volt which meets the requirement cited in paragraph 3.3.4.

The hysteresis characteristics are shown in Figure 8-3 for a supply pressure of 700 psi. Since the pressure is continuously decreasing, a shift in gain characteristic is apparent at the beginning and end of the run. The shift in gain characteristic is due to the null offset and changing gain with supply pressure. If the variation in null offset is factored out, the apparent hysteresis is negligible and is less than 3%.

All of the static test requirements were met by the FET #1 with the exception of null offset, stability and maximum thrust.

8-3

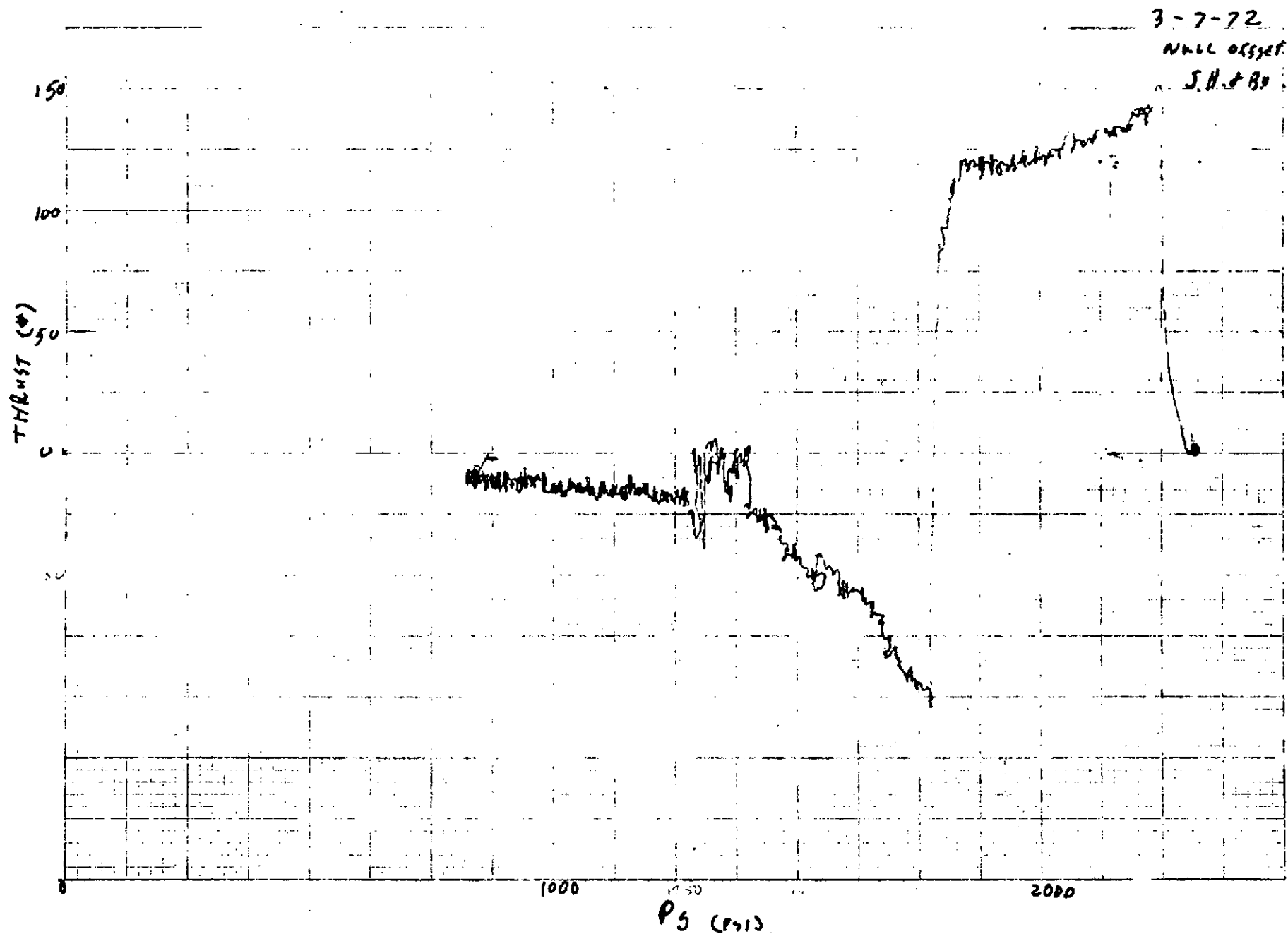


FIGURE 8-1 FET NULL OFFSET VS SUPPLY PRESSURE

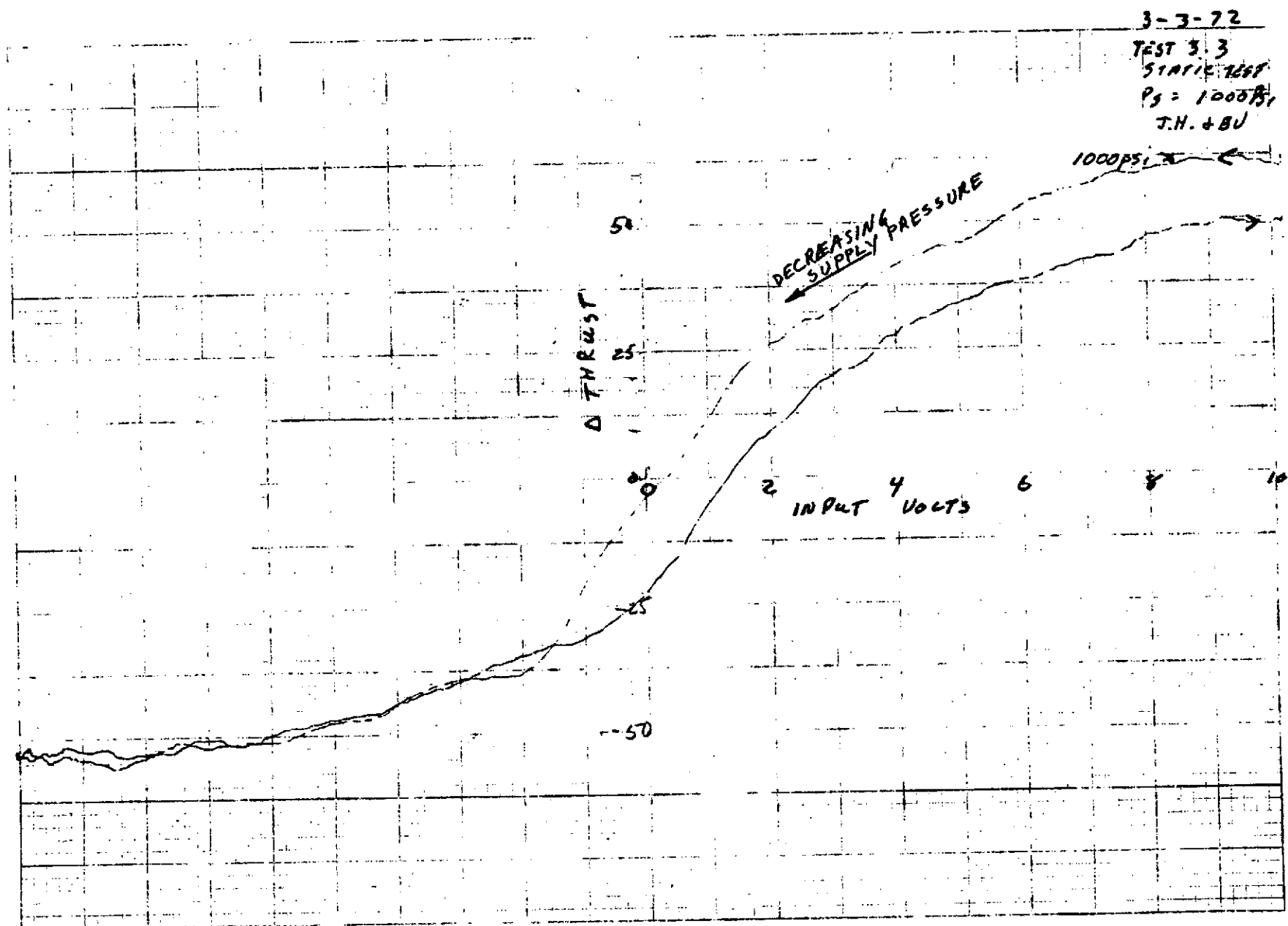


FIGURE 8-2 FET SATURATION CHARACTERISTIC

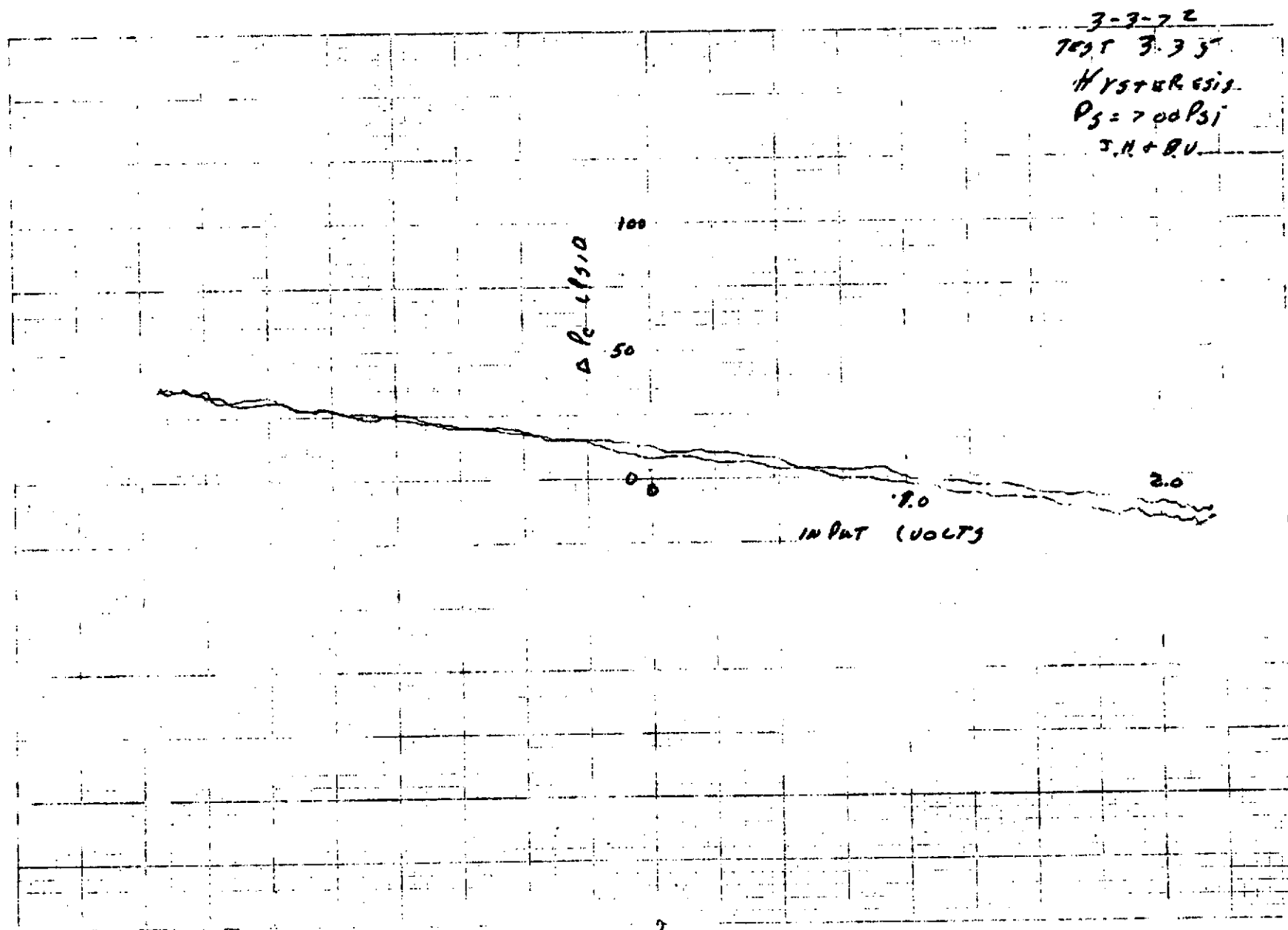


FIGURE 8-3 FET HYSTERESIS CHARACTERISTIC

Table 8-1 is a summary of the design goals and the measured values obtained with FET #1.

<u>Table 8-1</u>		
	<u>Goal</u>	<u>Actual</u>
Maximum Thrust	224	110
Hysteresis	3%	< 3%
Saturation Command	< 10 volts	< 10 volts
Gain @ 800 psia	10 lb/volt	10 lb/volt
Null Offset over entire pressure range	+15% max. saturated output	+15% max. sat. for pressures less than 1350
Stability	Proportional output for all pressures	Proportional for pressures less than 1700

#### DYNAMIC COLD GAS TESTS

Dynamic closed loop tests were conducted with unit #1 to determine the optimum loop gains and evaluate the dynamic performance. In order to retain the same stability characteristics as the simulated FET it is necessary to duplicate the gain of the simulation in terms of pounds thrust/volt between attitude control simulator and the analog computer. In the case of the simulation, a voltage of 3 volts at the analog computer input is equivalent to 100 lb. thrust. Calculations were made based on the FET static gain measurements and a gain distribution was selected to yield the desired overall system gain.

The tests were conducted by operating the system closed loop at various supply pressures and allowing the system to acquire from an initial angle of 25° and manually firing to demonstrate system response. The cold gas test setup did not permit a change in the supply pressure profile with time; therefore, each run was representative of the closed loop operation for a range of supply pressures. At the higher pressures, the system exhibited an unstable, or oscillatory characteristic which was to be expected since the system gain is too high, Figure 8-4. As shown in phase plane plot, Figure 8-5, the system demonstrated a response with no overshoot at 1300 psi, which is the anticipated proportional control range for

#43

2/13/72

P<sub>1</sub> = 2000-1800

8

66.6°/SEC

33.3°/SEC

+ 10° 20° 30° ⊖

8-7

FIGURE 8-4 COLD GAS TEST DATA FET-SIMULATED AIRCRAFT STABILIZATION CHARACTERISTIC

the emergency roll control. Satisfactory control was maintained by manual inputs for pressures in the 1000 psi range as demonstrated in Figure 8-6.

In Figure 8-4, there is a deadband due to hysteresis, but at the operating pressure level of 1300 psi, the hysteresis has virtually disappeared. Therefore, the hysteresis will not degrade the performance of the system when operating with the desired pressure profile.

Figure 8-7 is a photo of the test setup employed during the dynamic cold and hot gas runs. Data was recorded on a Sanborn and an X-Y recorder. As was mentioned in the cold gas test plan, the joy stick and electronics were mounted inside a Plexiglas carrying case to facilitate transporting and test setup. The aircraft simulation was mechanized on a 10 amplifier Donner Computer. All the instrumentation shown was employed on the hot gas runs with the exception of the Sanborn recorder.

#### HOT GAS TESTS

The initial setup and hot gas test of the first FET took a period of approximately one week. Delays were incurred due to other programs which were being conducted by Thiokol.

Dry runs were conducted employing a nitrogen bottle supply gas connected directly to the solid propellant case. Supply pressures of only 100 psi were generated due to the 1/8 diameter restricting orifice on the Nitrogen bottle. Although the supply pressures were low, the pressure output was of sufficient amplitude to check the operation of the FET prior to firing. Figure 8-8 is a photo of the FET and the hot gas generator plus instrumentation before firing. The hot gas generator was strapped to a fixed base with a chain clamp. The FET was connected to the generator by means of a Marman Clamp and sealed with Viton "O" rings.

During the dry runs the oscillograph data revealed that the attitude control simulator and Donner computer aircraft simulation performed as expected. The electronic firing circuit exhibited a 0.1 second delay which was attributed to the firing relay installed as a means of closing the firing circuit on the attitude control simulator. Although the delay results in a timing error between the attitude control simulator and the hot gas generator pressure profile, the percentage error is relatively small with respect to the total on time, therefore, it was decided to fire with the relay delay in the circuit. The 0.1 second delay does not degrade the performance of the system but does allow the angle and angular rate levels to reach a higher level before control is initiated.



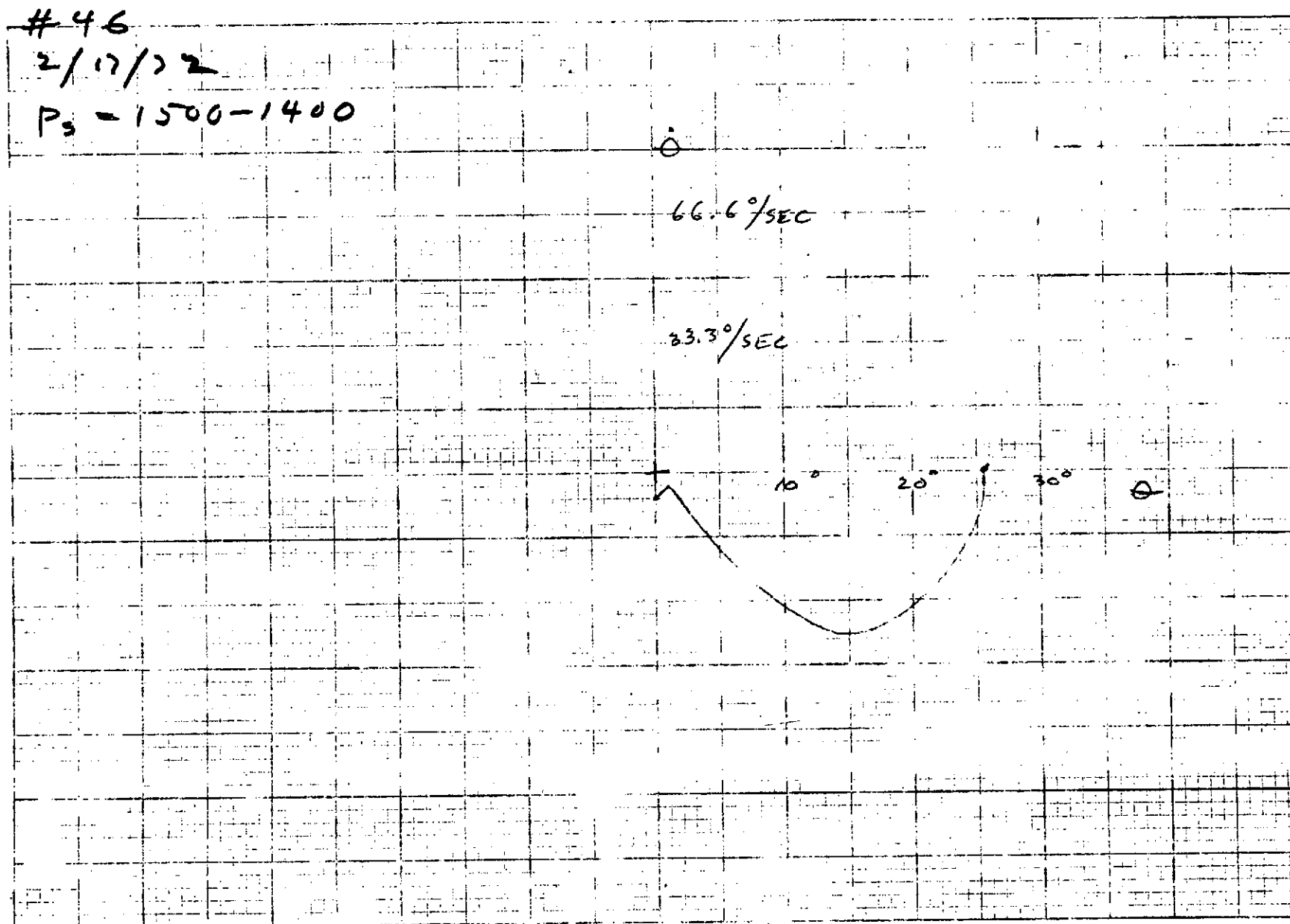


FIGURE 8-5 COLD GAS TEST DATA FET-SIMULATED AIRCRAFT STABILIZATION CHARACTERISTIC

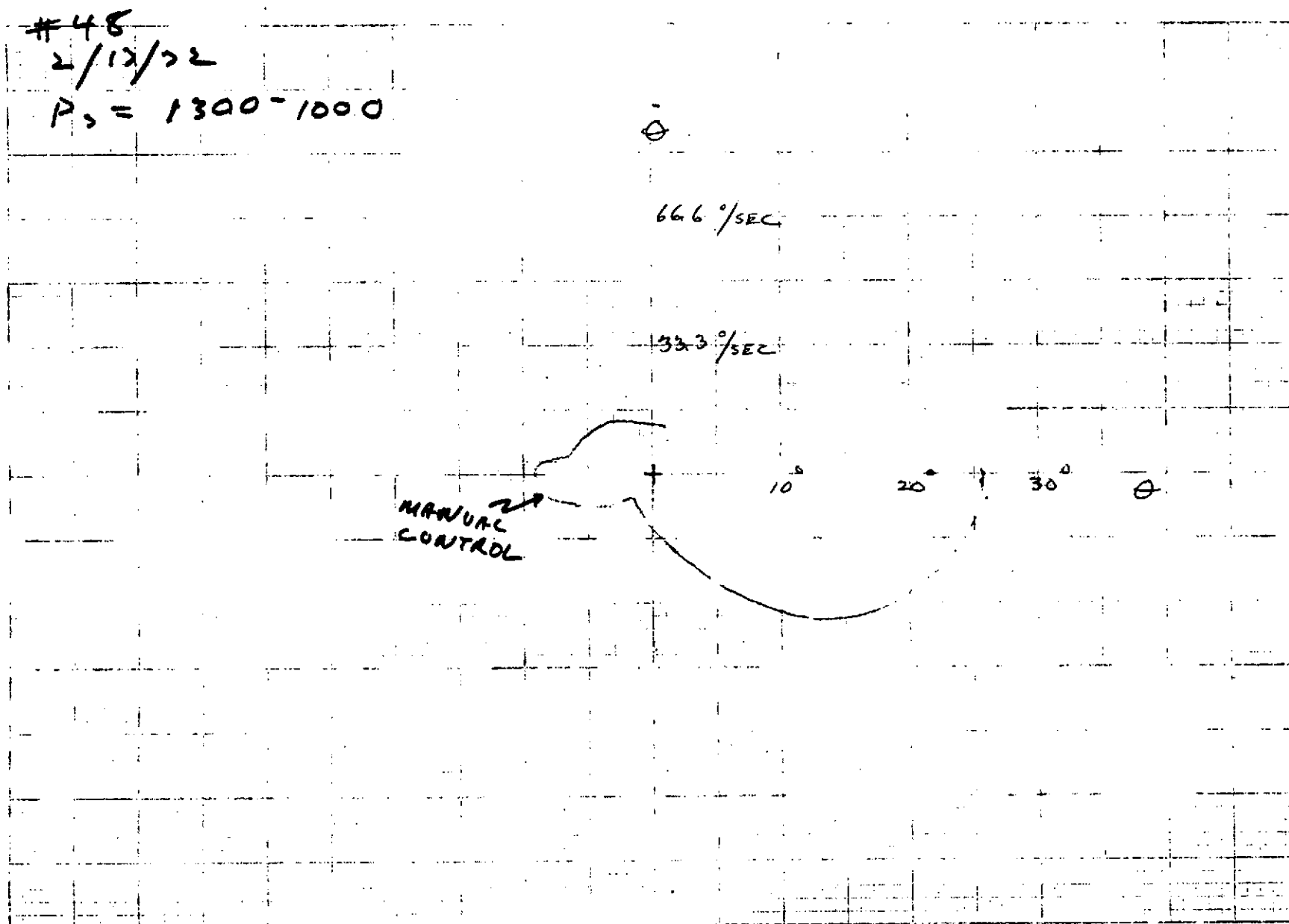


FIGURE 8-6 COLD GAS TEST DATA FET-SIMULATED AIRCRAFT STABILIZATION CHARACTERISTIC

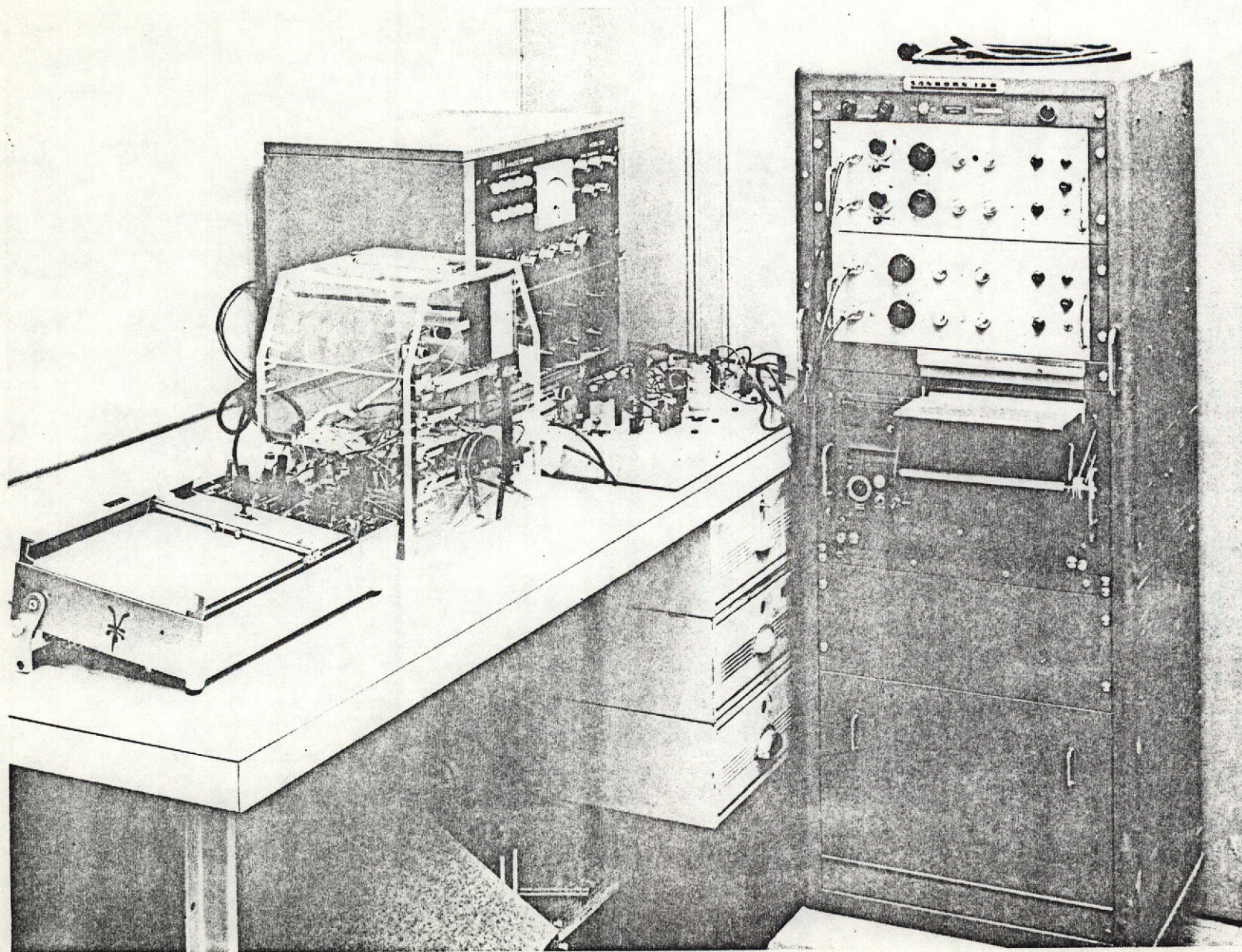


Figure 8-7 Photo of Test Setup



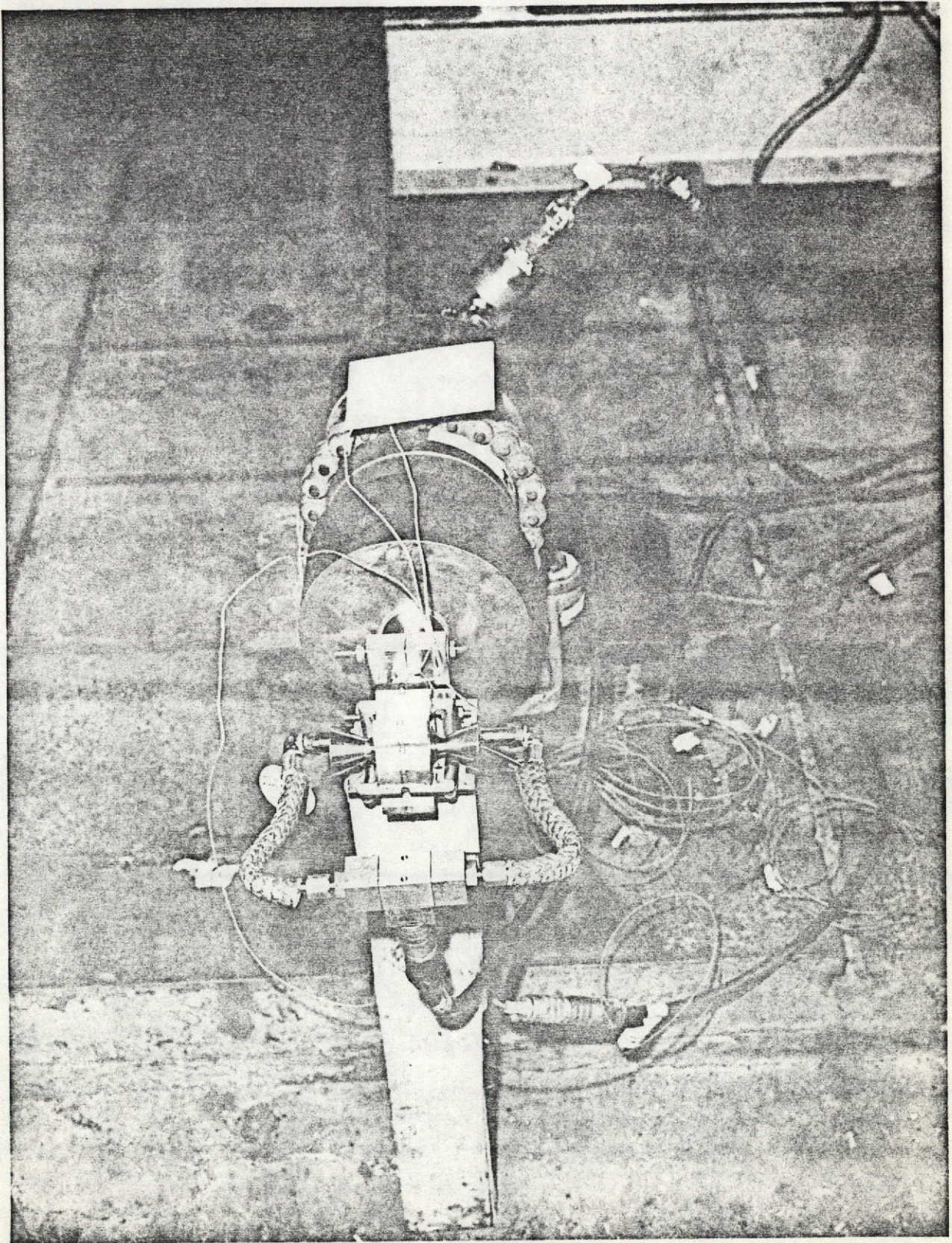


Figure 8-8 Test Setup Prior to Firing



The FET #1 was successfully fired using the automatic initiation of the firing circuit at the selected level of  $\theta$  plus  $\dot{\theta}$  as shown in the phase plane plot, Figure 8-9. The ERC performed satisfactorily during the first second of operation. The angle error was brought to zero in the minimum possible time, with no overshoot or oscillation. After the angle was reduced to zero, manual control of the ERC was initiated, but control of the simulated aircraft could not be maintained. The post firing inspection of the ERC revealed that the torque motor housing had developed a leak which resulted in a failure of the torque motor after one second of operation, Figures 8-10 and 8-11.

Inspection of the oscillograph data substantiated the fact that the ERC unit performed successfully during the first 1.4 second, and that control was lost due to overtemperature of the torque motor, Figure 8-12. The hot gas generator supply pressures were in excess of the 2500 psi design value and reached a value of 3300 psi, with a time duration 0.35 seconds, which was 0.05 seconds shorter than the expected 0.4 seconds. The second and third pressure levels were also higher than anticipated and were recorded as 1640 psi and 1040 psi. The entire pressure profile for the hot gas generator was 30% in excess of the design values.

The higher pressure produced by the hot gas generator was due to a reduced FET effective nozzle area. The hot gas generator was sized to a 0.350 diameter converging nozzle. A reduction in the effective area of the FET caused a 30% increased pressure output from the hot gas generator.

The cause of the leak was attributed to a failure of the base plate on which the torque motor cover was mounted. A definite bow in the base plate was evident after disassembly of the FET. The bowing of the base plate resulted in a failure of the "O" ring seal and subsequent failure of the torque motor due to excessive heat from the high flow of hot gases.

Cold gas tests of the assembly at 2500 psi indicated no evidence that structural failure would occur. The high initial pressure pulse, 3300 psi, and the "O" ring seal design were the most probable causes of FET failure.

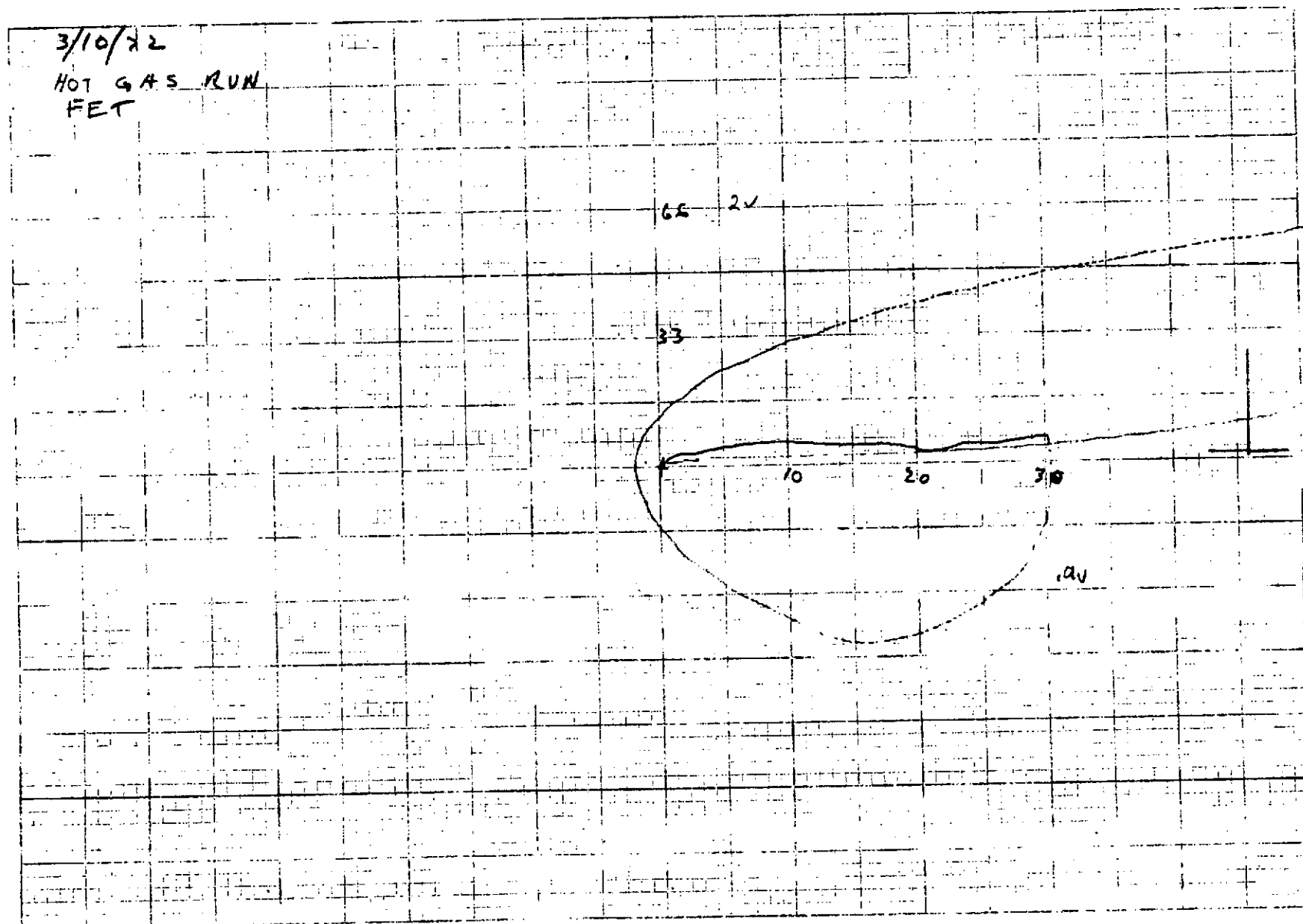


FIGURE 8-9 PHASE PLANE PLOT OF FET CLOSED LOOP PERFORMANCE ON HOT GAS #1

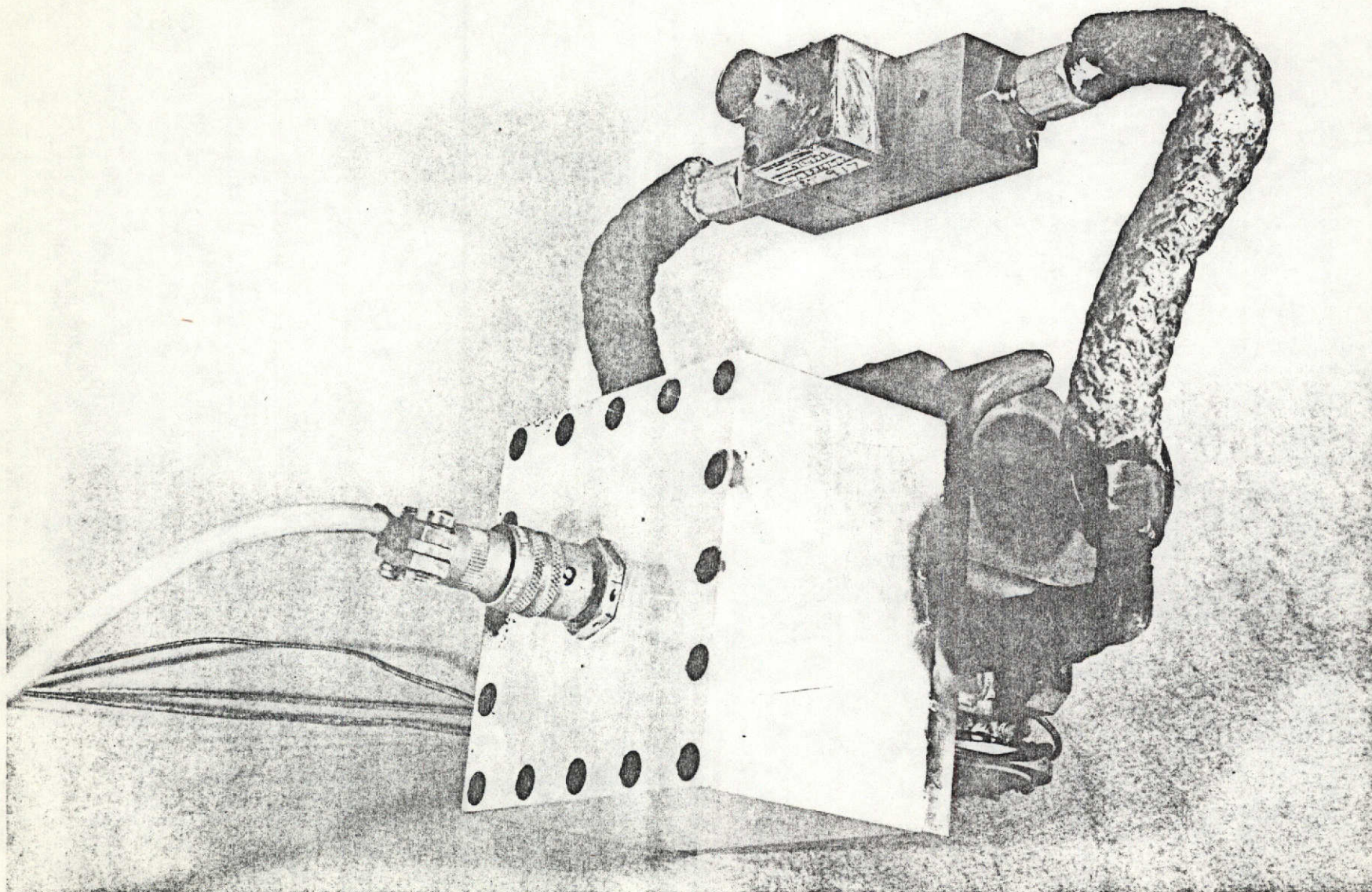


Figure 8-10 FET After Firing



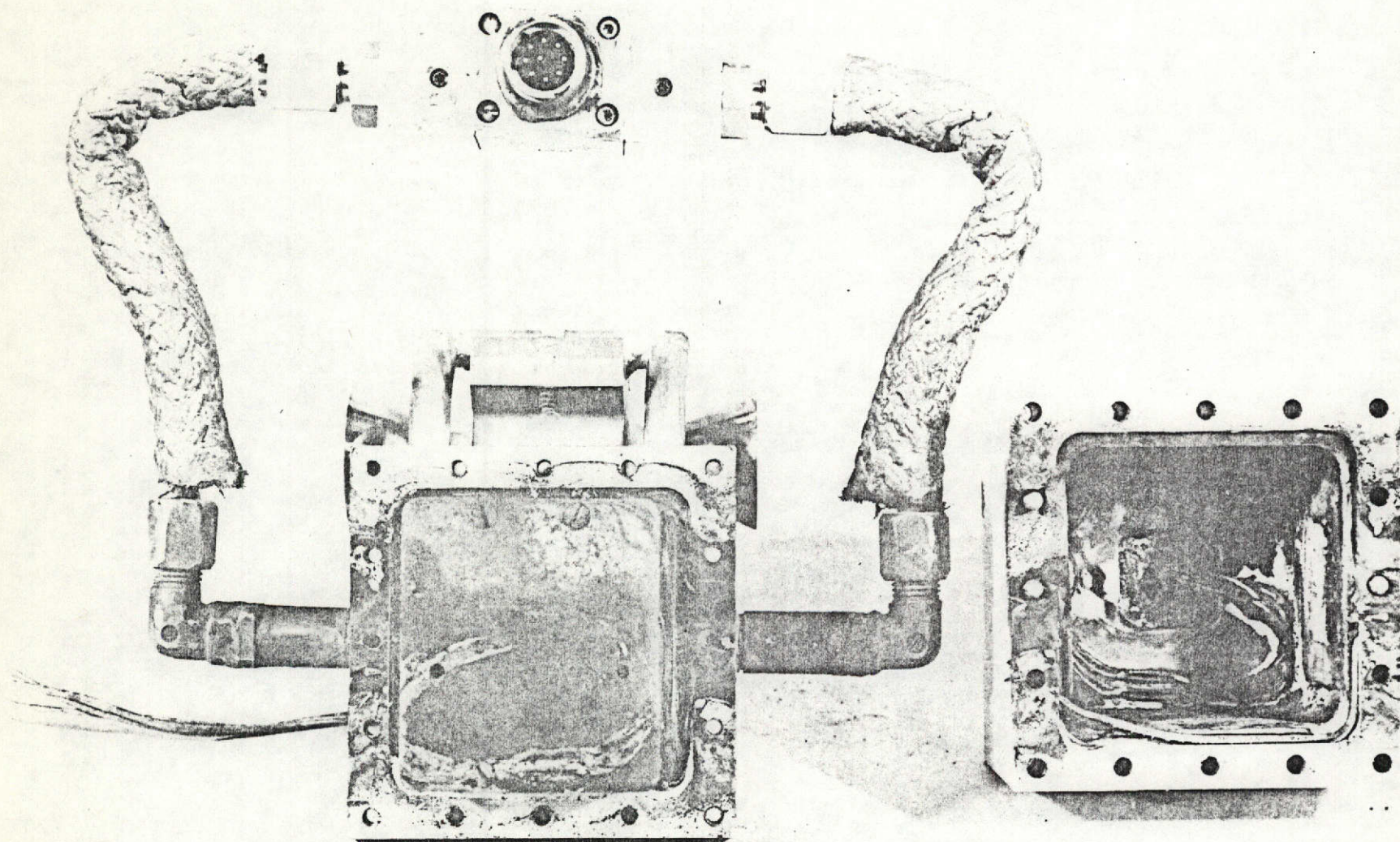


Figure 8-11 Torque Motor Housing After Firing



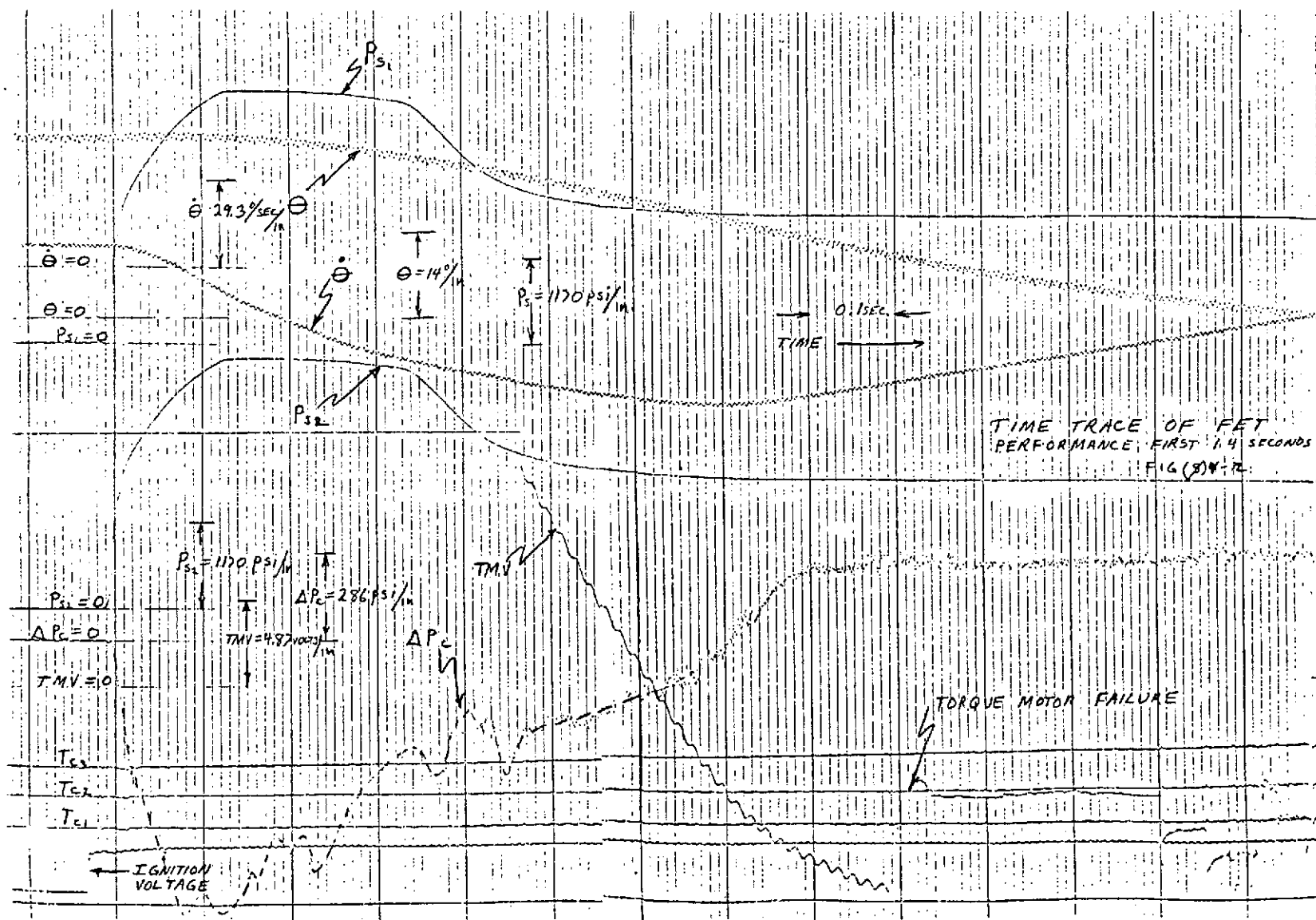


Figure 8-12

## Section 9

### FET MODIFICATIONS

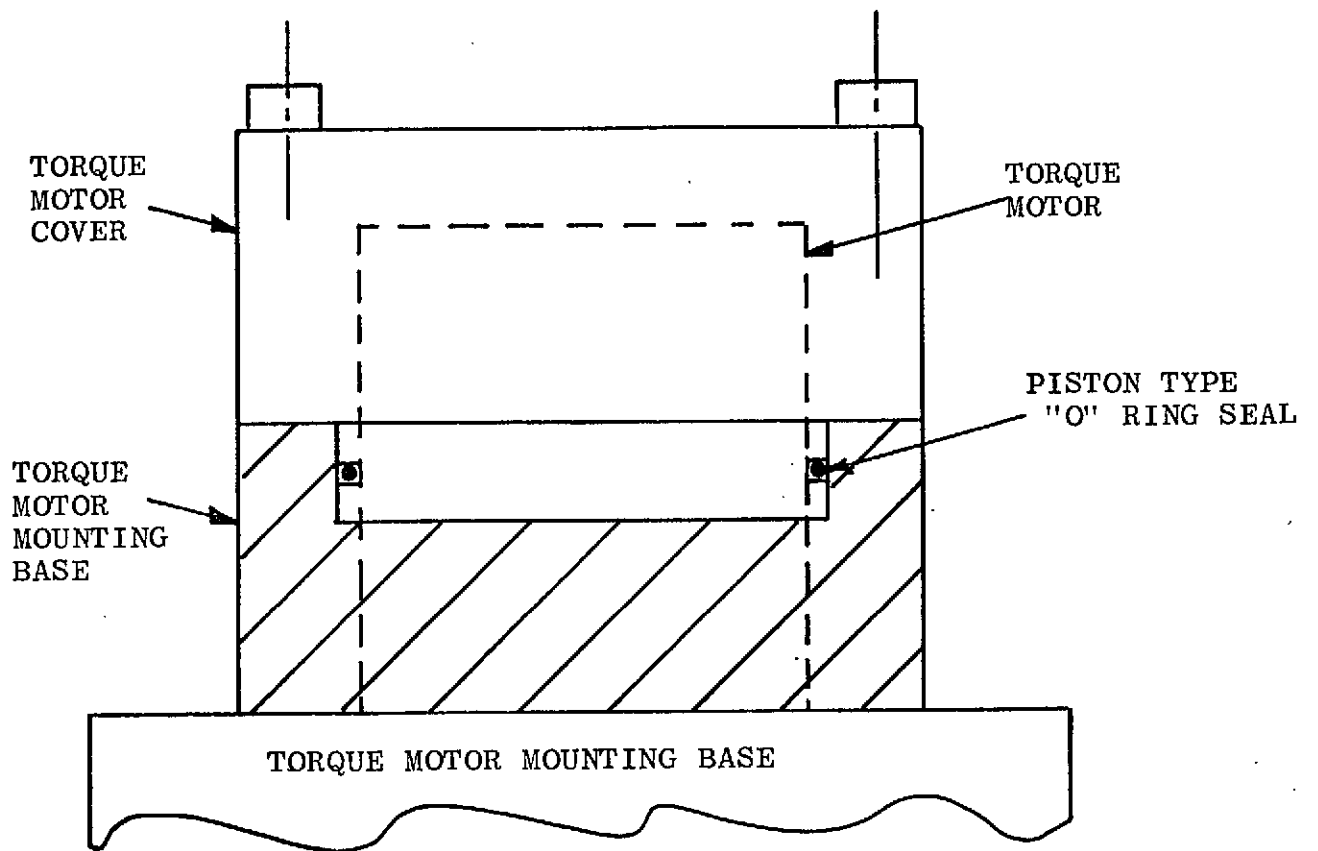
The failure of unit #1 was reviewed with the conclusion that the torque motor housing and mounting plate were not structurally strong enough to contain pressures of 3000 psi. Since minor leaks could be tolerated in the cold gas tests without degrading the performance, the structural weakness of the torque motor mounting plate was not detected. Some evidence of the structural weakness was evident during the initial cold gas tests in that after each run at 2500 psi, the torque motor null would shift and the bolts holding the torque motor would loosen. The first problem was corrected by strengthening the torque motor mount with added stiffeners under the base which rigidly attached to the base to the vortex valve structure. The addition of the stiffeners eliminated the change in null. A slot was also milled under the torque motor to allow a more uniform escape of gases when initially pressurized which solved the problem of the loosening bolts.

The FET was designed to operate on hot gas with a wet torque motor which would be subjected directly to the hot gases, but at a temperature well below the maximum gas temperature. If the torque motor housing experiences a continuous gas flow, as would be generated by a small leak, the temperatures in the torque motor housing quickly exceed the limits of the torque motor. Therefore, it was deemed essential that any subsequent firing of the FET would require a modification of the torque motor housing to insure that no leaks would occur.

After reviewing the data from unit #1 several modifications were made to unit #2. These modifications included:

- Increasing the structural strength of the housing
- Modify the torque motor seal design to eliminate leakage due to structural deflection
- Reduce magnetic field strength on torque motor to increase effective spring rate
- Provide bleed orifice on hot gas generator to reduce maximum pressure

The modification of the torque motor housing involved a major redesign of the structure. The strengthening of the housing was accomplished by using stainless steel rather than aluminum and fabricating the mounting base for the torque motor as an integral part of the housing (Figure 9-1).



SKETCH OF MODIFIED  
TORQUE MOTOR HOUSING

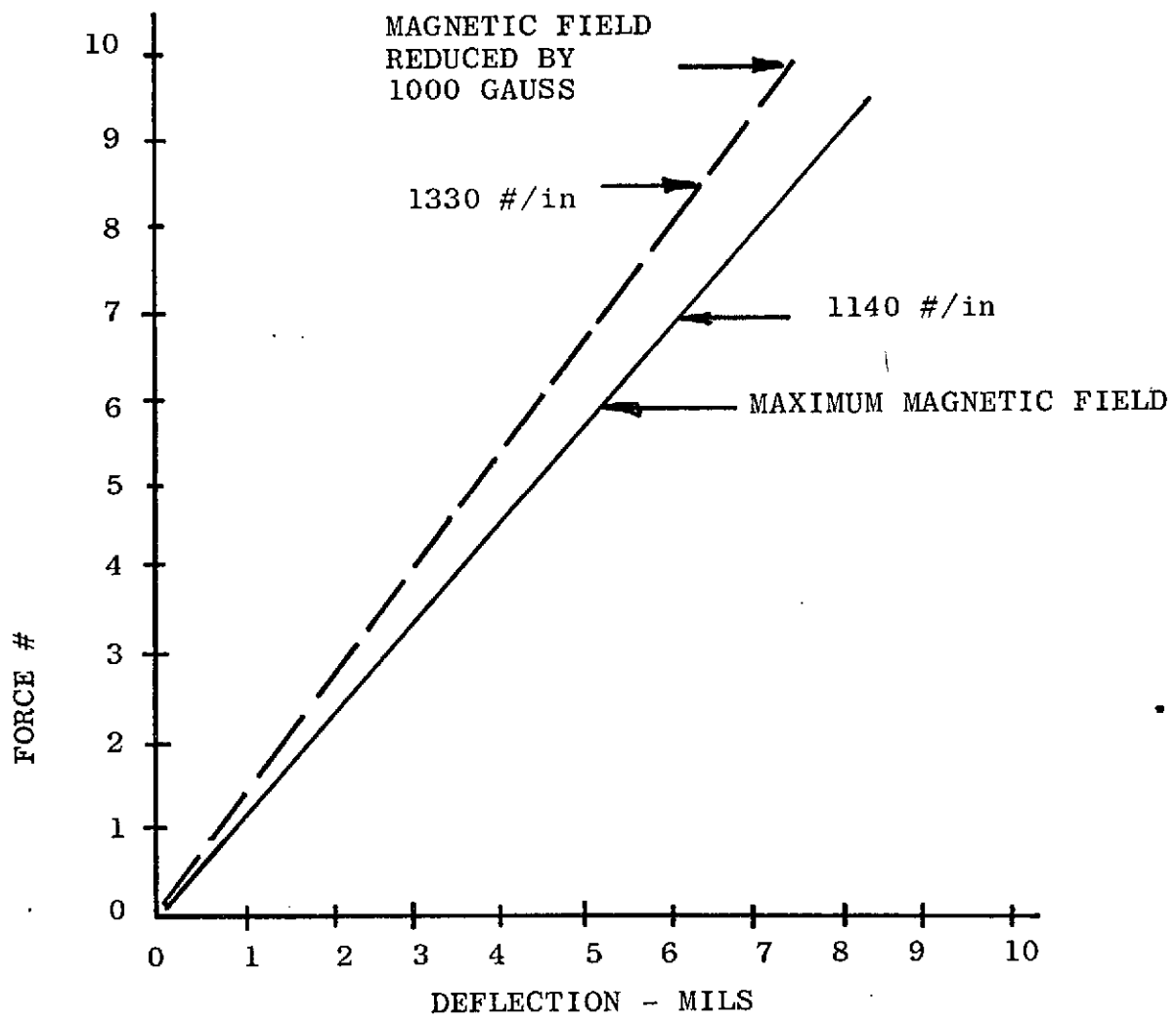
Figure 9-1

The redesign torque motor housing is a cubical volume which was split in half to allow the walls of the housing to contribute increased structural rigidity to both the cover and mounting base. The seal was formed between the cover and the mounting base by a piston "O" ring around the perimeter of the mounting base. This type of seal allows tolerance to structural elongation of the bolts holding the cover without leakage. The holddown cover bolts were also changed from stainless steel to heat tempered steel to further increase the strength of the torque motor housing. The torque motor housing was pressure tested to 4000 psi using hydraulic oil and found to be structurally sound with no evidence of leaks.

The torque motor magnets flux density was reduced by a 1000 gauss in an attempt to increase the effective spring rate of the torque motor, thus permitting higher operating pressures with no latching of the flapper. The 1000 gauss reduction was essentially equivalent to the previous attempt at increasing the spring rate by shorting the magnetic air gap with steel bars. The effective spring rate of the torque motor consists of the mechanical spring rate minus the magnetic spring rate. By reducing the magnetic spring rate, the overall effective spring rate can be increased, thus increasing the pressure at which the flapper latches. The reduction in magnet field strength is limited by the fact that the gain of the torque motor is also reduced. As a result of torque motor gain tests, it was determined that a reduction of 25% in magnetic flux density increased the effective spring rate by 17% but reduced the torque motor gain by 45%, Figure 9-2. Since the gain of overall FET was approaching the minimum specified value, it was decided not to reduce the flux density by more than 25%, which results in a latching pressure of 1700 psi. The gain of the torque motor prior to reducing the magnetic field was 0.00137 in/volt, Figure 9-3. By reducing the field strength the gain was reduced to 0.00091 in/volt. The reduction in field strength did not appreciably affect the linearity of the flapper travel vs. volt input or the maximum deflection. The addition of shorting bars in conjunction with the reduced field strength does reduce the maximum travel, which was another reason for not reducing the field strength less than 1000 gauss below the original level.

The last modification was accomplished by Thiokol on the hot gas generator. Since a modification to the FET to increase the effective orifice or change the design solid grain propellant would have required extensive modification in the original design, it was decided that the simplest method of reducing the pressure profile of the hot gas generator was to add a bleed orifice. The size of the orifice was determined by Thiokol based on the previous hot gas test conducted with unit #1. The bleed orifice was incorporated by drilling and tapping the case of the solid propellant grain for a pipe plug. The orifice was drilled in the plug to the desired size.

Each of these modifications was accomplished prior to the cold and hot gas static and dynamic tests on unit #2.



SPRING FORCE VS DEFLECTION  
Figure 9-2

FET TORQUE MOTOR GAIN CURVES  
WITH MAGNET FLUX DENSITY  
REDUCED BY 1000 GAUSS

DATE: 2 MAY 1972

9-6

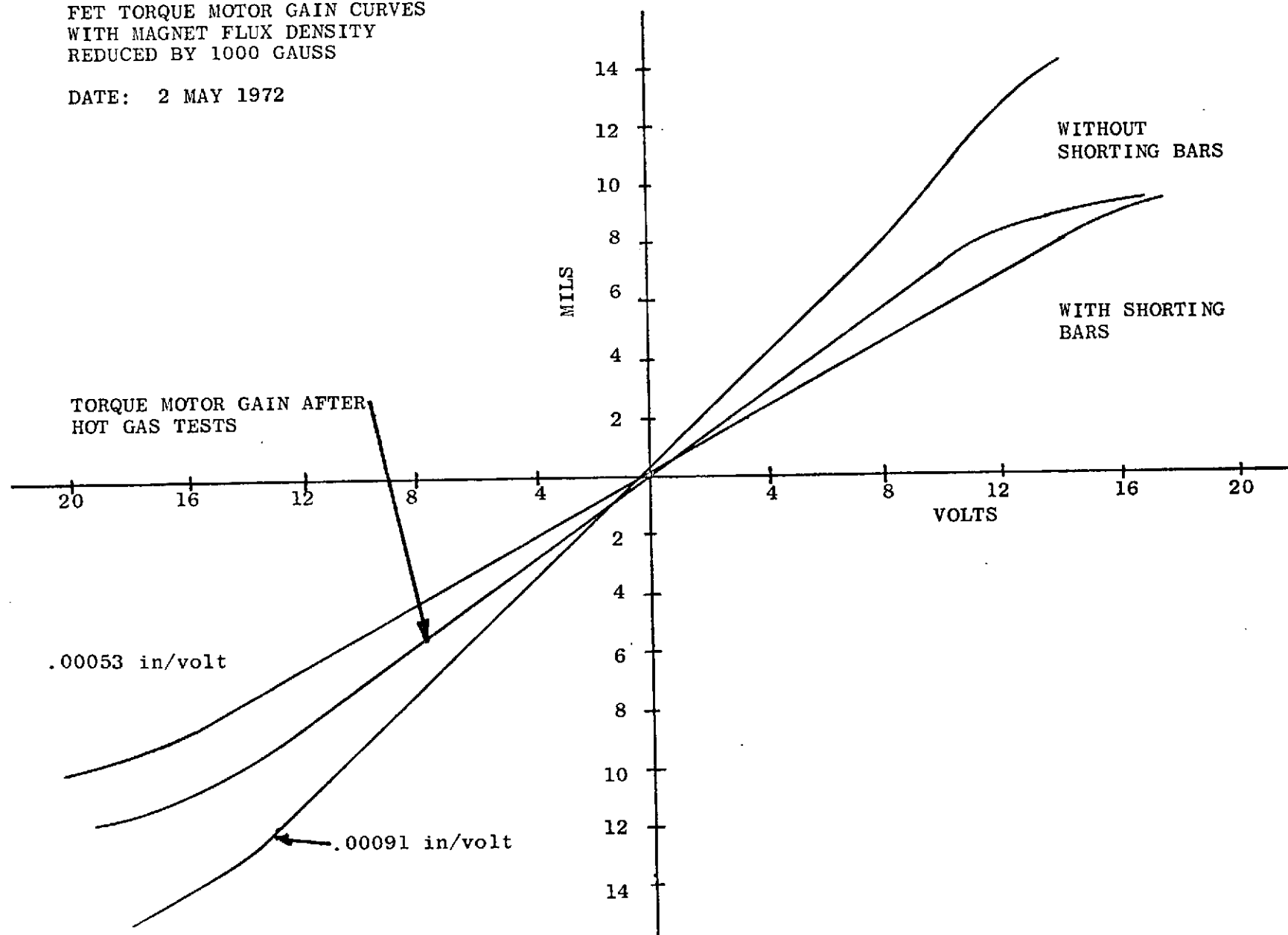


FIGURE 9-3 FLAPPER DEFLECTION VS VOLTS INPUT WITH MAGNETIC FIELD STRENGTH REDUCED BY 1000 GAUSS

## Section 10

### COLD AND HOT GAS TESTS-UNIT #2

#### COLD GAS TESTS

Cold gas static tests were performed with the NASA technical representative present. These tests were conducted prior to the hot gas tests which is contrary to the ES-PT-2. The main reason for performing these tests prior to the hot gas tests was to stay within the bounds of the program time scope. In lieu of a complete cold gas test at the completion of the hot gas test, a dynamic test of the torque motor displacement vs. voltage input was performed and a visual inspection of the FET housing and seals was accomplished.

The cold gas tests for unit #2 yielded essentially the same discrepancies cited on unit #1 - Figures 10-1, 10-2, 10-3, 10-4 and 10-5.

Figure 10-1 presents the performance of unit #2 over the pressure range of 2500 down to 800 psia with a zero input voltage. FET #2 still exhibits an unstable characteristic for pressures in excess of 1800 psi. From 1800 down to 1400 psi a steady state null of 30 lb. thrust is maintained which reverses direction at 1400 psi. The cause of this reversal was not determined during the cold tests, but it appears to be directly related to the relative position of the flapper and nozzles. The null offset curve was repeatable for a number of runs which verified that no structural deformation was taking place. When the pressure became less than 1400 psi, the null decreased in the expected manner and was within the ES-PT-1 limits of  $\pm 15\%$  at pressures less than 1300 psi. The adjustment of the torque motor null involved a considerable amount of time and effort and was difficult to set. The major reason for this difficulty in adjustment was due to the fact that the torque motor flapper had to be moved relative to the nozzles a small increment for each run until the optimum zero set point was obtained. Each run involved operating the FET over the entire pressure range of 2500 to 800 psi, which required approximately 4 hours for each test with the major time delay being the charging of the gas bottles. On the basis of the time available it was decided that once an acceptable null had been achieved for pressures less than 1400 psi, (the range of proportional control) the unit would be ready for hot gas firing. Although not shown in Figure 10-1 the maximum thrust for unit #2 was 110 lb. and as was the case with unit #1, the main reason for the low thrust was attributed to the low supply pressure on the vortex valves, and limited control of the first stage.

Figures 10-2 and 10-3 illustrate that unit #2 produces a saturated output for voltage inputs less than 10 volts for supply pressures greater than 800 psi.

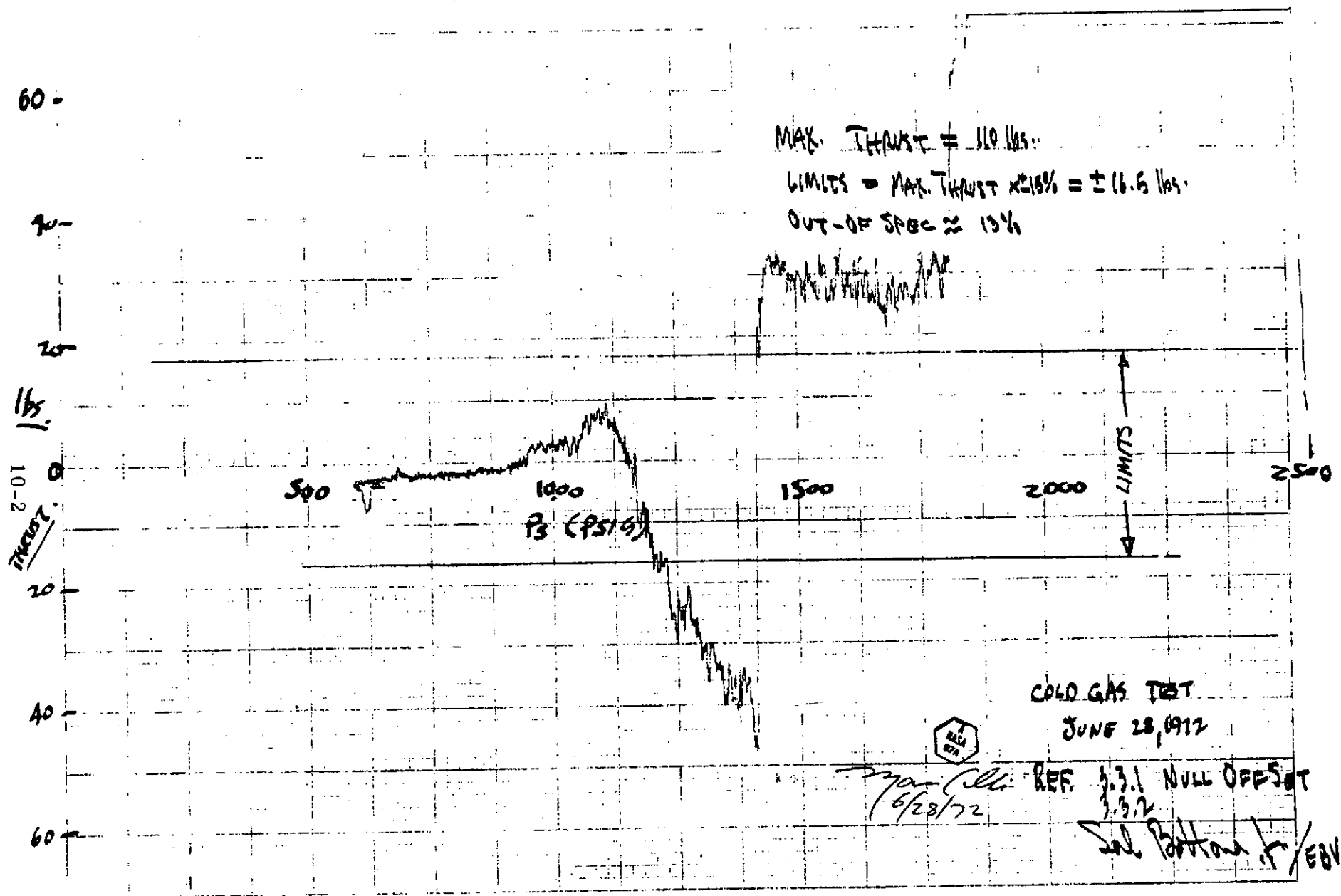


FIGURE 10-1 COLD GAS TEST



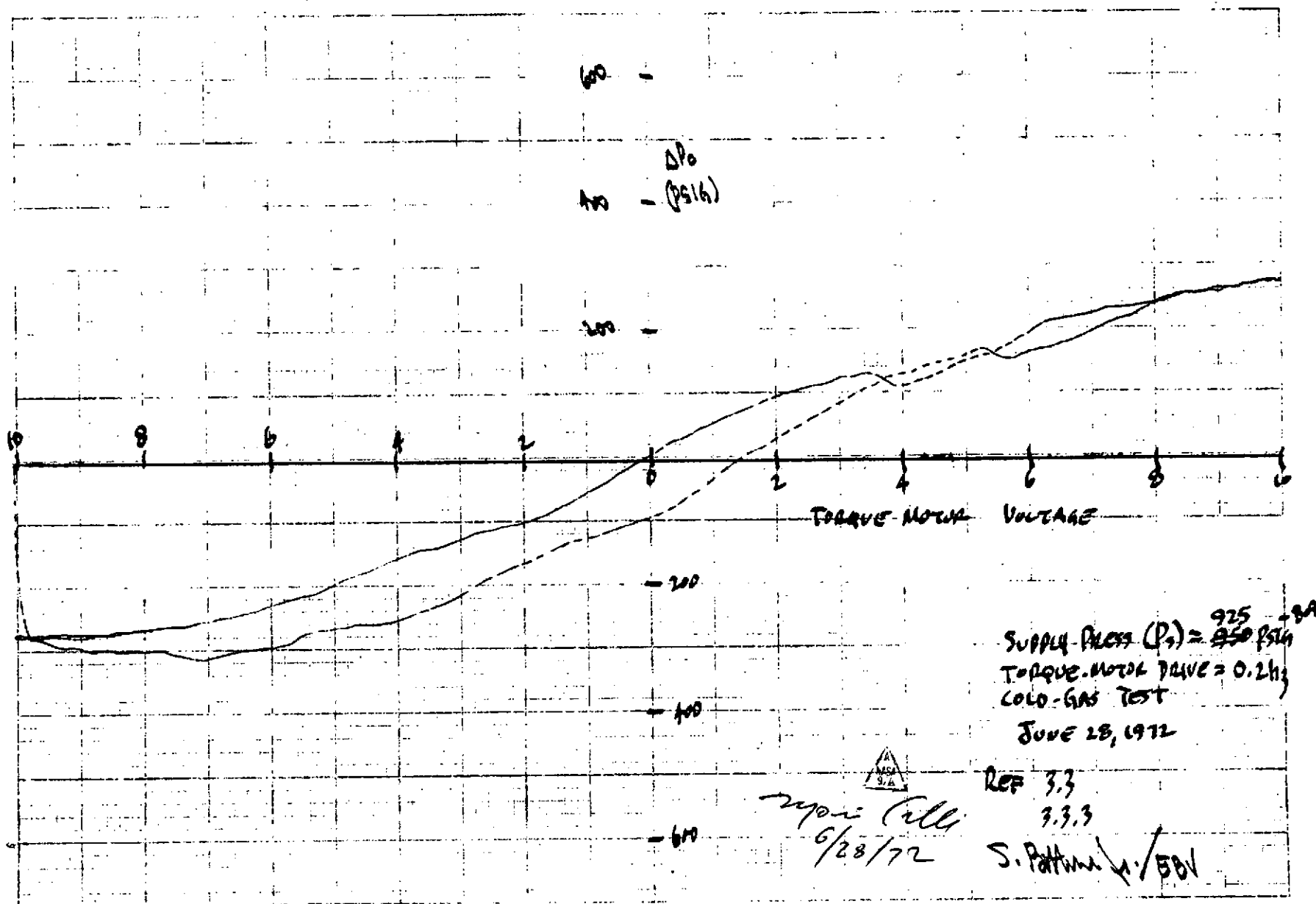


FIGURE 10-2 COLD GAS TEST

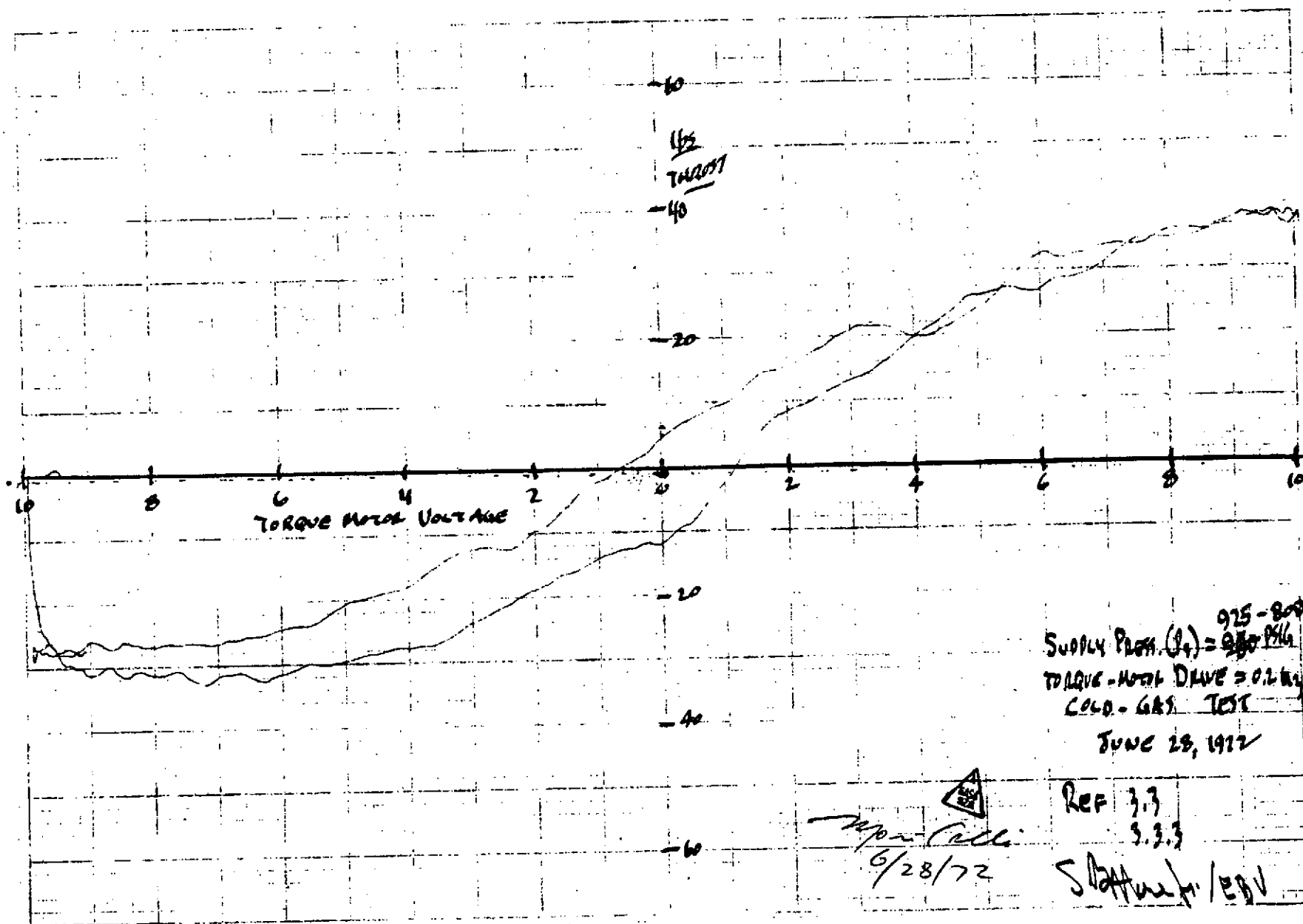


FIGURE 10-3 COLD GAS TEST

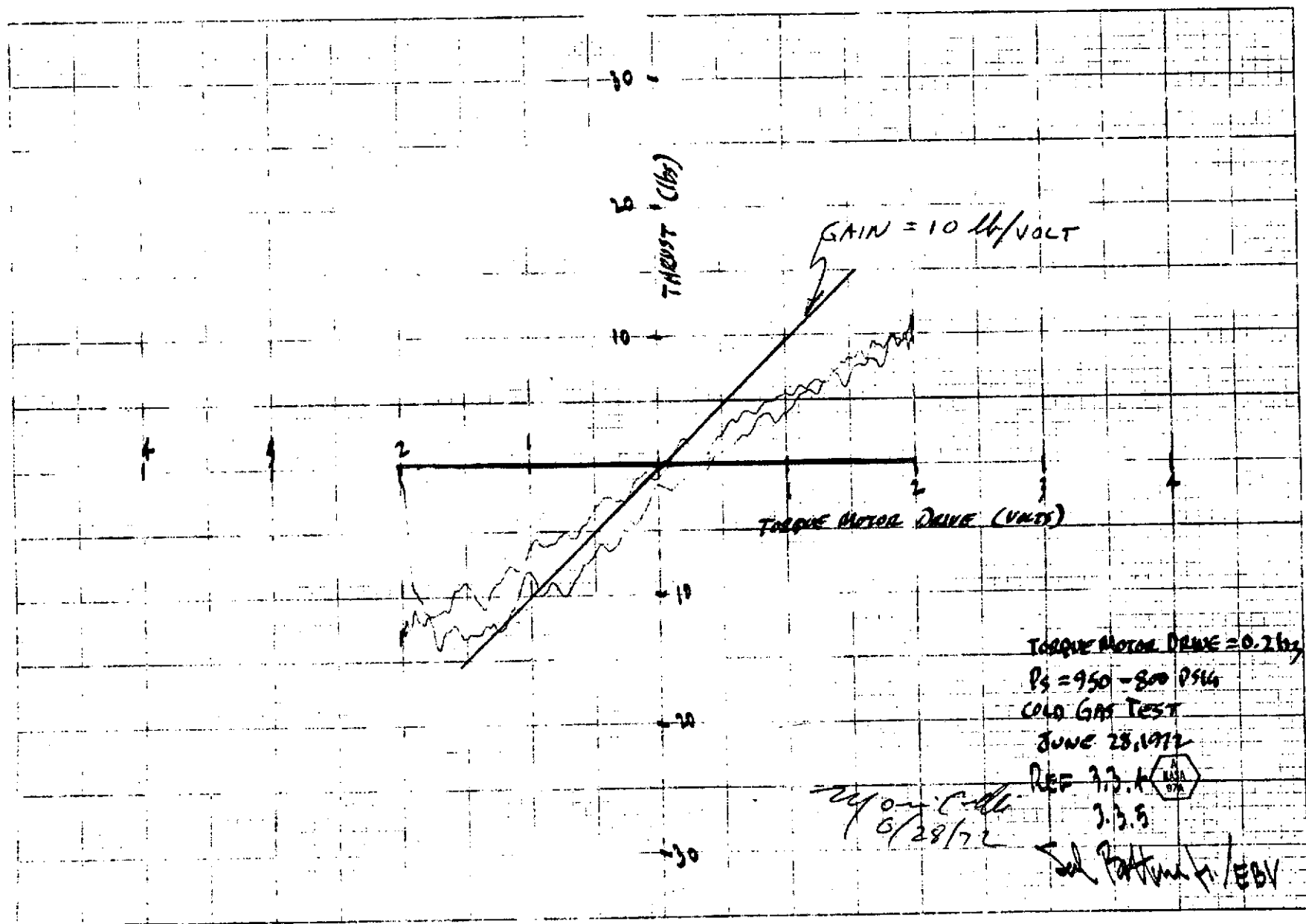


FIGURE 10-4 COLD GAS TEST

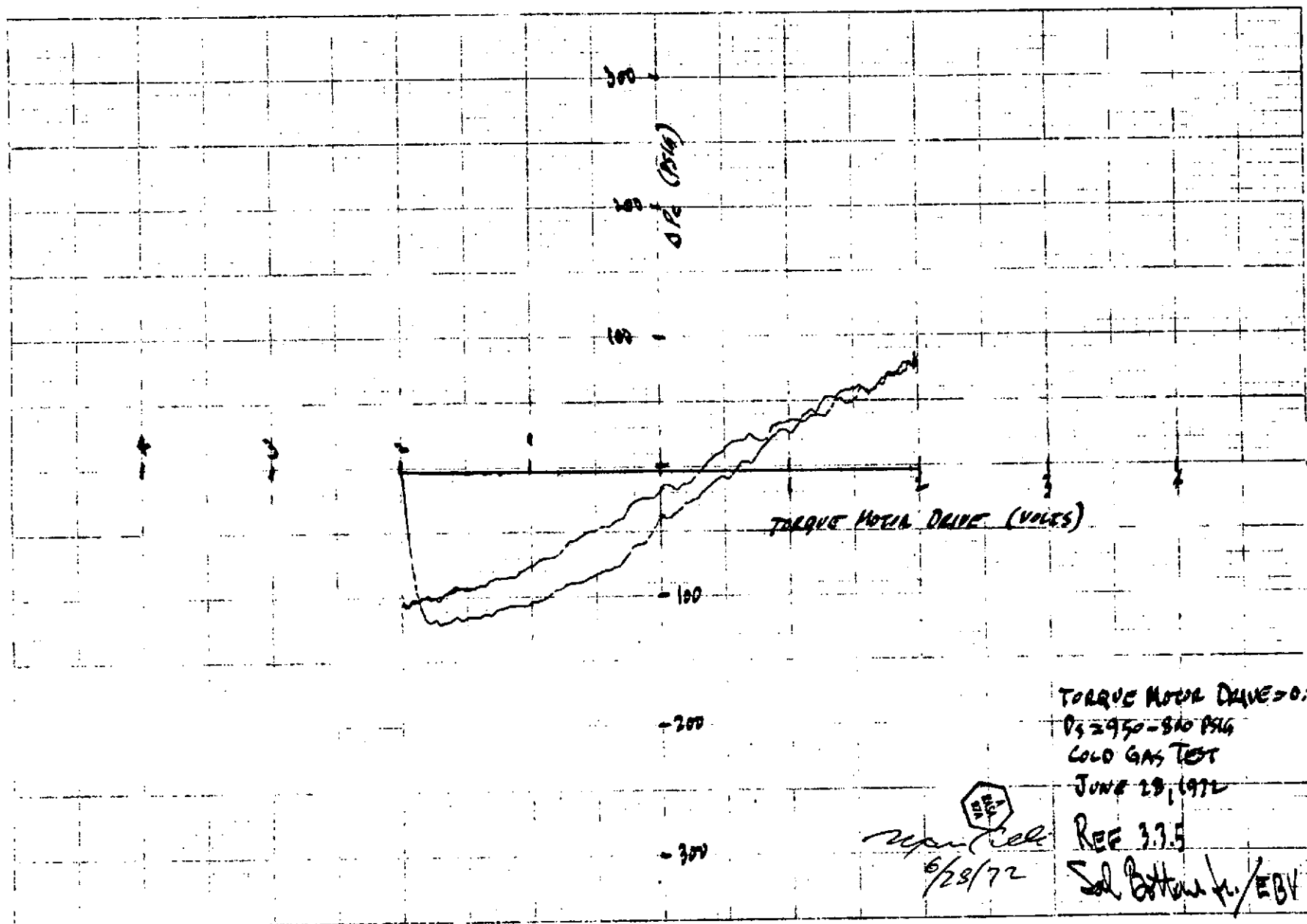


FIGURE 10-5 COLD GAS TEST

In each trace, 10-2 and 10-3, there is a significant drop in supply pressure from the beginning to the end of the run.

Figure 10-4 is a trace of thrust vs. voltage at a supply pressure of 950 to 800 psig and was performed to show the gain of unit #2. For the lower pressures the gain is less than the goal of 10 lb/volt specified in ES-PT-1, but as the pressure increases, the gain of the FET increases as a result of the increased torque motor gain. The gain as shown in Figure 10-4 is 5 lb/volt. At supply pressures of 1000 to 1300 psi the gain of 10 lb/volt is achieved. The reason for the low gain is most likely a result of the reduced magnetic field strength on the torque motor. This discrepancy can be corrected by employing a stiffer torque motor operating at maximum magnetic field strength.

Figure 10-5 complies with the hysteresis data required for ES-PT-1, paragraph 3.3.5. Since the pressure is varying it is difficult to obtain an accurate assessment of the hysteresis. If no compensation is made for pressure change, the hysteresis at null is approximately 10%. The change in null with pressure accounts for a large portion of the measured hysteresis.

The following table summarizes the performance of FET #2 and the goals specified in ES-PT-1.

<u>Table 10-1</u>		
<u>Specification</u>	<u>FET #2</u>	<u>Goal</u>
Pressure Range of Stable Operation	1300 psi	2500 psi
Null $\pm 15\%$ of Max. Output	In limits up to 1300 psi	In limits up to 2500 psi
Max. Thrust	110 lb.	220 lb.
Hysteresis	10%	3%
Saturation	$> 10$ volts	$> 10$ volts
Static Gain @ 800 psi	5 lb/volt	10 lb/volt

Although most of the goals were not met by the FET, the performance was deemed acceptable for accomplishing the hot gas firing. Since the major emphasis for this development program was placed on fabricating an entire ERC system capable of demonstrating successful operation on hot gas, no additional design changes were made to correct the deficiencies. Limited cold gas dynamic tests operating

closed loop with the simulated aircraft and attitude control simulator were also conducted on unit #2 and demonstrated equivalent performance to the data obtained with unit #1.

#### HOT GAS TESTS

The time required for performing the hot gas tests on unit #2 was two days, which was considerably less than unit #1. The hot gas tests were conducted in the same manner as the test on unit #1.

For the hot gas firing, the rate was kept close to zero prior to ignition with the automatic fire taking place at 30° angle. Figure 10-6 demonstrates the recovery of the simulated vehicle for a successful hot gas firing of the ERC. As is evident from the X-Y plot, the initial angle for auto fire was 37°. Although the initial angle was in excess of the desired 30° angle, the simulated vehicle was automatically returned to zero rate, but with a positive angle offset. The data seems to indicate that a bias was present in the system during the run of 7°. A rerun of the system with the simulated FET attitude control did not show the presence of the offset.

After the initial automatic acquisition, the vehicle was manually flown with an input introduced by the potentiometer connected to a 'joy' stick. At the conclusion of the manual control, the rates appear to diverge, which is a result of the hot gas generator pressure going to zero before the timing sequence had been completed by the electronics.

Figure 10-7 is a photo of the unit after the hot gas test in the bay at Thiokol. No apparent physical damage to the hardware was evident in the post firing examination.

The TV recording of the FET operation showed a very definite modulation of the output as indicated by the variation of the flame magnitude emanating from the thrust nozzle.

The data from the oscillograph was reduced and is presented in Figure 10-8 through 10-10.

The hot gas generator pressure profile for test #2 was still greater than the desired pressure levels of 2500, 1300, and 800 psi. In each case the levels were approximately 25% in excess of the design goals. The incorporation of the bleed orifice did not seem to produce any significant difference from the pressures generated during the first hot gas test.

The only explanation which can be offered for not achieving the desired pressures is that the bleed orifice was sized for unit #1 without compensating for the leak in the torque motor housing. Although the pressures were higher than predicted, the overall

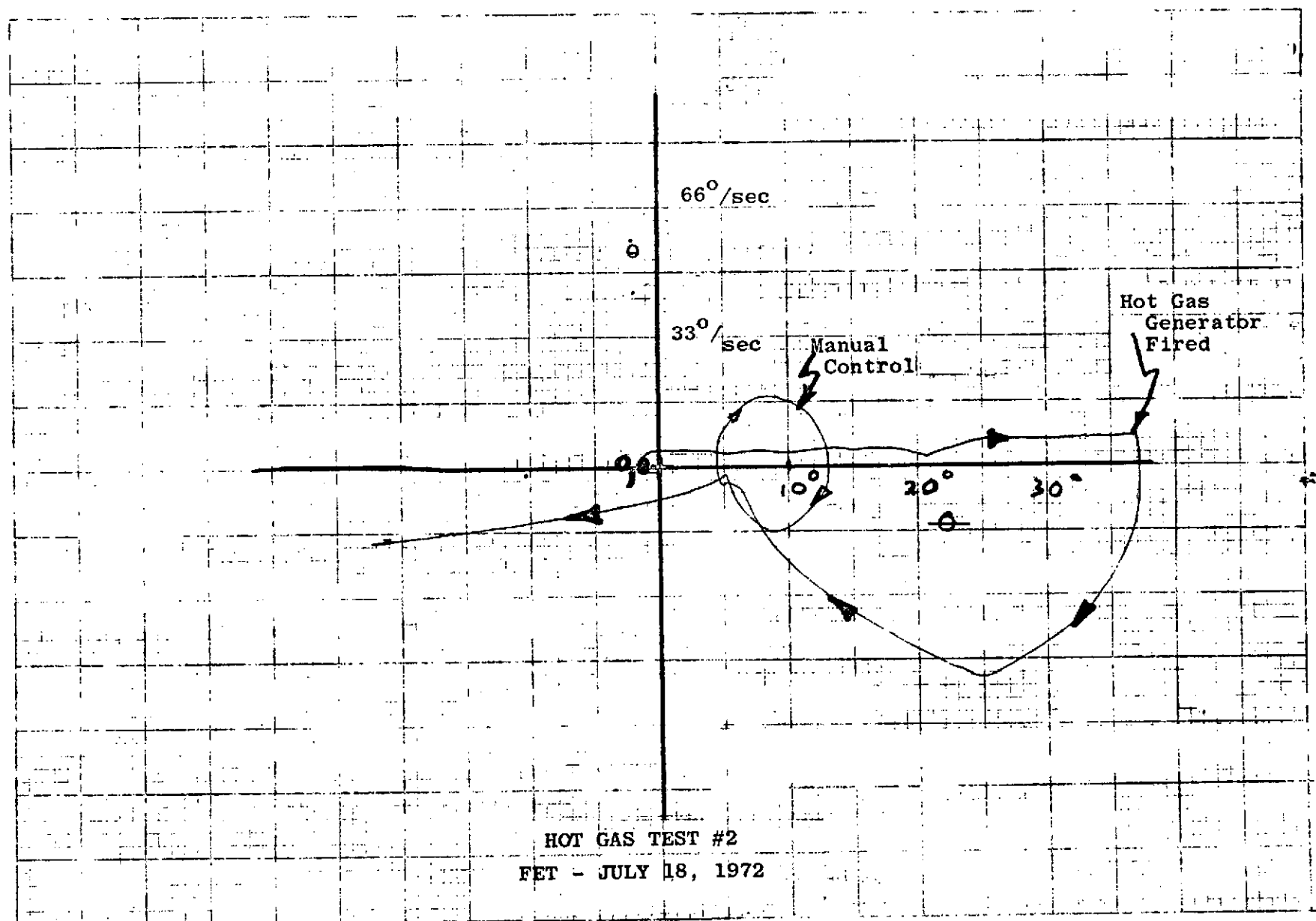


FIGURE 10-6 HOT GAS TEST #2



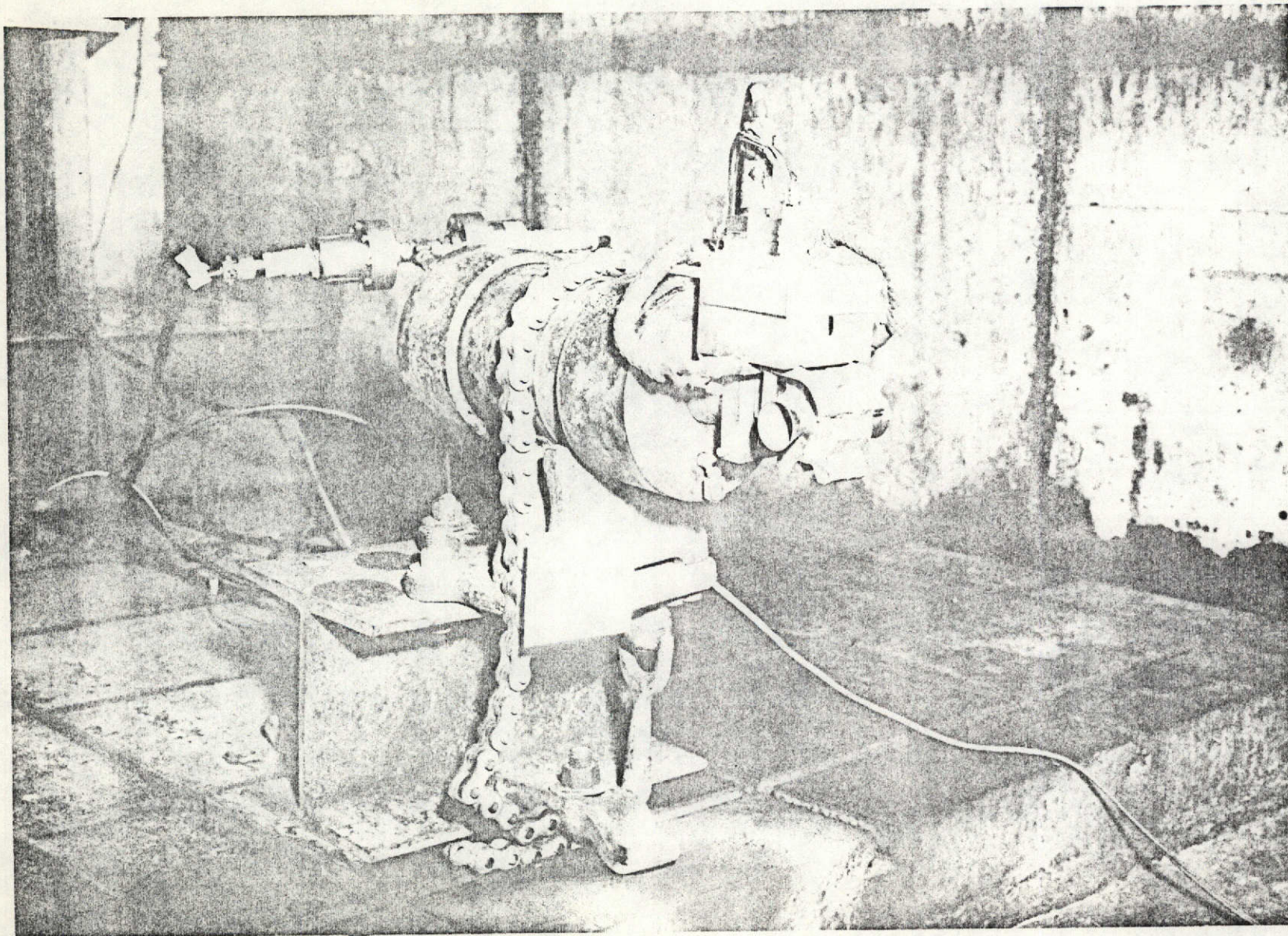


Figure 10-7 Photograph of Post Firing Unit #2



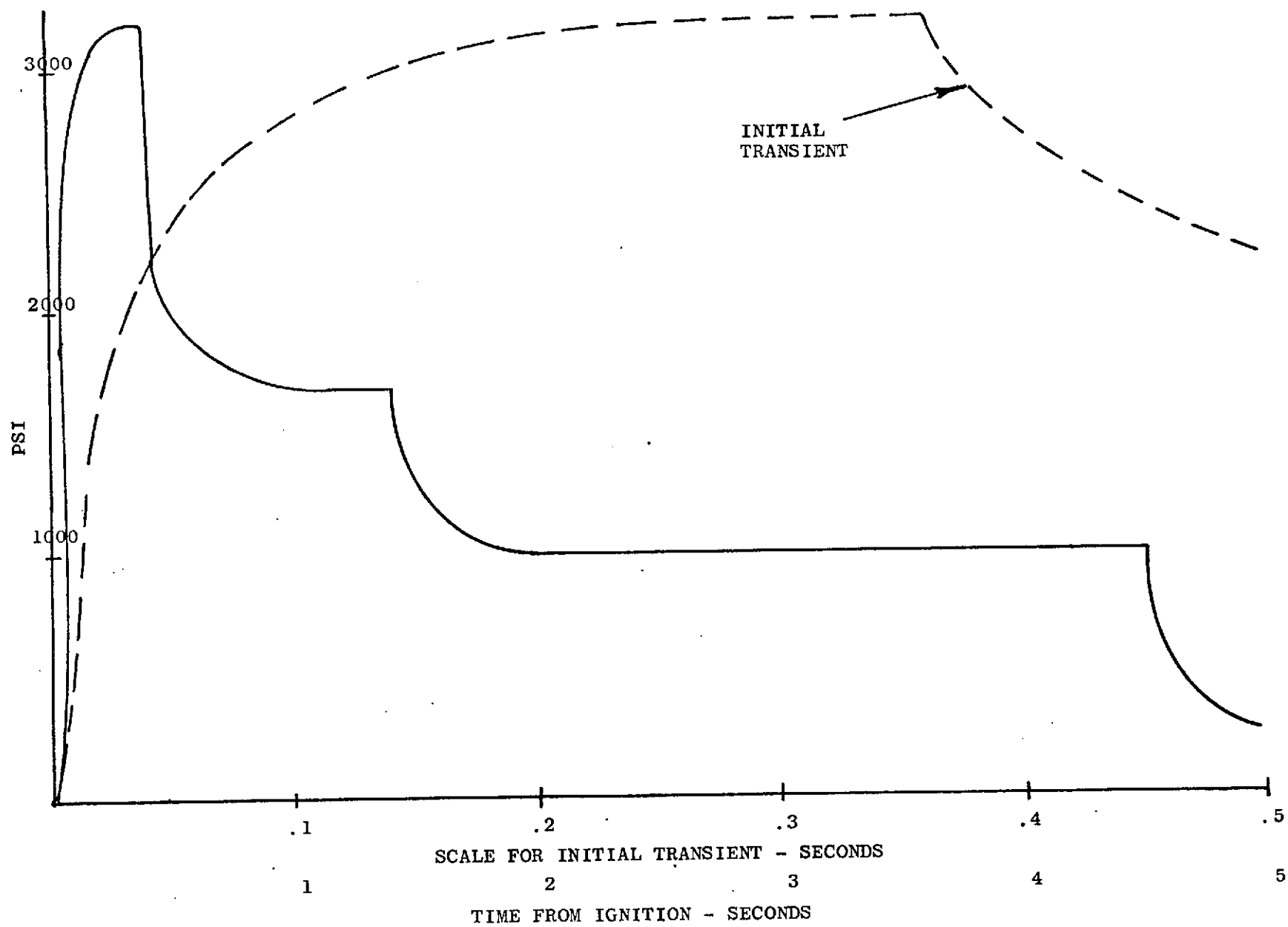
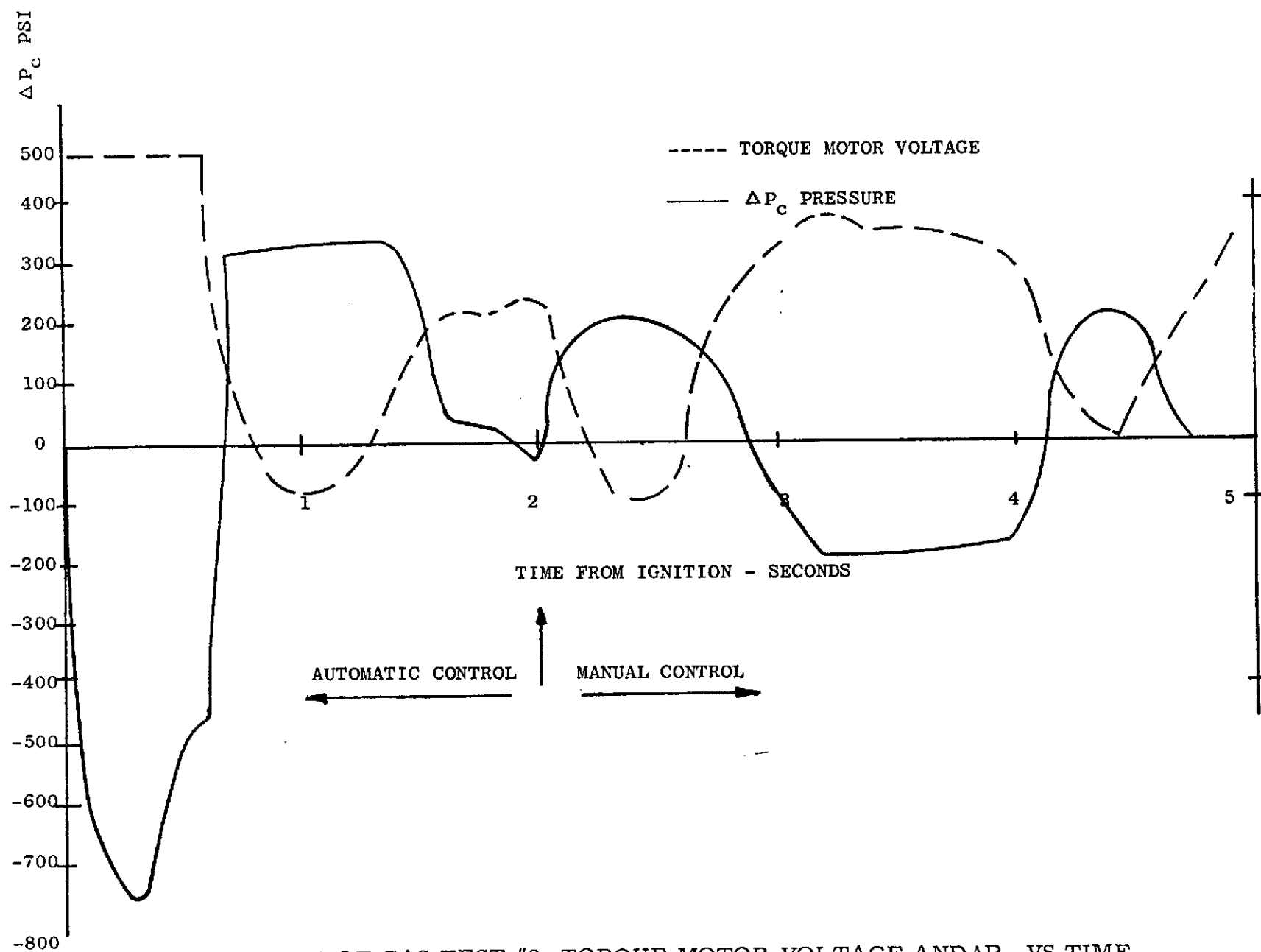


FIGURE 10-8 HOT GAS TEST #2 PRESSURE VS TIME

FIGURE 10-9 HOT GAS TEST #2 TORQUE MOTOR VOLTAGE AND  $\Delta P_c$  VS TIME

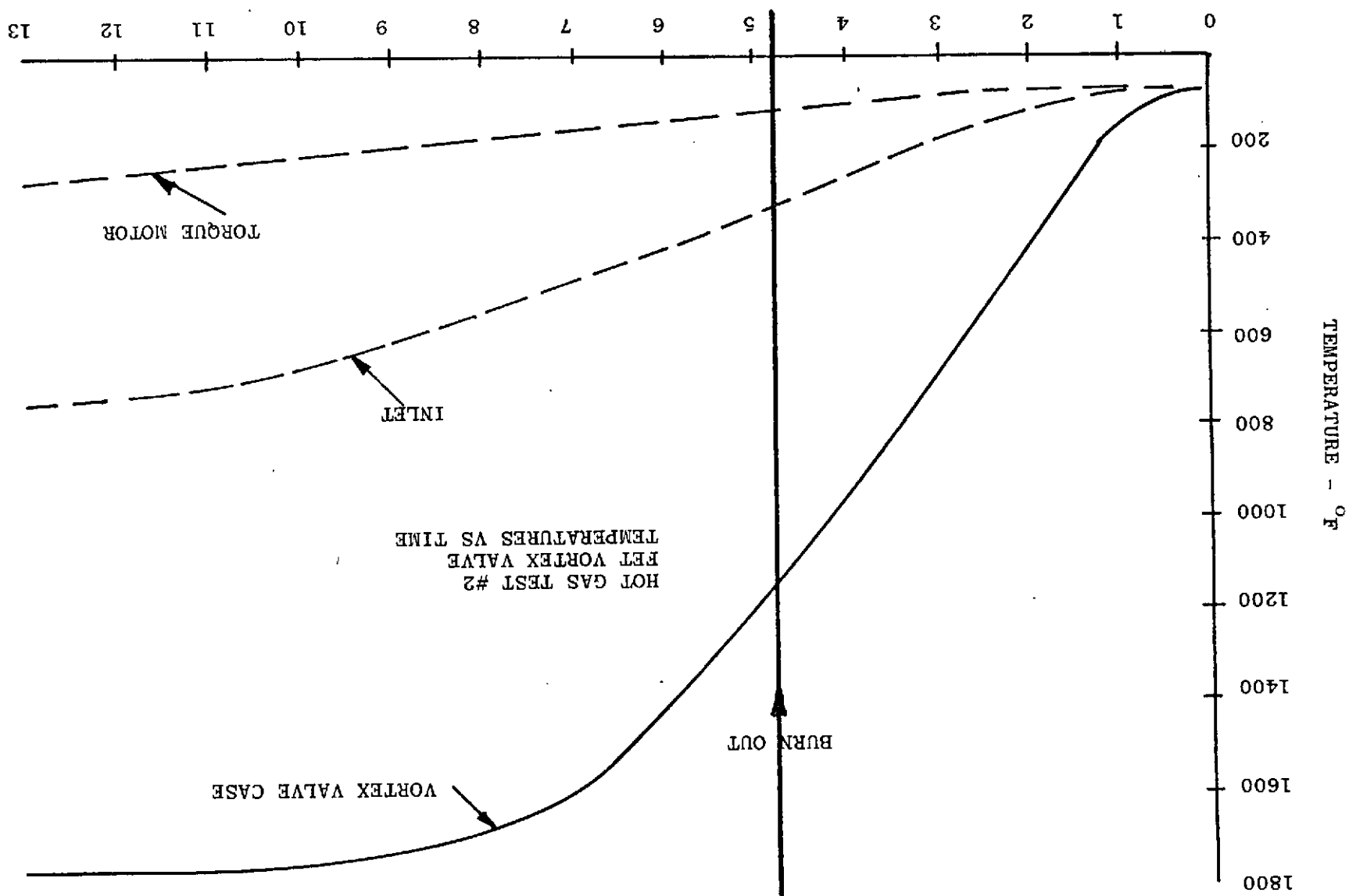


FIGURE 10-10 HOT GAS TEST #2 FET VORTEX VALVE TEMPERATURES VS TIME

operation of the gas generator was satisfactory. As shown by initial pressure transient plotted on Figure 10-8, the rise time of the initial pressure pulse is more than adequate in terms of meeting the design specification of 0.1 seconds.

The time traces of torque motor voltage and control pressure are plotted in Figure 10-9. A definite correlation can be made from the phase plane plot of  $\theta$  and  $\dot{\theta}$  in Figure 10-6. During the initial 0.6 seconds the angular rate was increased to 53°/sec at which time attitude control function calls for a reversal in rate. Maximum thrust is commanded for a time period of 0.8 seconds and a total time of 1.4 seconds from time of ignition. The programmed 1.4 second time period should represent the termination of automatic control and the initiation of manual control by the pilot, but the data indicates that automatic control was maintained for 2 seconds and that the timing of the attitude control simulator logic was not in correspondence with the time from ignition. From 1.6 seconds to 2 seconds, the simulated vehicle was maintained in a zero rate condition with a bias of 7°. During that same time period the supply pressure was reduced from 1700 psi to 1000 psi. The  $\theta$  bias error is due to the fact that there is a null offset in the FET for supply pressures from 1700 psi to 1000 psi, and in order to compensate, the closed loop control system has to maintain an angular error to generate the torque motor voltage for zero thrust. At 2 seconds after ignition, manual control is activated by the control logic. As shown on Figure 10-6 the sign of the acceleration went through a sequence of plus, minus and then plus, which is in agreement with the reversals of the  $\Delta P_c$  signal. The  $\Delta P_c$  signal is proportional to the thrust output or acceleration from the FET. The  $\Delta P_c$  signal goes to zero at 4.6 seconds after ignition as a result of expending the hot gas generator. The rate on the phase plane plot proceeds to increase at the end of the run due to the timing mismatch between the hot gas generator ignition and the attitude control simulator timing logic. With the exception of the delayed ignition and the attitude bias error, the hot gas test of the ERC was an unqualified success.

Figure 10-10 is a reduction of the thermocouple data from the oscillograph for the vortex valve case, the FET inlet, and the torque motor case. Even though data was taken for 10 minutes after generator cutoff, the data beyond 13 seconds is not shown due to the fact that the thermocouple readings had reached a saturated condition at 13 seconds. As was expected, the temperature on the torque motor case was the lowest of the three, and did not exceed 300F. The inlet temperature reached a value of 800F, which is well below the level where the structural strength of steel is degraded. The temperature on the vortex valve case did reach an excessive value of 1800F and appeared to be white hot from the TV recording. Although the temperatures were excessive after generator burnout, the temperatures during the period of maximum pressure, where maximum strength is required, were less than 400F. The 347

stainless steel used for fabricating the FET does not exhibit any significant degradation in tensile strength for temperatures less than 1000F.

After the hot gas tests, the unit was returned to Schenectady General Electric and static gain tests made on the torque motor. The torque motor was found to be functionally intact with a gain which was 25% less than the pre-test measurements (Figure 9-3). The reduced gain is attributed to the heat soak of the magnets at the completion of the hot gas test which resulted in a lower magnetic flux density. The unit was disassembled as shown in Figures 10-11 and 10-12, and revealed no damage to the seals or torque motor. A small amount of residue from the hot gas generator products of combustion was present in the torque motor housing along with water condensate. Examination of the thrust nozzle throat did not show any evidence of erosion or material failure.

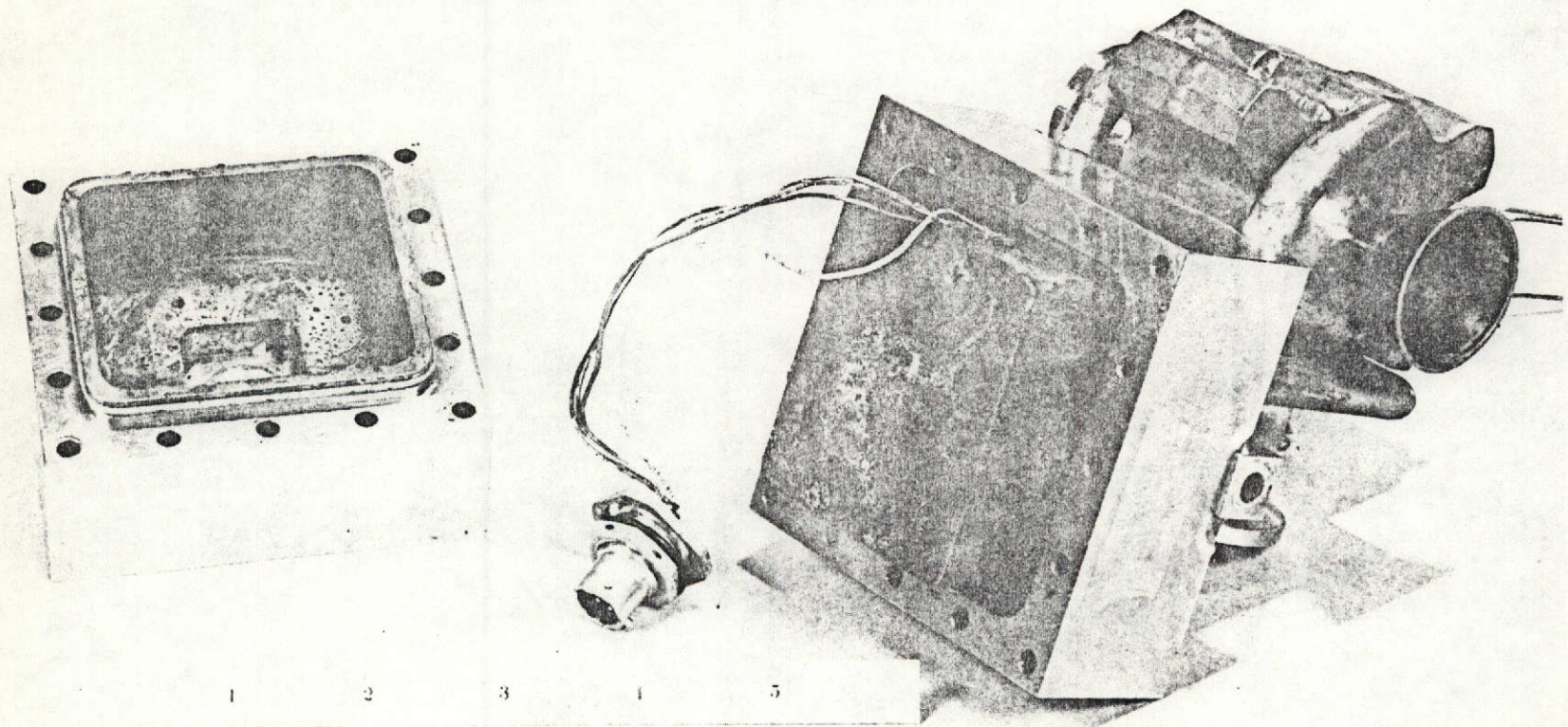


Figure 10-11 Partial Disassembly of FET After Hot Gas Test #2



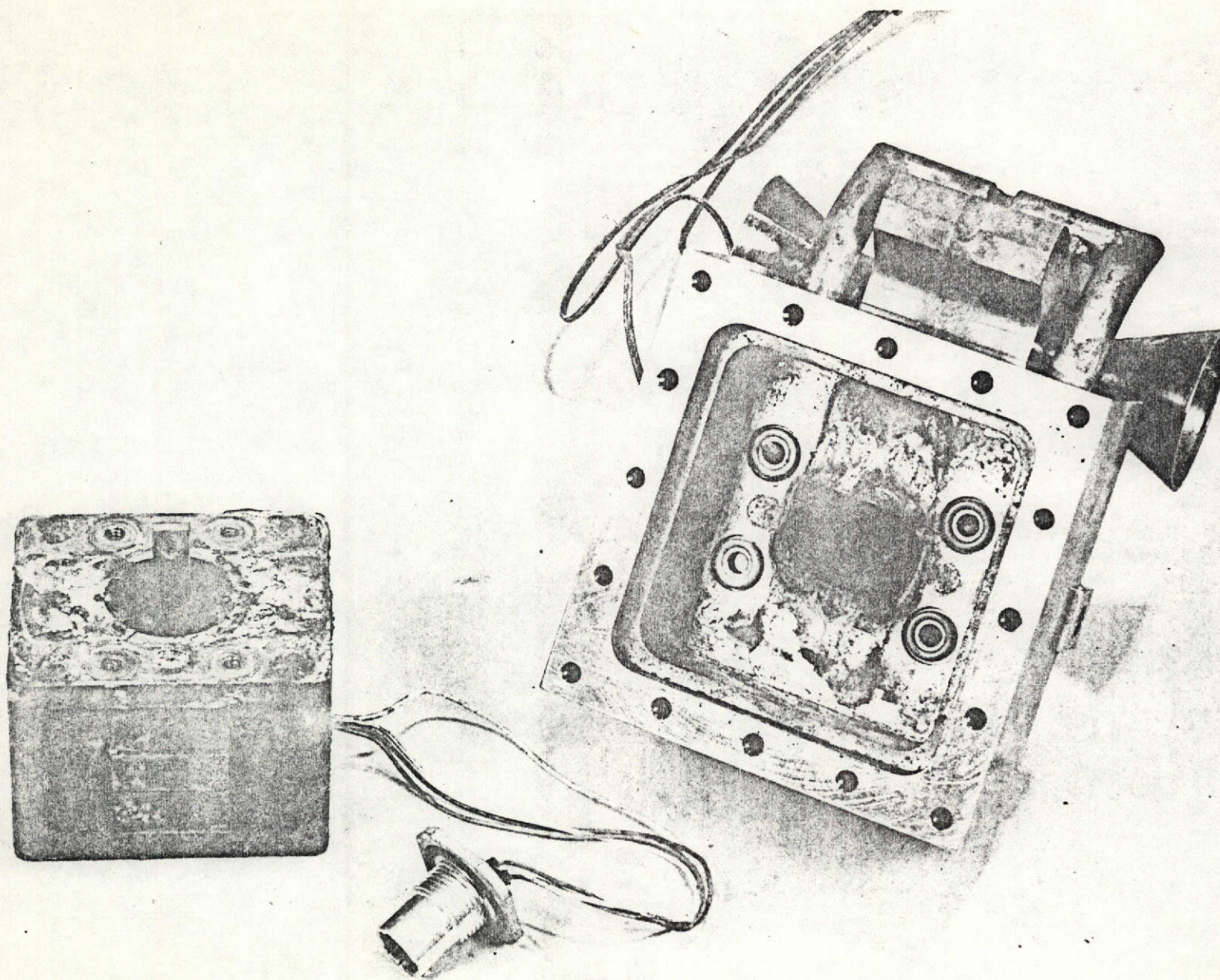


Figure 10-12 Complete Disassembly of FET After Hot Gas Test #2

## ENGINEERING SPECIFICATION

SPECIFICATION NO.: ES-PT-1

Title: ENGINEERING PERFORMANCE TEST PROCEDURE		Issue Date: 28 December 1971 Revision: A	
Product: Fluidic Emergency Thruster		Contract or Task No. NAS 2-5467 Task IV	
Model No. CR280PT32AA0000 CR280PT32BA0000	Prepared T. S. Honda	Distribution:	
Checked <i>[Signature]</i>	Proj Engr	D. M. Chisel - NASA/ARC	
Approved <i>[Signature]</i>	Mfg Mgr	M. Celli - DCAS	R. H. Warner
	Engr Mgr	W. T. Rauch	T. F. Conroy
		R. C. Kumpitsch	T. S. Honda
		S. Bottone	E. B. Voorhees

## Reference Drawings:

G.E. Drawing 55-518081

This test procedure, in accordance with Attachment Q-2 of Contract NAS 2-5467, provides detailed instructions for conduct of engineering performance tests on the fluidic emergency thrusters (FET) prior to delivery to NASA/ARC. The final engineering performance tests shall be conducted after the operation of the FET with a solid propellant hot gas generator.

## REVISIONS

Ltr	Pages	Description	Date	Approved
A	2	Par 3.0	3-7-72	<i>[Signature]</i>
A	3	Par 3.1, 3.2, 3.3.1, 3.3.3	3-7-72	<i>[Signature]</i>



Fluidic Emergency Thruster  
Engineering Performance Test Procedure

1.0 General Instructions

1.1 Scope - This test procedure; in accordance with Attachment Q-2 paragraph 4 of Contract NAS 2-5467, provides detailed instructions for conduct of Fluidic Emergency Thruster (FET) engineering tests. The tests shall be conducted by the FET contractor prior to and after the operation of the FET with hot gas.

1.2 Hardware Identification - The FET test hardware shall be designated:

Fluidic Emergency Thruster  
G.E. Part Number: CR28OPT32AA0000  
CR28OPT32BA0000

1.3 Applicable Documents - G.E. Drawing No. 55-518081 FET Assembly.

1.4 Inspection Plan - Tests shall be witnessed by G.E. Engineering and Quality Assurance personnel. The NASA/ARC designated representative shall be notified forty-eight (48) hours in advance and four (4) hours on retest.

1.5 Inspection Verification - Prior to engineering tests, conformance to applicable drawings and specifications shall be provided by inspection personnel.

1.6 Failure Report - Nonconformance reports shall be submitted in accordance with attachment Q-3 of Contract NAS 2-5467.

2.0 Test Conditions: The following test conditions apply to all tests described in Section 3.0 of this specification.

2.1 Test Fluid - The fluid used in the performance of all tests shall be compressed air. The fluid temperature shall be room ambient.

2.2 Test Set-up Environment - Unless otherwise noted:

- a. Ambient temperature shall be 70  $\pm$ 15F.
- b. Ambient pressure shall be normal sea level (28-32 inches of mercury).

2.3 Test Measurements - Instruments shall be calibrated to commercial standards.

2.3.1 Pressure - All pressures shall be measured with gauges or pressure transducers which have been calibrated with a standard dead weight tester.

2.3.2 Temperature - Laboratory thermometers or thermocouples shall be used for temperature measurement.

2.3.3 Thrust Measurement - The thrust measurement shall be made using a standard force gauge with a range of at least  $\pm$ 250 pounds.

2.4 Test Pressures - The test pressure shall be in the range from 700 to 2750 psig.

3.0 Test Methods: The following tests shall be performed on the fluidic emergency thruster provided under the contract containing this specification.

3.1 Examination of Product - The FET shall be carefully examined visually and dimensionally prior to any other test to determine conformance with the requirements of specification in regard to workmanship, identification, marking, finish, and conformance to applicable drawings.

3.2 Torque Motor Resistance - The two coils in the torque motor shall be connected in parallel so that a voltage applied across the coils causes the flapper to deflect. The resistance of the coils in parallel shall not exceed 40 ohms.

3.3 Static Test - With +10 volts maximum applied to the input of the torque motor, the voltage shall be cycled at 0.2 Hz to -10 volts and back to +10 volts. The vortex valve control and the output differential thrust shall be recorded on the ordinate of an X-Y recorder with the torque motor input voltage recorded on the abscissa. This test shall be repeated with an input sufficient to produce a peak amplitude of 25% saturation.

3.3.1 Null Offset - With zero input to the torque motor, the supply pressure shall be varied over a range from 700 to 2500 psig. The differential thrust shall be recorded on the ordinate of an X-Y recorder with the supply pressure on the abscissa. The thrust null offset between 700 and 1500 psig shall not exceed  $\pm 15$  percent of the maximum thrust.

3.3.2 Stability - In the test under paragraph 3.3.1, the FET shall exhibit no bistable characteristic at supply pressures below 2500 psig.

3.3.3 Saturation - The output of the FET shall saturate at input amplitudes of less than  $\pm 10$  volts with supply pressure greater than 800 psig.

3.3.4 Static Gain - The static gain (thrust vs volts input) around null shall be determined from the X-Y plot. It shall be determined in the supply pressure range from 800 to 900 psig and shall be greater than 10 lb/volt.

3.3.5 Hysteresis - The hysteresis shall be determined from an X-Y plot of the FET input voltage vs vortex valve differential control pressure and differential thrust output for an input amplitude from zero to +25% of maximum then through zero to -25% of maximum and then back to zero input. The hysteresis shall not exceed 3% when the input amplitude is within the saturation limits and when the supply pressure is less than 1000 psig.

PRELIMINARY

APPENDIX B(a)

THIOKOL CHEMICAL CORPORATION  
ELKTON DIVISION  
ELKTON, MARYLAND

TEST PLAN 1290-141

FOR

FLUIDIC EMERGENCY THRUSTER SYSTEM

AUTHORIZATION: \_\_\_\_\_

PREPARED BY: \_\_\_\_\_

APPROVED BY: \_\_\_\_\_

APPROVED BY: \_\_\_\_\_

APPROVED BY: \_\_\_\_\_

\_\_\_\_\_  
Date

\_\_\_\_\_  
Date

\_\_\_\_\_  
Date

\_\_\_\_\_  
Date

\_\_\_\_\_  
Date

PRELIMINARY

1.0 OBJECTIVES

1.1 The test objectives are to demonstrate:

- a. functional performance of the thruster
- b. temperature rise in critical areas during burn and stabilization after burn
- c. generator ballistic performance

and, thus, to evaluate the compatibility of the TE-T-614-1 and the General Electric Fluidic Emergency Thruster.

2.0 TEST DESCRIPTION

2.1 To obtain the test objectives, the TE-T-614-1 gas generator and the fluidic thruster system will be tested utilizing an electronic Aircraft Control Simulator to provide flight simulation and to demonstrate the error correction function of the thruster system.

3.0 DATA PARAMETERS TO BE RECORDED

	<u>Range</u>	<u>Range</u>	<u>No.</u>	<u>Type of Record</u>
3.1	Chamber Pressure	0 - 3000	2	Oscillograph
3.2	Differential Pressure	$\pm$ 3000	2	Oscillograph
3.3	Roll Rate Signal		1	X-Y plotter and oscillograph
3.4	Wing Position	$\pm$ 30°	1	X-Y plotter and oscillograph
3.5	Thruster Temperature (Chromel-Alumel)	0 - 2000°F	3	Oscillograph
3.6	Torque Motor Input	$\pm$ 15 volts	1	Oscillograph
3.7	Ignition Zero	Indication	1	Oscillograph
3.8	Valve Actuation	Indication only (on cold gas test only)	1	Oscillograph
3.9	Nitrogen Pressure	0 - 3000 psi (on cold gas test only)	1	Oscillograph

4.0 REQUIRED EQUIPMENT

	<u>No.</u>
4.1 Pressure Transducer (0-3000 psi)	2
4.2 Differential Pressure Gage ( $\pm$ 3000 psi)	1
4.3 Thermocouples (Chromel-Alumel)	3
4.4 X-Y Plotter (8-1/2 x 11)	1
4.5 Power Supply ( $\pm$ 15 volts DC minimum)	1
4.6 Power Supply (5 volts DC, 2 ampere, minimum)	1
4.7 TV Camera and Monitor	1
4.8 Pallets of Nitrogen with Controls (2000 psi minimum)	2
4.8.1 Regulator	
4.8.2 Solenoid Valve	
4.8.3 One-inch plumbing system	
4.9 Aircraft Simulator (GE-furnished)	1
4.10 Analog Computer (GE-furnished)	1
4.11 Fluidic Thruster (GE-furnished)	1
4.12 Hot Gas Adapter (TE-M-509 to Fluidic Thruster) (GE-furnished)	1
4.13 TE-M-509 Gas Generator (TCC)	1

5.0 SEQUENCE OF EVENTS

5.1 Receive the aircraft simulator, fluidic thruster, analog computer, television tape recorder, and associated equipment.

5.2 Provide support services for interfacing the above items into the Thiokol control and instrumentation systems.

5.2.1 All operations on or with the above equipment shall be at the direction of the General Electric personnel only.

5.3 Provide cold gas test plumbing and control system.

5.3.1 The cold gas system shall consist of a source of dry nitrogen connected to a pressure regulator, solenoid valve controlled by the fire control system, and manually operated ball valve, all with a minimum port size of 3/4 inch and connected by means of one-inch tubing.

5.3.2 The nitrogen source shall supply 2500 psig.

5.3.3 The solenoid valve shall be connected to be actuated by the GE flight simulator when the sum of the aircraft wing position  $\phi$  and the roll rate  $\dot{\phi}$  exceeds the safe value. The actuation of the valve simulates the rocket motor firing.

- 5.4 Setup all instrumentation and perform dry run of the systems.
- 5.5 On approval of the dry run, prepare for the cold gas test.
- 5.6 Connect nitrogen plumbing to the fluidic thruster input.
- 5.7 Ensure that the solenoid valve to the nitrogen system is "CLOSED".
- 5.8 Close the manual ball valve.
- 5.9 Open the nitrogen regulator and adjust to 1000 psi.
- 5.10 Prepare the instrumentation for a simulated flight.
- 5.11 Open the manual ball valve to the nitrogen bank.
- 5.12 Install area jumpers.
- 5.13 Start the recording equipment.
- 5.14 General Electric personnel will perform a simulated flight program.
  - 5.14.1 When an unsafe position of the wing is assumed, the solenoid valve will apply pressure to the input of the fluidic thruster to make corrections.
- 5.15 Record all data parameters.
- 5.16 Develop and review all records.
- 5.17 Upon satisfactory completion of the cold gas test, the hot gas adapter will be installed onto the assigned TE-M-509 gas generator and attached to the fluidic thruster.



- 5.18 Prepare instrumentation for the hot gas test and prepare to arm the gas generator.
- 5.19 Clear the area and arm the gas generator.
- 5.20 Install safety jumpers.
- 5.21 Start firing sequence and proceed through calibration sequence, allow recorders to run.
- 5.22 Switch control of the fire control to the electronic flight simulator.
- 5.2.1.1 GE personnel shall begin the simulated flight program and simulate an "unsafe attitude" condition which will signal the gas generator ignition.
- 5.23 Record all data parameters and develop records.
- 5.24 Record output of TV camera on tape.
- 5.25 Monitor the thermocouple output at one-minute intervals for 10 minutes after firing.

## 6.0 SPECIAL SYSTEM REQUIREMENTS

- 6.1 A control system will be provided to allow the ignition voltage to be held "ON" and delivered to the igniter on command of the electronic simulator computer.
- 6.1.1 All other control, calibration, and recording functions shall occur in their normal sequence.

6.2 A system shall be provided to allow recording of roll rate and position on an X-Y plotter and oscillograph at the same time.

6.3 Circuits for recording television on tape shall be provided.

7.0 DATA REDUCTION

7.1 A copy of the oscillograph trace with all gage factors imprinted on it shall be provided.

7.1.1 General Electric will do their own reduction and analysis.

# ENGINEERING SPECIFICATION

This test procedure, in accordance with Item 5 of Task IV of Contract NAS 2-5467, provides an outline for hot gas tests to be conducted on the fluidic emergency thrusters at Thiokol Chemical Corporation, Elkton, Maryland. The facilities and instrumentation are to be provided by General Electric Company and Thiokol Chemical Corporation. The electronic aircraft system simulator (Par. 3.2.1) is provided as GFE by NASA/ARC.

## REVISIONS

Ltr	Pages	Description	Date	Approved

Fluidic Emergency Thruster System  
Hot Gas Test Procedure

1.0 General Instructions

1.1 Scope - This test procedure, in accordance with Attachment Q-2 paragraph 4 of Contract NAS 2-5467, provides detailed instructions for conduct of Fluidic Emergency Thruster System (FETS) hot gas tests. The tests shall be conducted by the FET contractor.

1.2 Hardware Identification - The FET test hardware shall be designated:

Fluidic Emergency Thruster  
G.E. Part Number: CR280PT32AA0000  
CR280PT32BA0000

Gas Generator  
Thiokol - TE-T-509 Modified

1.3 Applicable Documents - G.E. Drawing No. 55-518081 FET Assembly.  
Thiokol Drawing No. E24847.

1.4 Inspection Plan - Tests shall be witnessed by G.E. Engineering personnel. The NASA/ARC technical monitor shall be notified forty-eight (48) hours in advance.

2.0 Test Conditions - The following test conditions apply to all tests described in Section 3.0 of this specification unless specified otherwise.

2.1 Test Fluid - The fluid used in the performance of hot gas tests shall be the products of combustion of Thiokol propellant TP-Q-3074A.

2.2 Test Set-up Environment - Unless otherwise noted:

- a. Ambient temperature shall be outdoor ambient (-20F to 110F).
- b. Ambient pressure shall be normal sea level (28-32 inches of mercury).

2.3 Test Measurements - Instruments shall be calibrated to commercial standards.

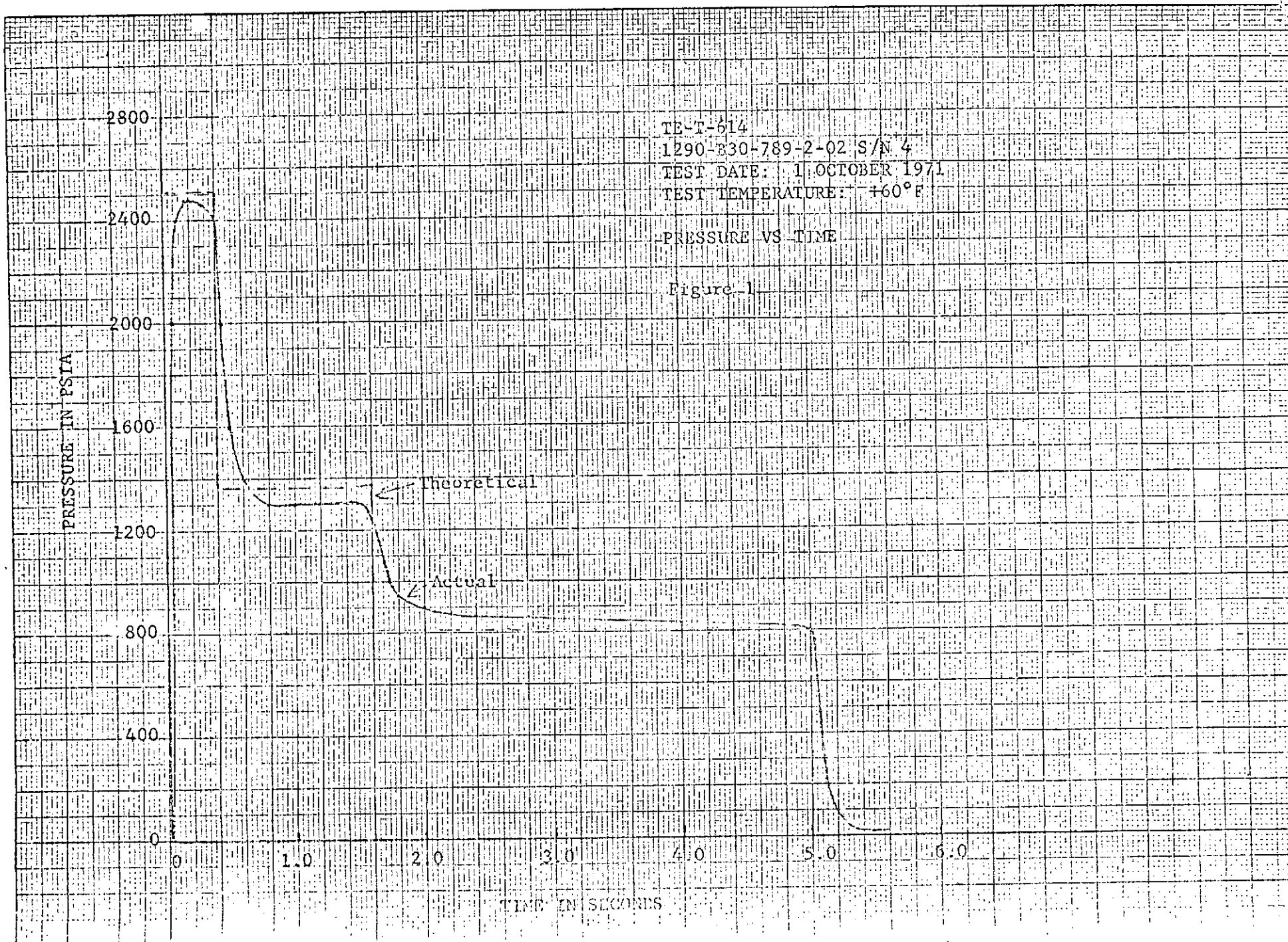
2.3.1 Pressure - All pressures shall be measured with gauges or pressure transducers which have been calibrated with a standard dead weight tester.

2.3.2 Temperature - Laboratory thermometers or thermocouples shall be used for temperature measurement.

2.4 Test Pressures - The test pressure shall be within  $\pm 10\%$  of the actual schedule (solid line) as shown in Figure 1.

3.0 Test Methods - The following tests shall be performed on each of the three (3) fluidic emergency thrusters provided under the contract containing this specification.

3.1 Cold Gas Test - The FET static characteristics shall be established on high pressure air tests as defined in Specification No. ES-PT-1 dated 12/28/71.



3.2 Hot Gas System Test - The FET shall be mated with a modified Thiokol high pressure control test motor, TE-T-509 and operated with the products of combustion of Thiokol propellant TP-Q-3074A. The grain shall be shaped to provide the pressure-time characteristics defined in Figure 1.

3.2.1 FET and Aircraft System Simulation - The FET shall be tied into the electronic aircraft system simulator through the torque motor driver amplifier and the vortex valve control pressure transducer output as shown in Figure 2. The simulated vehicle inertia shall be 2340 slug ft<sup>2</sup> and the lever arm shall be 16.1 ft.

3.2.2 Hot Gas Generator Initiation - The hot gas generator initiation logic shall be set up to fire when the sum of the vehicle wing position  $\theta$  and roll rate  $\dot{\theta}$  exceeds the safe region shown in Figure 3. During the test run, the simulated aircraft shall be flown manually into an unsafe condition to automatically activate the FET system. Manual control at wings level and near zero rate shall be maintained after the hot gas generator ignition.

3.2.3 Simulated Emergency Control Data - The following data vs time shall be recorded during the simulated emergency control operation.

3.2.3.1 Wing Position Signal from the Simulator.

3.2.3.2 Roll Rate Signal from the Simulator.

3.2.3.3 Torque Motor Input Voltage.

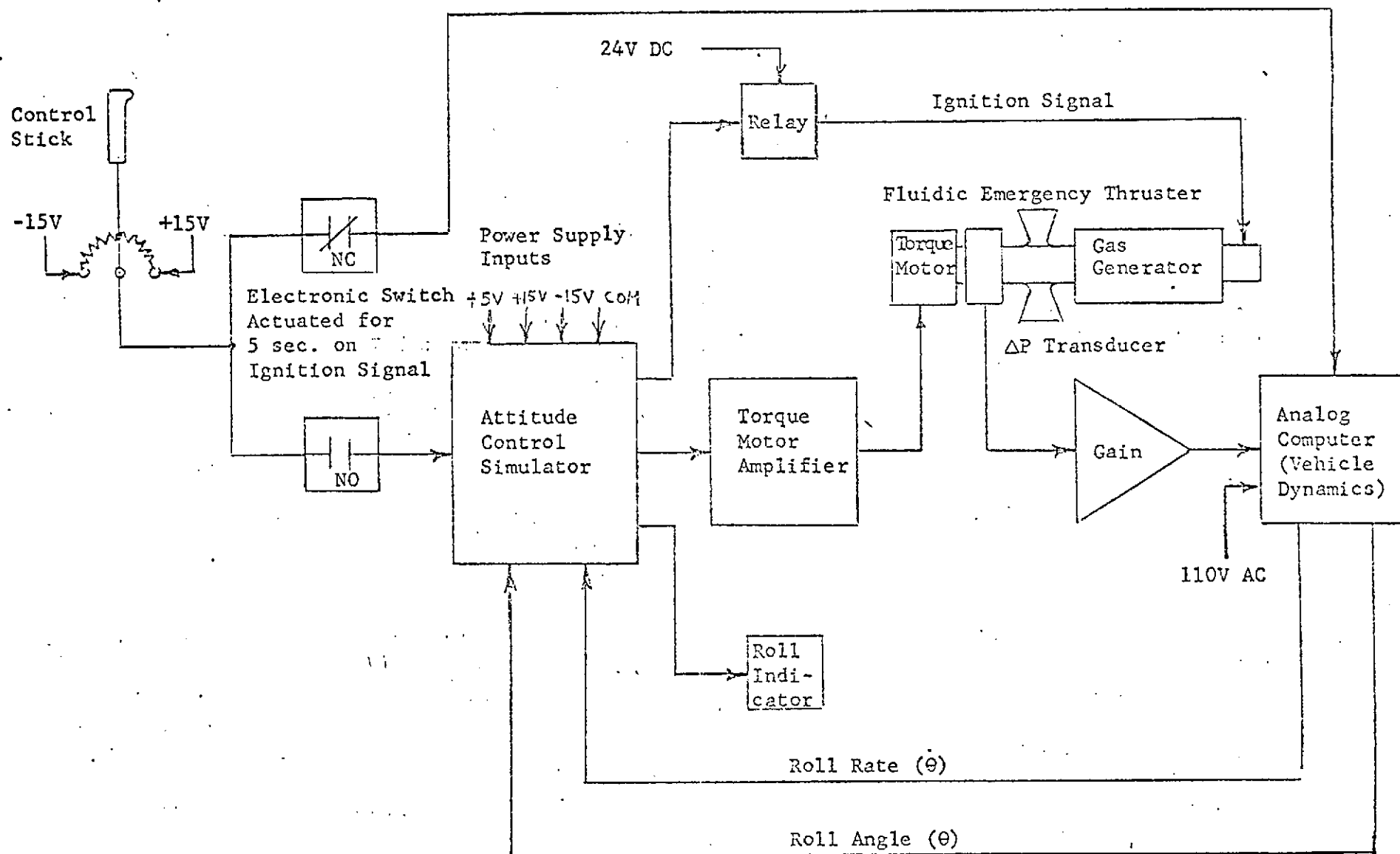
3.2.3.4 Hot Gas Generator Ignition Signal.

3.2.3.5 Hot Gas Generator Pressure.

3.2.3.6 Vortex Valve Control Differential Pressure.

3.2.3.7 FET surface temperatures at the torque motor base, supply inlet and vortex valve body. The temperature measurements shall be recorded for at least 10 minutes after propellant burn out.

3.3 Cold Gas Retest - The test procedure outlined under Section 3.1 shall be repeated after hot gas operation of the FET.



Functional Diagram  
Fluidic Emergency Thruster  
and Aircraft System Simulator

Figure 2



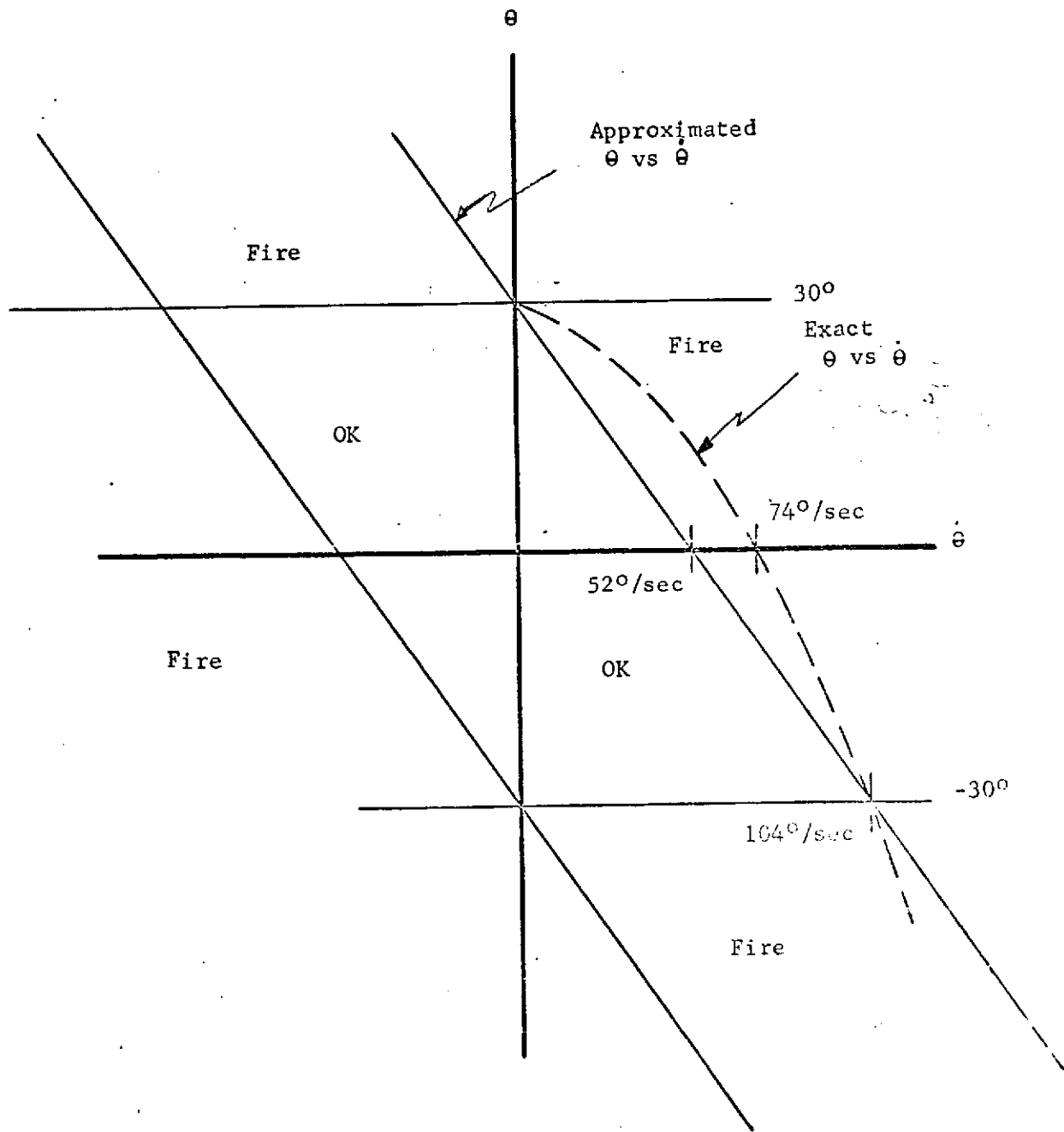


Figure 3

VTOL EMERGENCY FLIGHT CONDITIONS